SCINTILLATORS AND SILICON PHOTOMULTIPLIERS

PHD PHYSICS COURSE – XXXIII CYCLE

UNIVERSITÀ DI BARI

Dott.ssa Elisabetta Bissaldi

RTDa – Politecnico & INFN Bari

Light pipes

- **Coupling** between scintillator and PMT
  - Used if size or shape of scintillator does not match the circular PMT area
- Optically **transparent solids** with **high refractive index**
  - **Guide** for the scintillation light
- Used e.g. in case of strong magnetic fields in order to put the scintillator at some distance

➔ Averaging of photocatode nonunifo
resolution

- Operate on total internal reflection
- Surface highly polished
- Example: Lucite (Plexiglas)

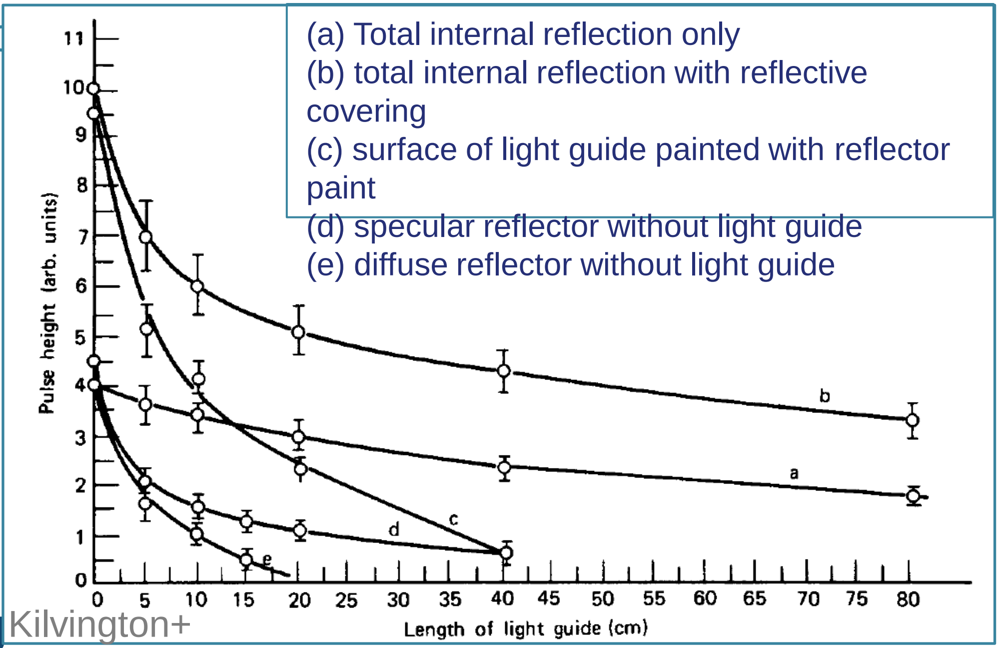

Variation of pulse heig

Kilvington+ 1979

Light pipes

- Estimation of the **fraction of light** that will be **conducted** in one direction along the length of a rod (stick) by successive **internal reflections**

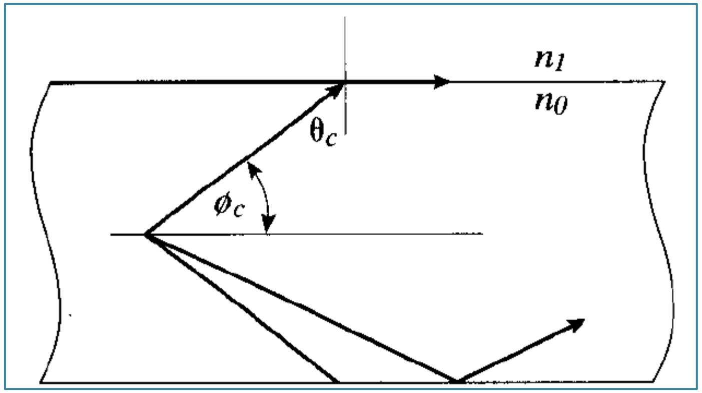

- Only the light emitted within the cone angle ϕ_c will be incident on the rod surface at the critical angle θ_c or greater→ **total internal reflection**
- BUT: angle of reflection = angle of incidence!

  ➔ Subsequent arrivals of the reflected light at the rod surface will also be **above the critical angle**

  ➔Light is "piped" along the rod length as in an optical fiber

  ➔Fractional solid angle subtended by ϕ_c in a rod: $F = \frac{1}{2}(1 - n_1/n_0)$

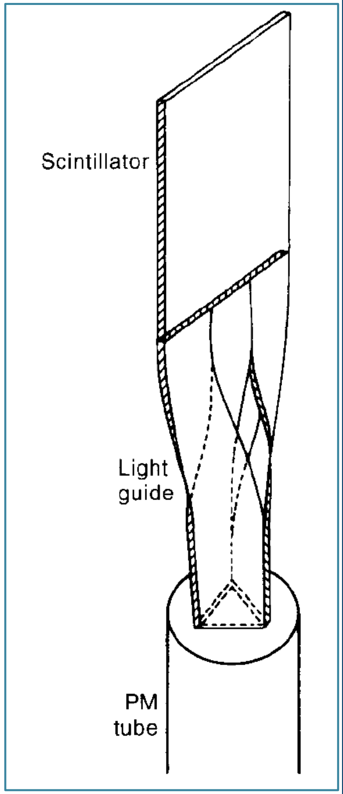

Fiber scintillators

- **Small diameter fibers** in which a fraction of the scintillation light is conducted over **substantial distance** by **total internal reflection**

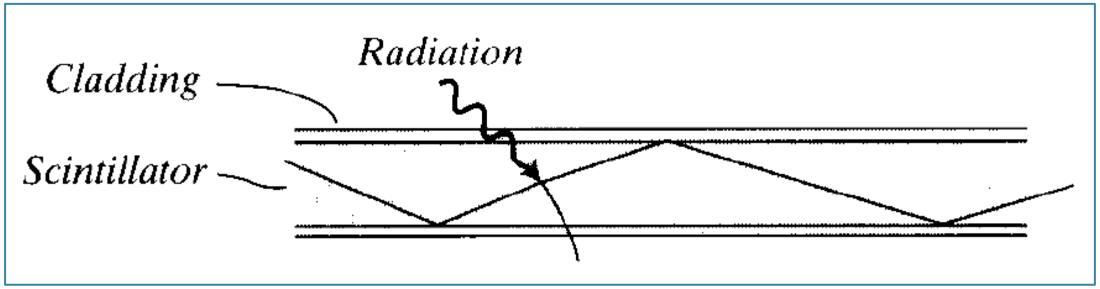

- Common configuration
  - Scintillator core surrounded by thin layer of cladding material
    - Core and cladding are transparent materials

      ➔ $n_{core} > n_{cladding}$
    - Light rays that arrive at the core-cladding interface with $\theta > \theta_c$ are "piped" down the length of the fiber
      - Optical isolation provided by "extramural absorber" to the outer surface of the cladding

Plastic and liquid core fibers

- Plastic scintillators fabricated into fibers with **round, square**, or other shapes
  - Core material: Polystrene (n=1.58) with few % of organic fluor
  - Cladding material: Polymethyl (n=1.49)
- Diameters:
  - From few tenths to some millimeters
- Emission spectrum typically peaked in the **blue region**
  - Decay times from **2 to 4 ns**
- Can be grouped together to form ribbons or bundles

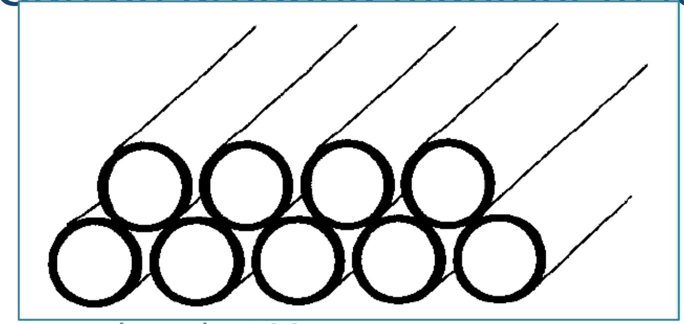

Baumbaugh+1994

Glass capillaries filled with liquid scintillator

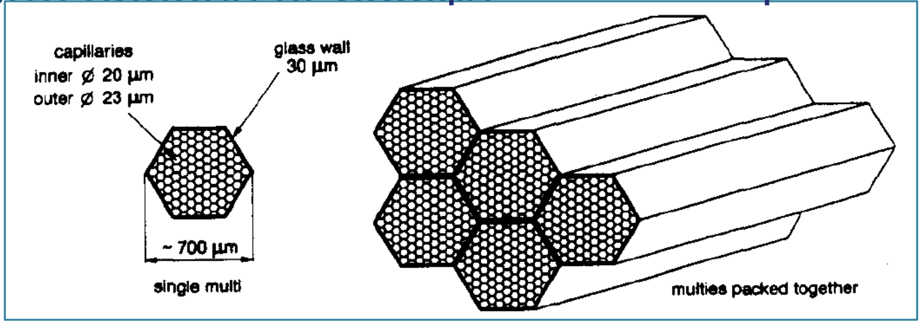

Ferroni & Martellotti 1995

Plastic and liquid core fibers

- Attenuation processes in glass fibers:
  - High number of reflections
  - Imperfections at the core-cladding interface
  - Reabsorbtion of scintillation light
  - Deflections due to Rayleigh scattering

➔ Cumulative effect expressed as ATTENUATION LENGTH L of the fiber

  - Typical values of L from a few tens of centimeters to several meters

- Light Intensity at distance x from the original scintillation site (where $I = I_0$)

$$I = I_0 e^{-x/L}$$

  - Short wavelengths tend to be more readily reabsorbed

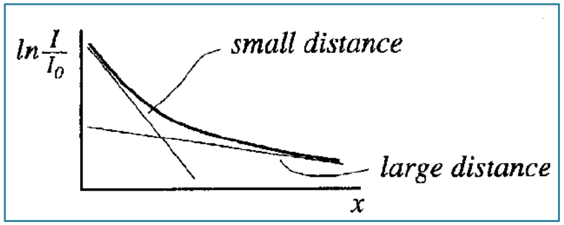

Typical Light yield for fiber scintillators

Core material	photons/keV	λ_{peak} (nm)
Glass scintillator	3–5	400
Plastic scintillator	8–10	420
Liquid scintillator	11–13	420
For comparison:		
NaI(Tl)	38	415

Quoted yields are for low dE/dx particles such as fast electrons and will be lower for heavily ionizing particles such as recoil nuclei

Radiation spectroscopy with scintillators

GAMMA-RAY INTERACTIONS

- **Photoelectric absorption**: single peak appears a total electron energy corresponding to the energy of the incident gamma rays.

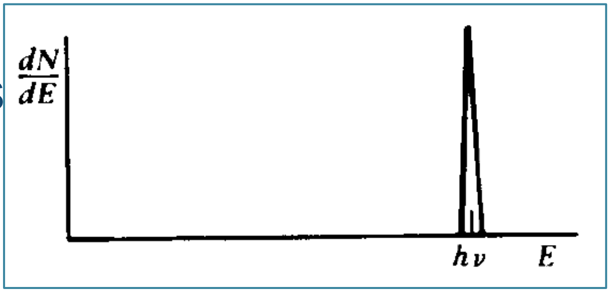

- **Compton Scattering:** all scattering angles will c in the detector. A continuum of energies can be transferred to the electron, ranging from zero up the maximum predicted one.

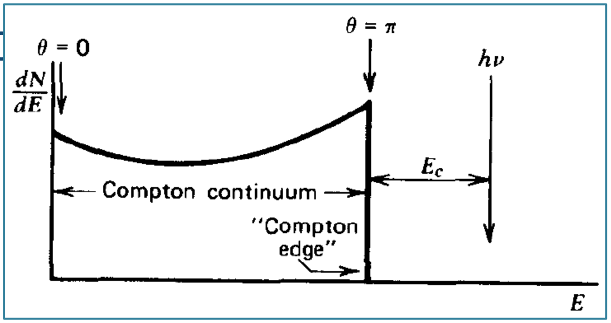

- **Pair production**: The total (electron-positron) ch particle kinetic energy created by the incident gamma ray is now located 2 $m_e c^2$ below the incid gamma-ray energy

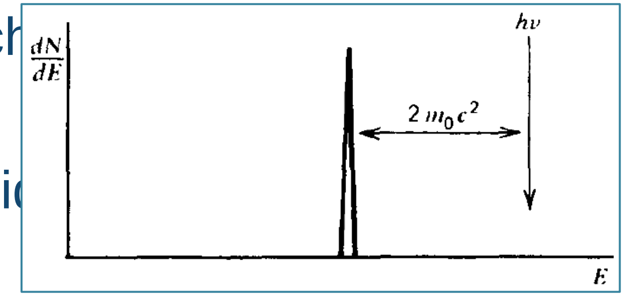

Knoll 1999

Radiation spectroscopy with scintillators

- **Small Size Detectors** (1–2 cm)

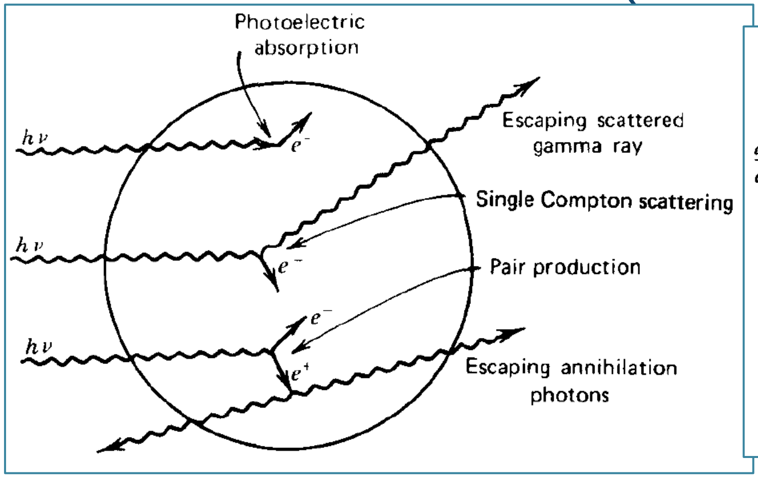

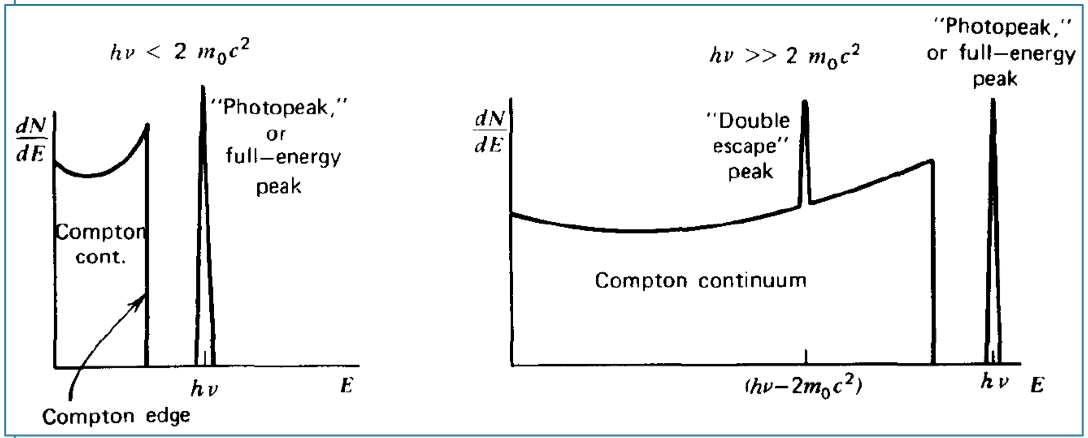

Knoll 1999

- **Very large detectors** (tens of cm)

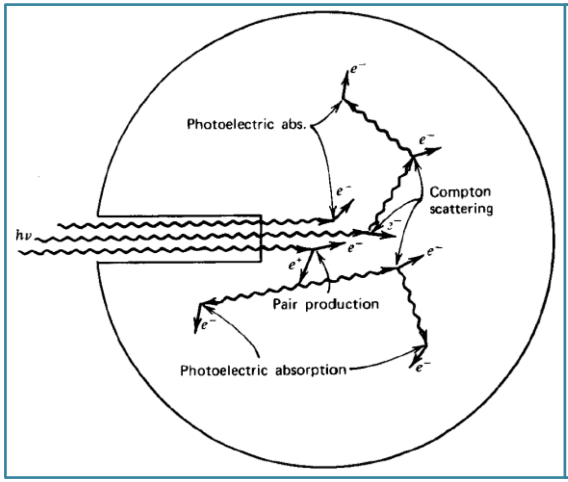

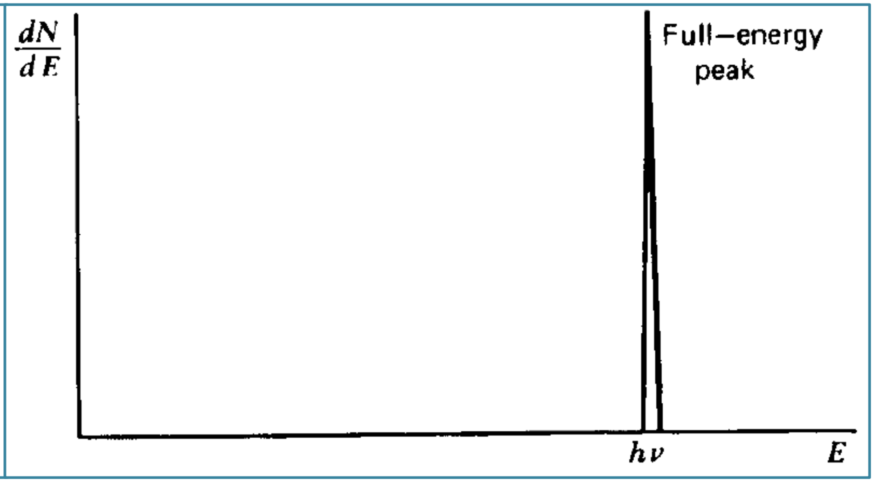

Radiation spectroscopy with scintillators

- **Intermediate Size Detectors**

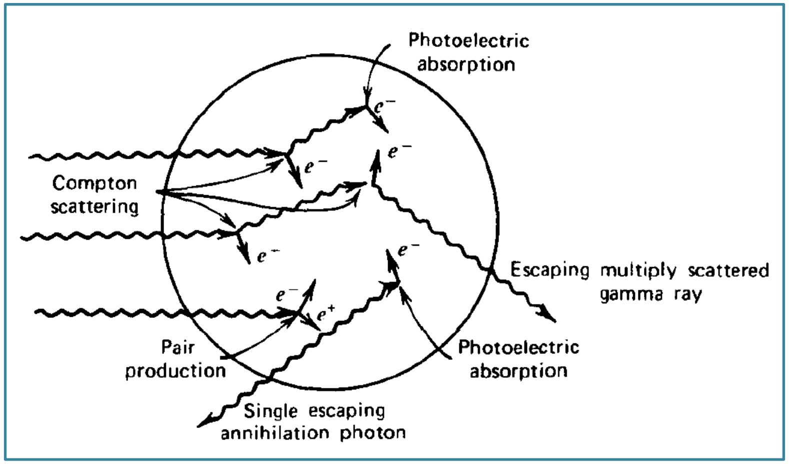

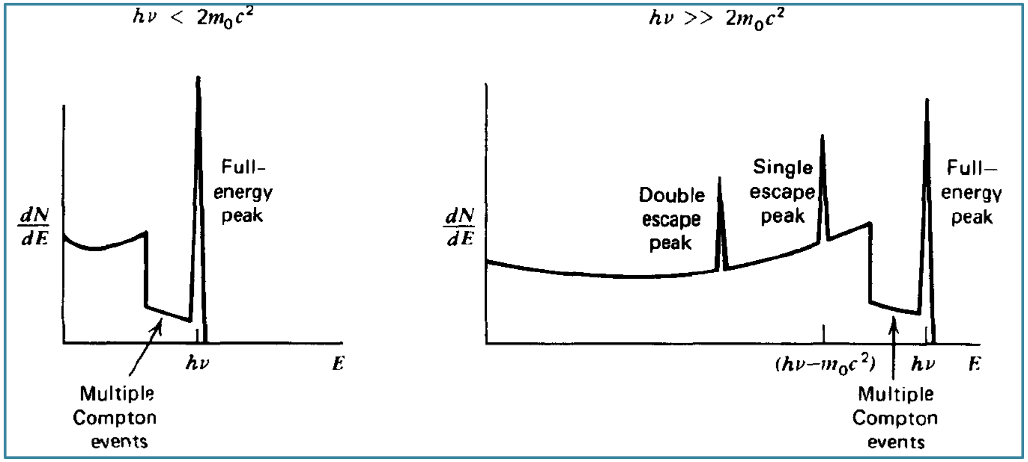

Knoll 1999

- **At medium energies:**
  - Multiple Compton scattering followed by escape of the final scattered photon can lead to a **total energy deposition** that is **greater** than the **maximum predicted for single scattering**
    - **Events fill in the gap** between the Compton edge and the photopeak
- **At high energies:**
  - One annihilation photon escapes but **the other is totally absorbed**
    - Events that contribute to a **single escape** peak

COMPLICATIONS IN THE RESPONSE FUNCTION

1. Secondary electron escape
2. Bremsstrahlung escape
3. Characteristic x-ray escape
   - In the photoelectric absorption process a characteristic X-ray often is emitted by the absorber atom. If the photo-electric absorption occurs near a surface of the detector, the X-ray photon may escape

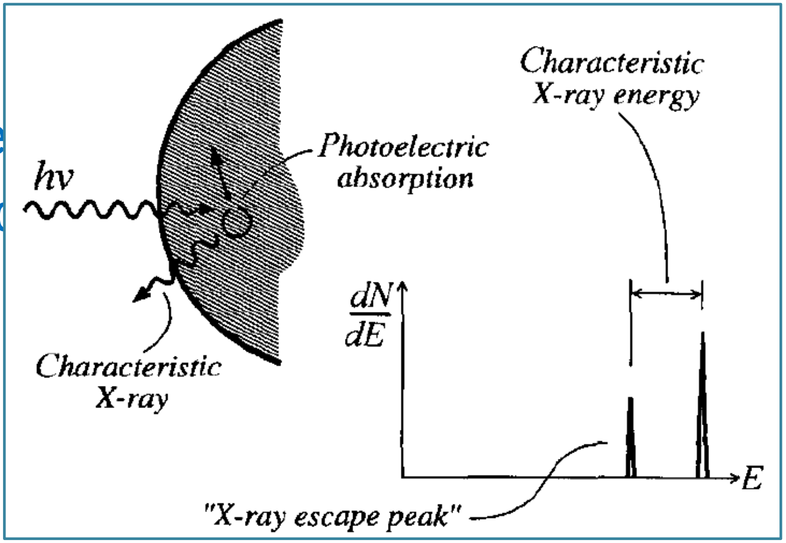

Knoll 1999

Radiation spectroscopy with scintillators

- EFFECTS OF SURROUNDING

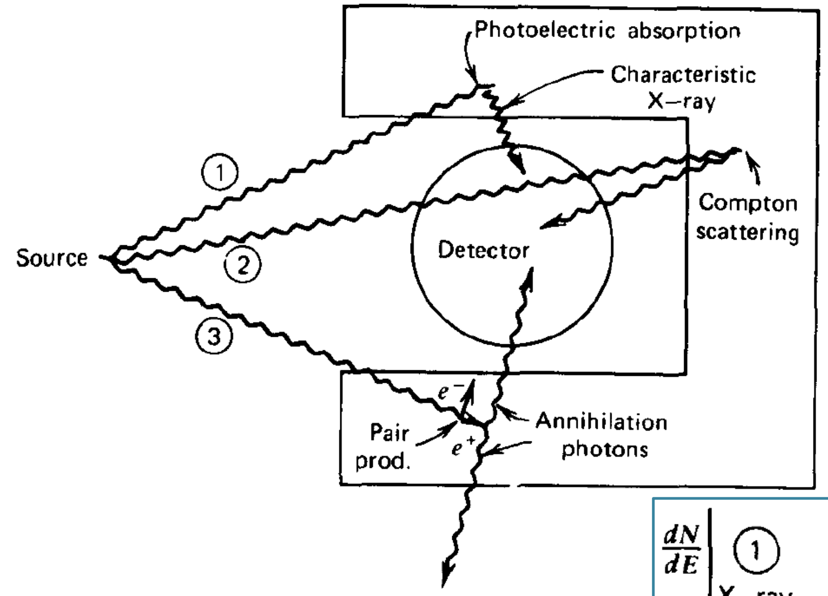

- **Backscatter peak:**
  caused by gamma rays from the source that have first interacted by Compton scattering in one of the materials surrounding the detector

Knoll 1999

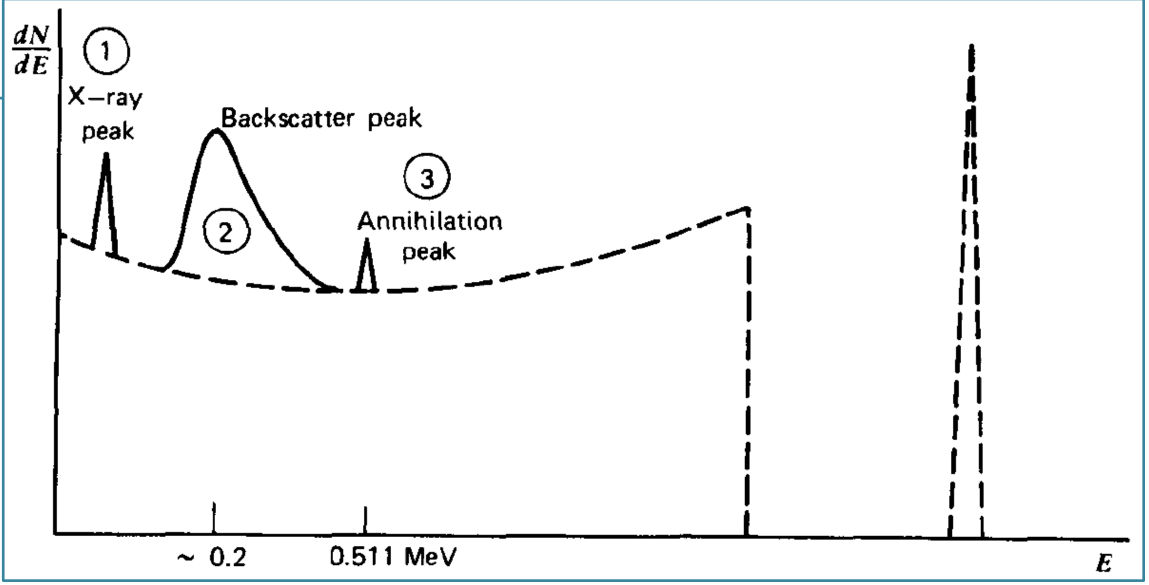

Fermi-GBM detector characteristics

- **Fermi-GBM Response Functions**
  - NaI(Tl) spectra measured with monochromatic synchrotron radiation

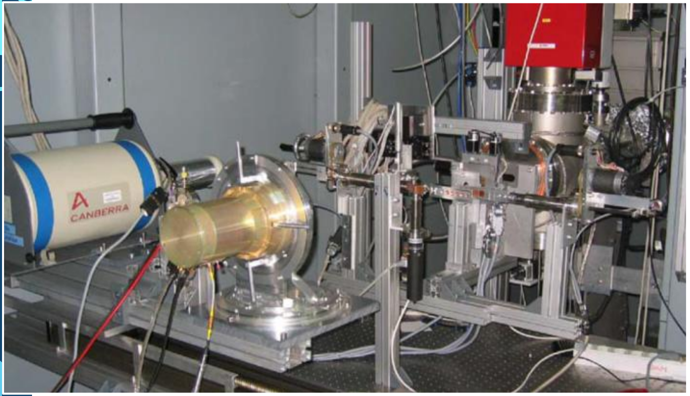

Calibration at Electron storage ring PTB/BESSY II in Berlin (2005)

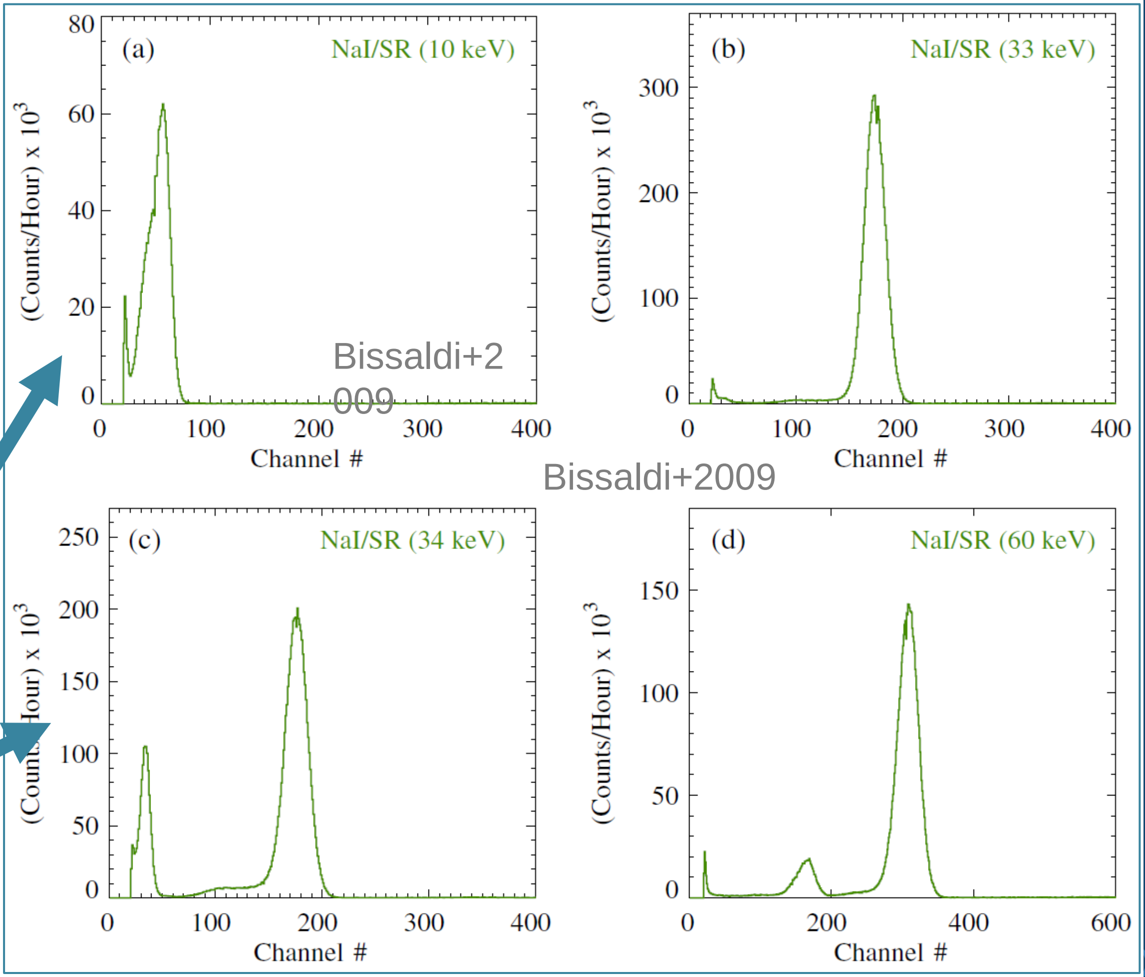

Below K-edge energy

Above K-edge energy

➔characteristic Iodine escape peak

Fermi-GBM detector characteristics

- NaI(Tl) spectra measured with various radioactive sources

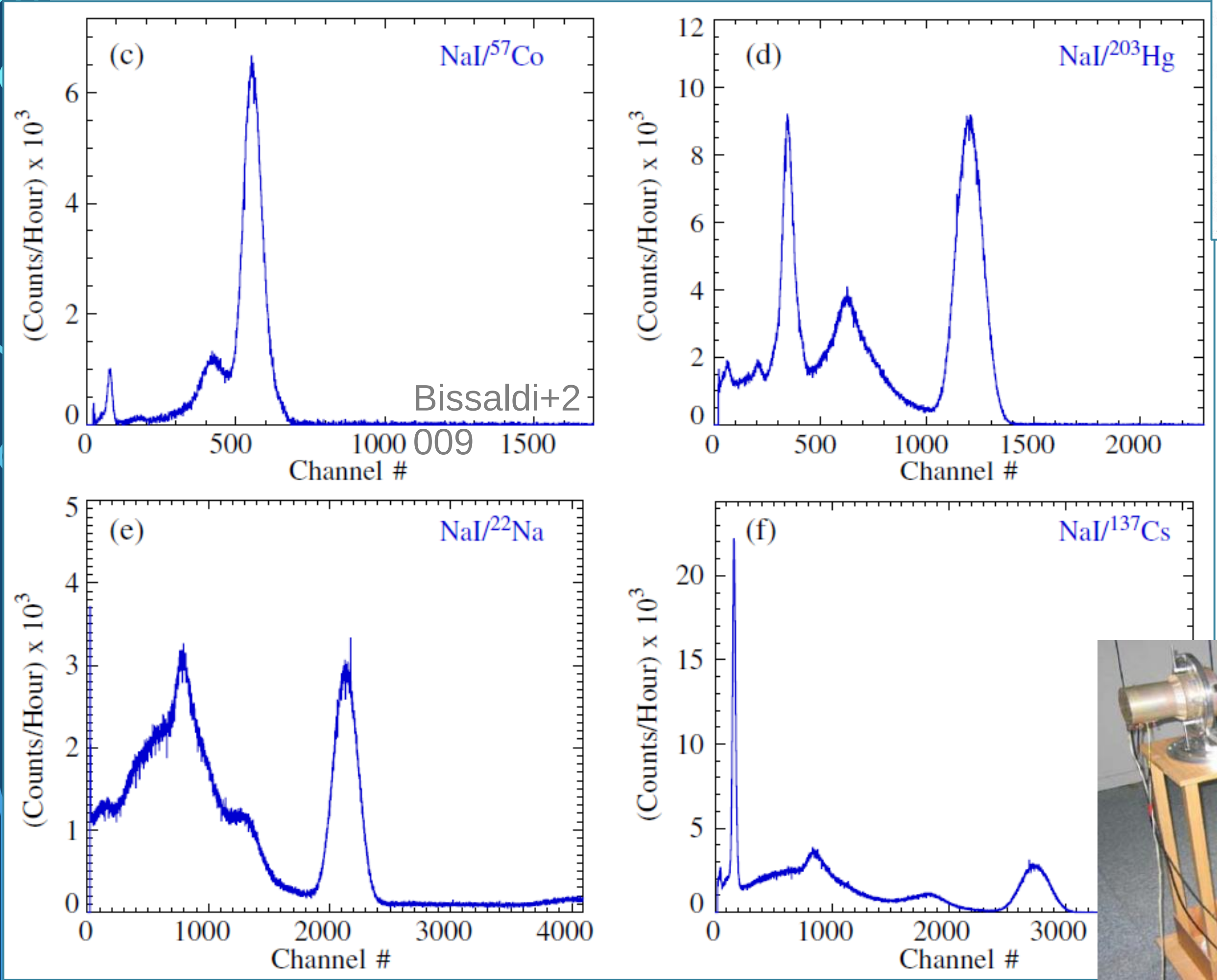

Bissaldi+2009

Nuclide	(1) Half-life	(2) Line origin	(3) Line Energies (keV)	(4) Transition Probability
^{22}Na	950.5(4) d	Annih.	511	1.798
		γ	1274.54	0.9994
^{40}K	1.277(8)E9 y	γ	1460.83	0.1067
^{54}Mn	312.15(8) d	γ	834.84	0.999750(12)
		γ	14.41	0.0916(15)
^{57}Co	271.83(8) d	γ	122.06	0.8560(17)
		γ	136.47	0.1068(8)
^{60}Co	5.2712(11) y	γ	1173.23	0.9985(3)
		γ	1332.49	0.999826(6)
^{88}Y	106.630(25) d	γ	898.04	0.940(3)
		γ	1836.06	0.9933(3)
		Ag−SumKα	22.1	0.836(6)
^{109}Cd	462.1(14) d	Ag−SumKβ	25	0.1777(19)
		γ	88.03	0.03626(20)
		Ba−SumKα	32.06	0.0553(10)
^{137}Cs	30.13(24) y	Ba−SumKβ	36.6	0.01321(27)
		Ba−137m	661.66	0.8500(20)
^{203}Hg	46.604(17) d	γ	279.2	0.8146(13)
^{232}Th	1.405(6)E10 y	^{208}Tl (γ)	2614.53	0.3564
^{241}Am	432.2(7) y	γ	59.4	0.359(4)
^{241}Am/^{9}Be	432.2 (7) y	γ	4430	0.00004

Fermi-GBM detector characteristics

- BGO spectra measured with various radioactive sourc

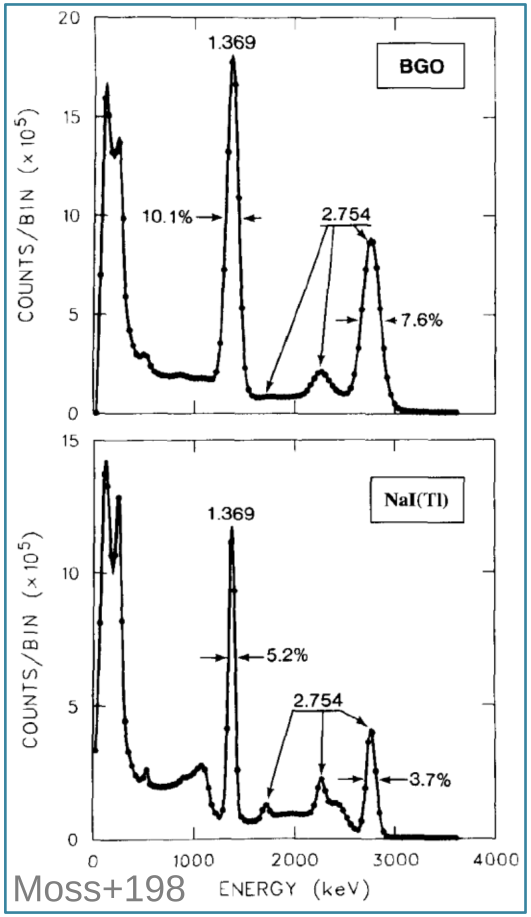

Moss+1984

Comparative pulse height spectra measured for BGO and NaI(Tl) scintillators of equal size (7.6 x 7.6 cm) for gamma rays from ^{24}Na

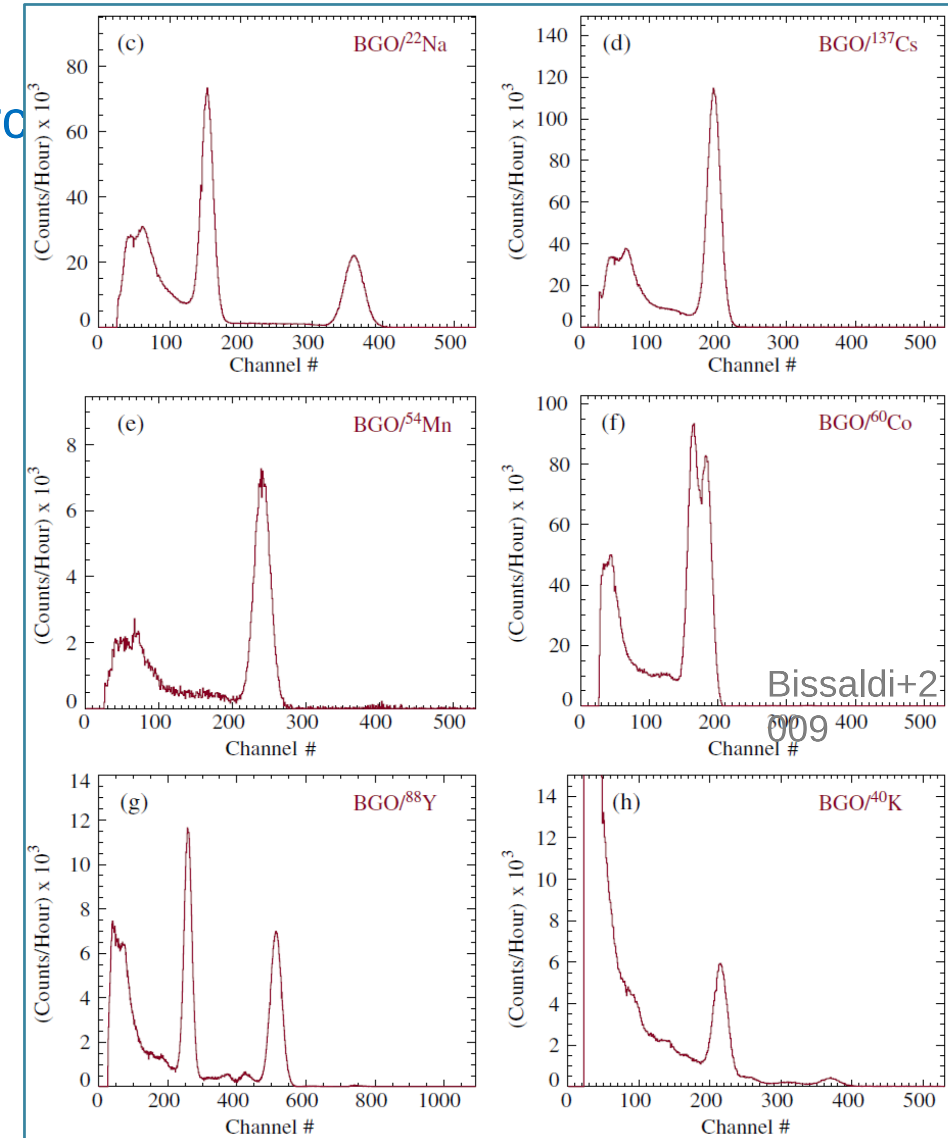

Bissaldi+2009

Fermi-GBM detector characteristics

Fermi-GBM Response Functions

- Full energy peak analysis
  - **Gaussian** fits with 3 parameters
    - Area
    - Center
    - FWHM
  - **Important**: background subtraction from the continuum

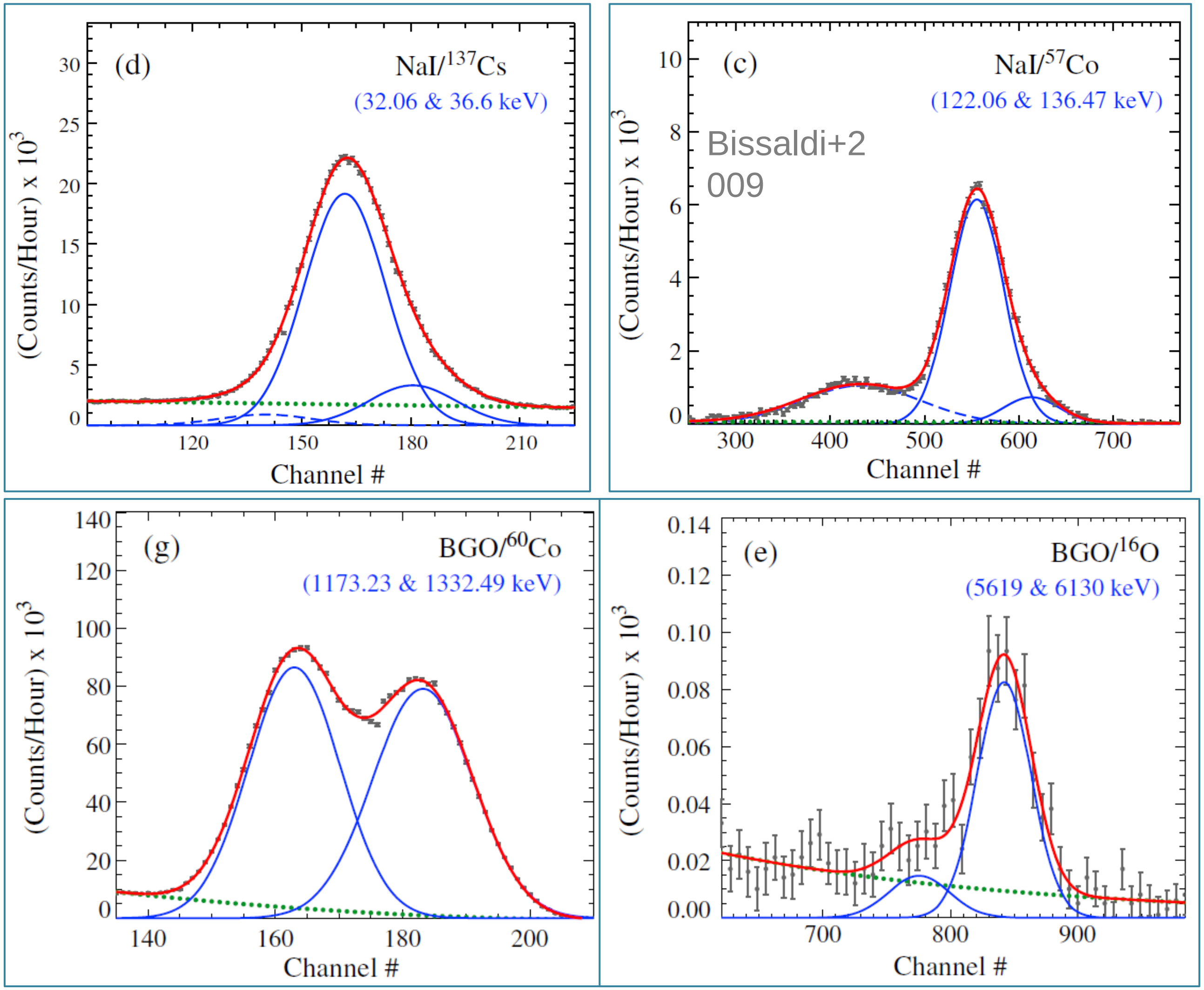

Fermi-GBM detector characteristics

CHANNEL-ENERGY RELATION (CALIBRATION)

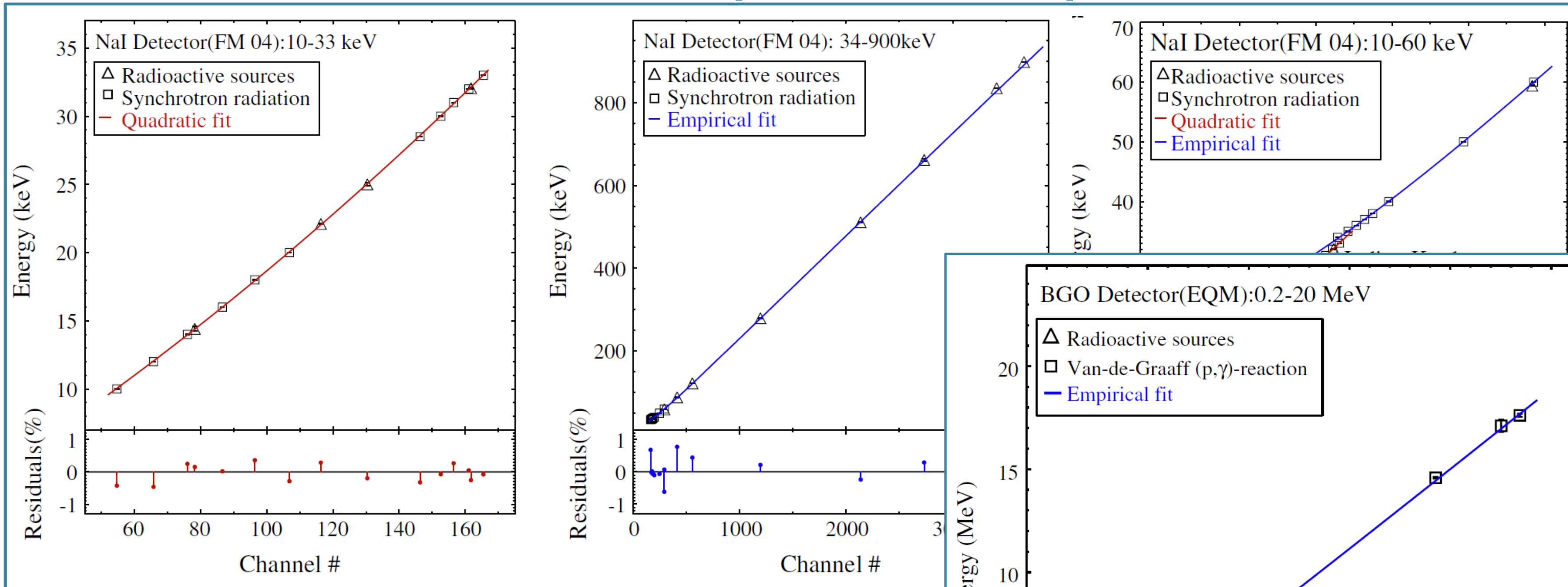

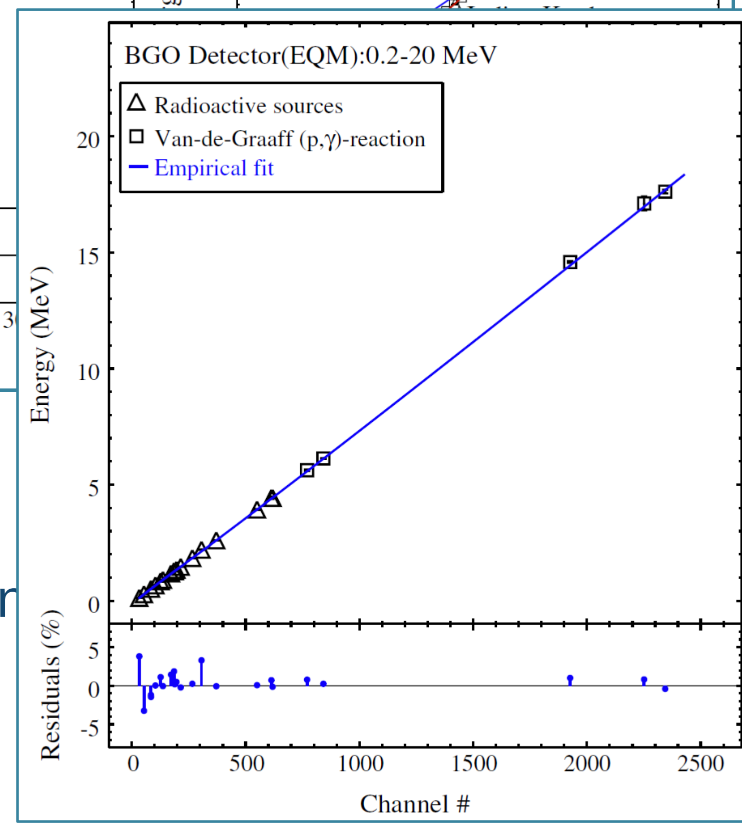

Bissaldi+2
009

➔ Both Nai(Tl) and BGO scintillators show **good linearity** over the whole energy ran

Fermi-GBM detector characteristics

ENERGY RESOLUTION

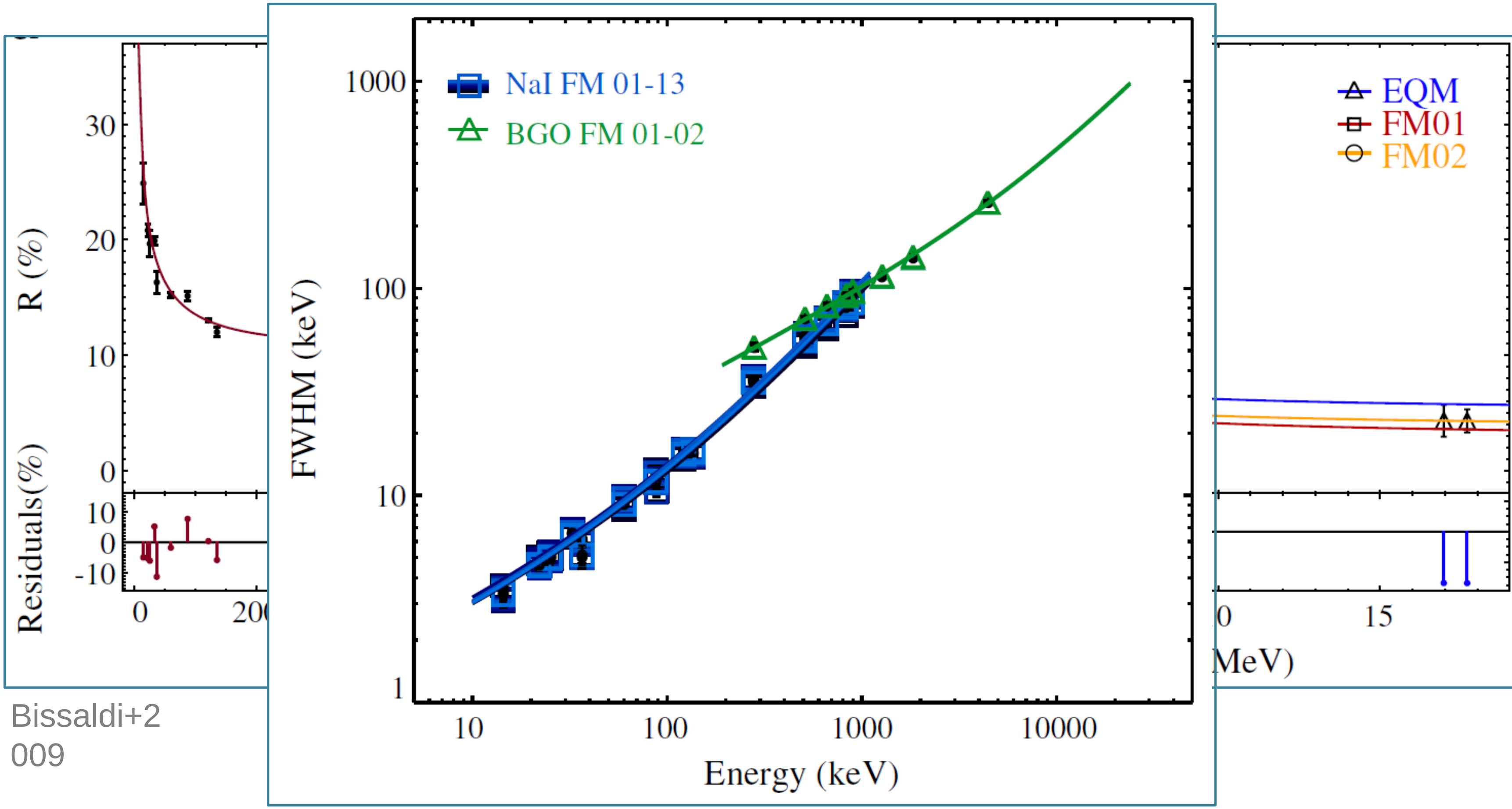

Bissaldi+2009

Fermi-GBM detector characteristics

NAI(TL) SCINTILLATOR CRYSTAL UNIFORMITY

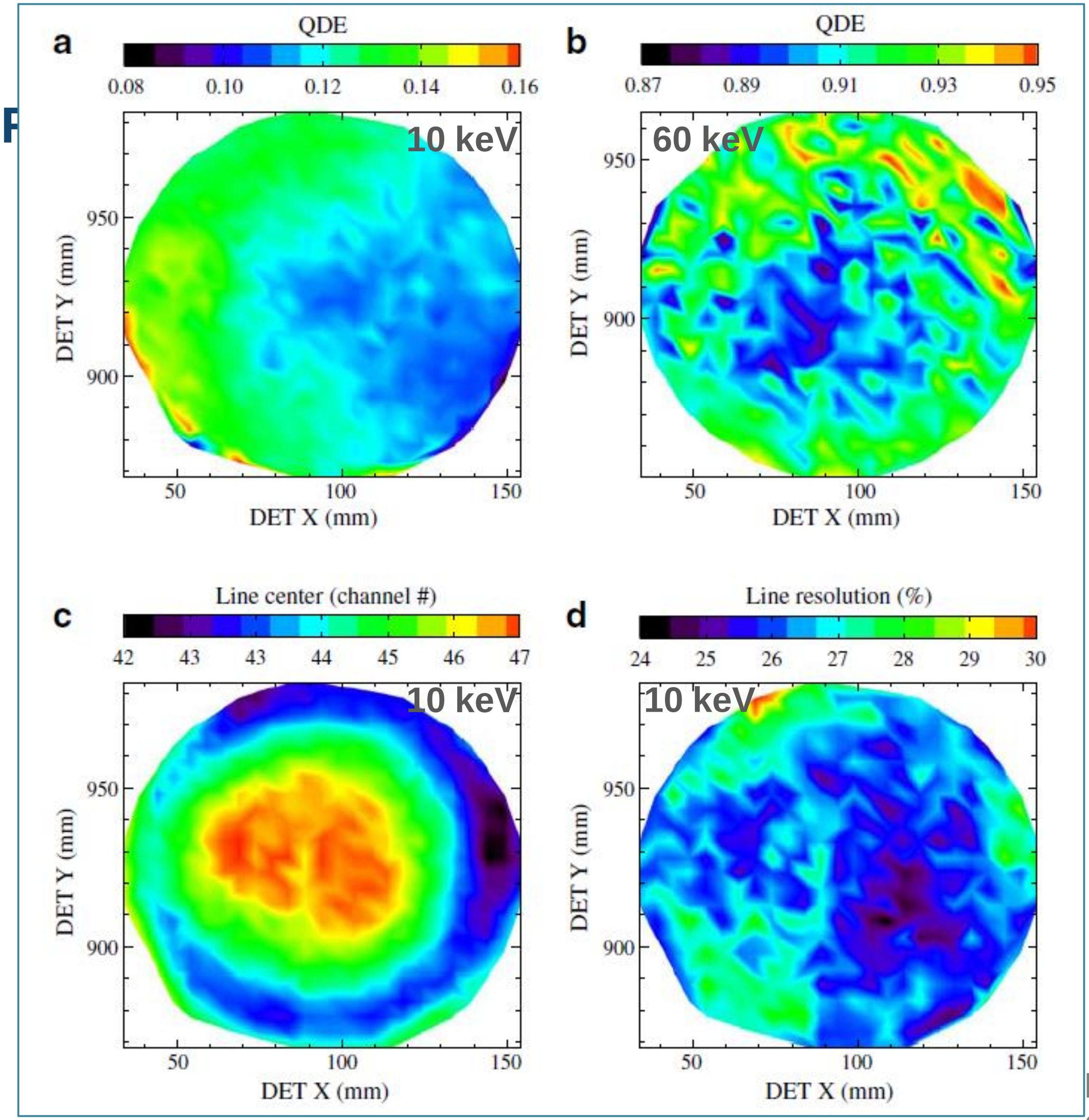

Bissaldi+2009

Fermi-GBM detector characteristics

NaI(Tl):

- **511 keV line** from positron annihilatio in the atmosphere and nearby materials → **Used for AGC**
  - 2 lines from excited ^{127}I energy levels of (57.6 and 202.9 keV)
  - Passive materials in front the detectors limit the response o the detectors significantly at ~8-20 keV (low energy drop)

BGO:

- **2.2 MeV line** due to neutron capture in the large amount of H contained in the hydrazine tanks of the spacecraft → **Used for AGC**
  - 1.46 MeV line is due to ^{40}K from the

Fermi-GBM 2.4 hr accumulations of background

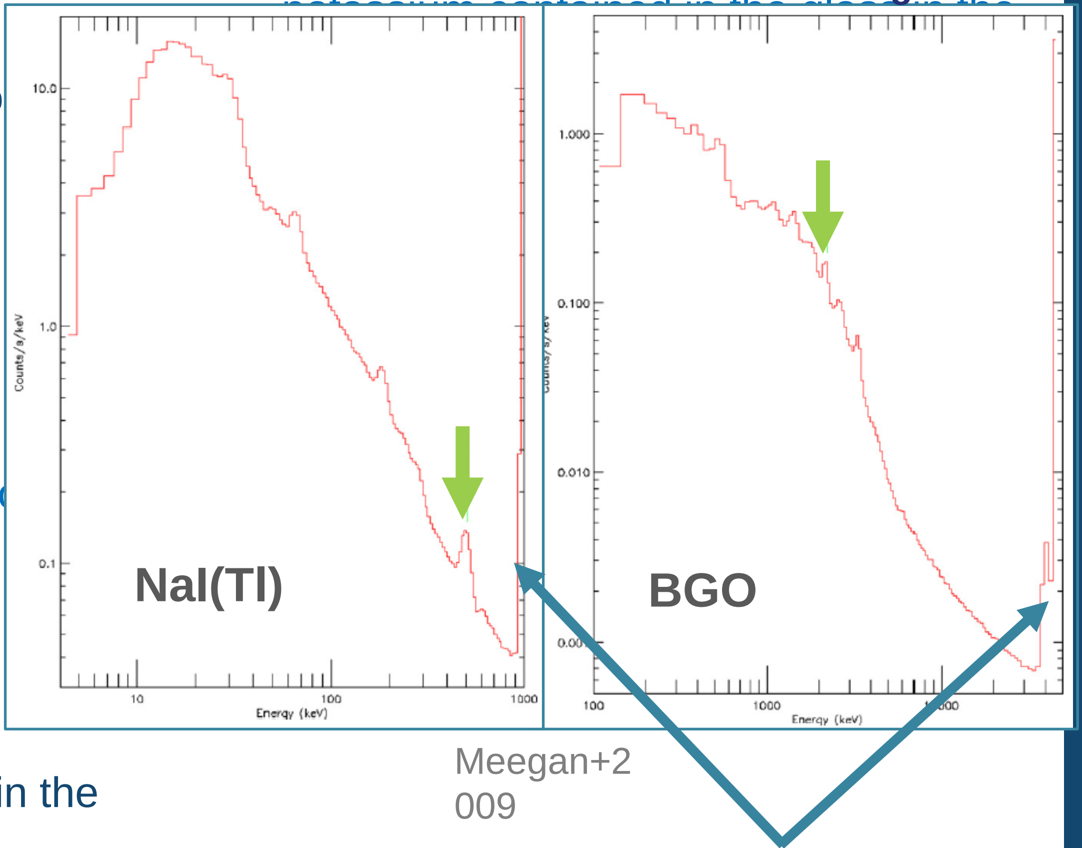

Meegan+2009

“Overflow channels”
(NaI: ~1MeV BGO: ~45 MeV)

Fermi-GBM detector characteristics

Bacground rates: Temporal plots over 1 day (86400 s)

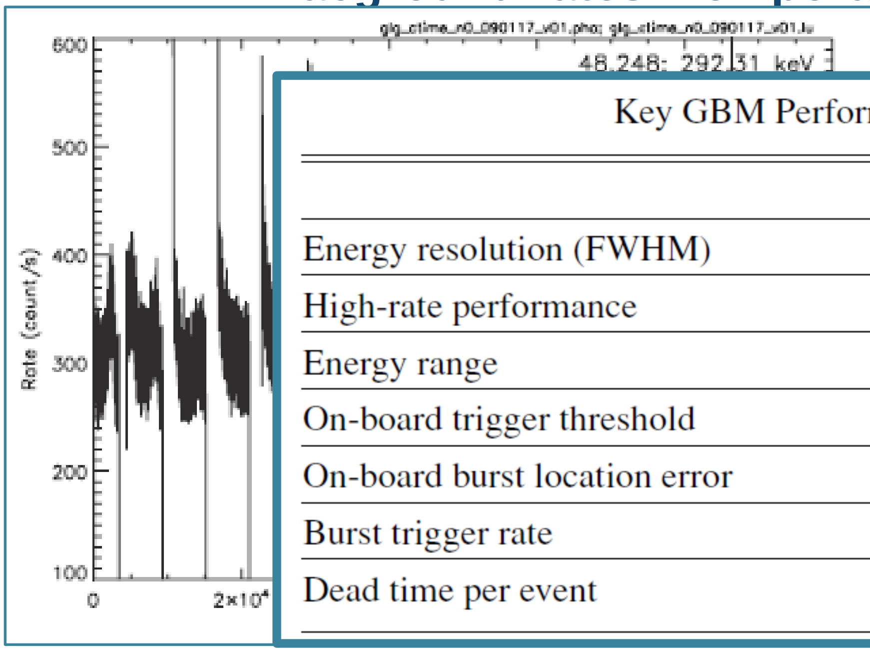

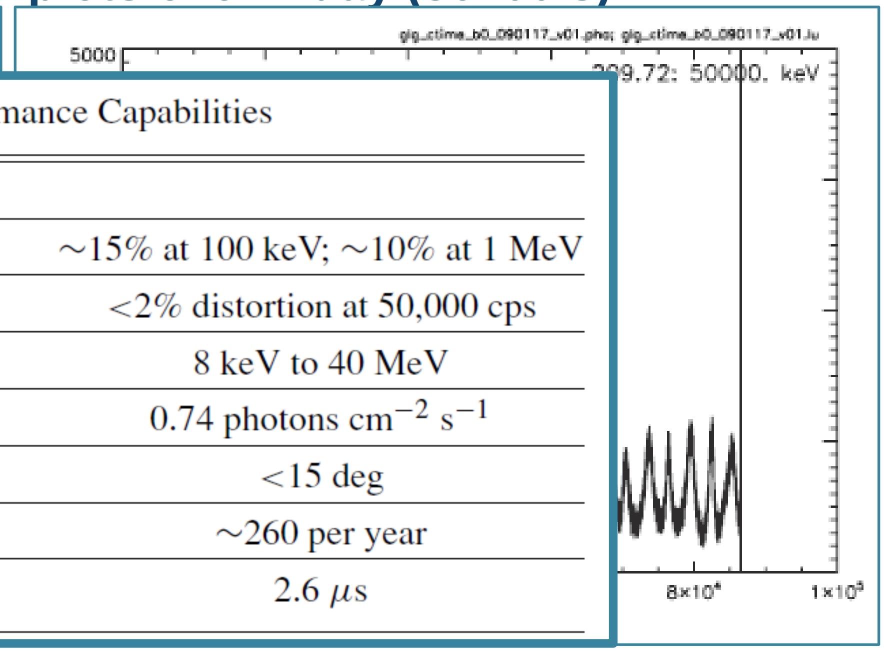

Key GBM Performance Capabilities

Energy resolution (FWHM)	~15% at 100 keV; ~10% at 1 MeV
High-rate performance	<2% distortion at 50,000 cps
Energy range	8 keV to 40 MeV
On-board trigger threshold	0.74 photons cm^{-2} s^{-1}
On-board burst location error	<15 deg
Burst trigger rate	~260 per year
Dead time per event	2.6 μs

Meegan+2009

- Times of zero rate due to **turning off the PMTs** during **South Atlantic Anomaly (SAA) passages**
- High rates near the SAA boundaries
  - Effect of **activation** by the SAA **more pronounced in BGO** detectors
- NaI rates are shown for the **primary trigger energy range of 50–300 keV**

Photon detection

Purpose: Convert light into a detectable electronic signal

Principle: Use photo-electric effect to convert photons to photo-electrons (p.e.)

- **Requirement:**
  - High Photon Detection Efficiency (PDE)
    - High quantum efficiency ($QE = N_{p.e.}/N_{photons}$), low surface reflection, …

PMT collection

- **Available devices:**
  - Photomultipliers [PMT]
  - Micro Channel Plates [MCP]
  - Photo Diodes [PD]
  - Hybrid Photo Diodes [HPD]
  - Visible Light Photon Counters [VL

Photomultiplier tubes (PMTs)

- **Convert** the extremely weak **light output** (no more than a few hundred photons) of a scintillation pulse into a corresponding **electrical signal**, without adding a large amount of random noise to the signal
  - Still the most widely used devices
- Two major components:
  1. **Photocathode**
     - Converting as many of the incident light photons as possible into low-energy electrons
  2. **Electron multiplier structure**
     - Efficient collection geometry + electron number amplification

1 pulse → 10^7 –10^{10} electrons

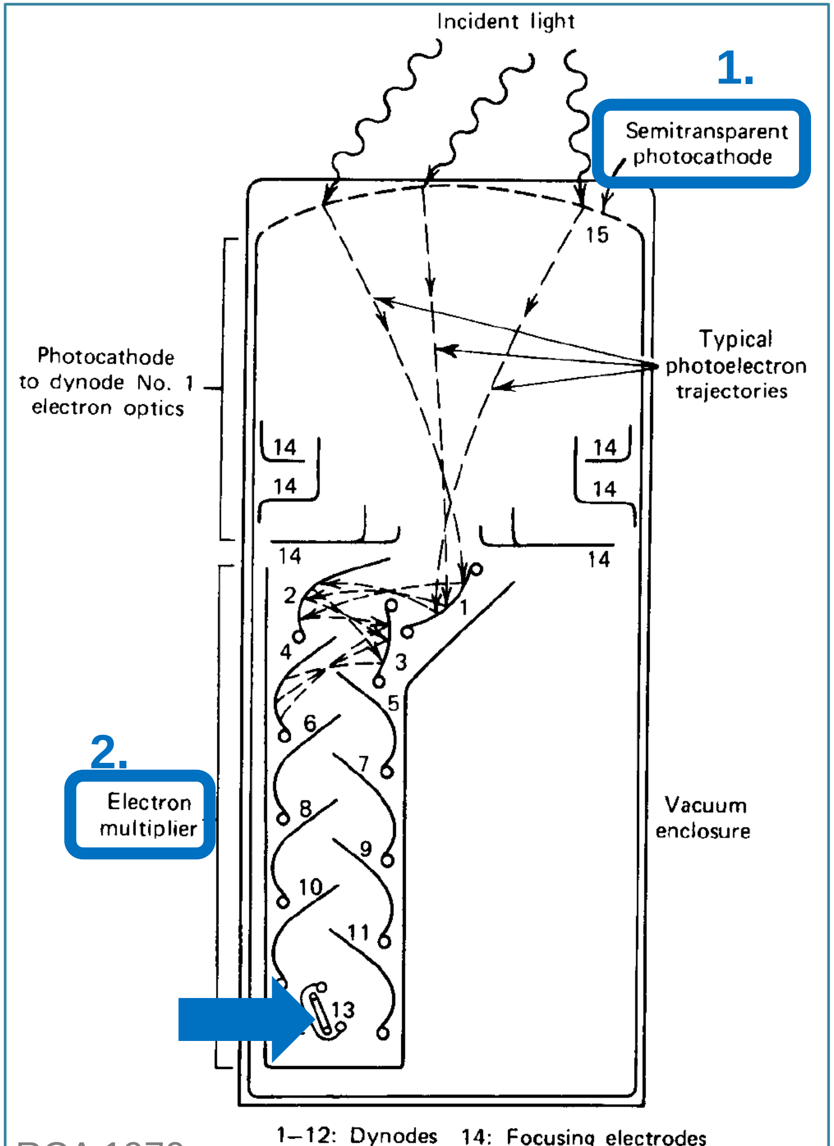

RCA 1970

Photomultiplier tubes (PMTs)

PHOTOEMISSION PROCESS – 3 steps!

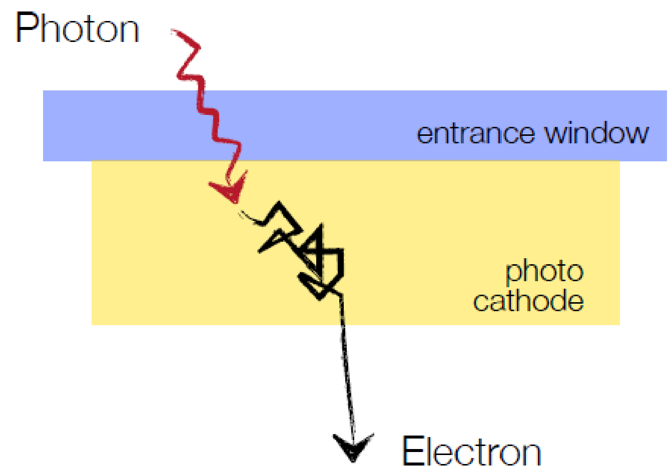

1. **Absorption** of the incident photon: gamm convertion through photoel. effect: electro generation within the photoemissive mate
   - Incident photon energy ~3 eV (blue light, from most scintillators)
2. **Migration** of that electron through the photocatode
   - Some energy will be lost
3. **Escape** of the electron from the surface of the photocathode into vacuum
   - Electron has to overcome the inherent potential barrier that exists at the interface between material and vacuum
     - This imposes a minimum energy on the incoming light photon

Photomultiplier tubes (PMTs)

Photocathodes (opaque or semitransparent layer)

- Great thickness uniformity over the entire area

- **Quantum efficiency**

$$Q = \frac{\textit{number of photoelectrons emitted}}{\textit{number of incident photons}}$$

  - Practical photocathodes show maximum **quantum efficiencies of 10-30%**
  - Stron function of energy of incident light

- Materials include multialkali ($Na_2K\,Sb$) or bialkali ($K_2Cs\,Sb$) compounds
  - thermionic emission in **bialkali** tends to be lower than in multialkali materials
    ➔ lower spontaneous noise rates

EMI
GENCOM
1999

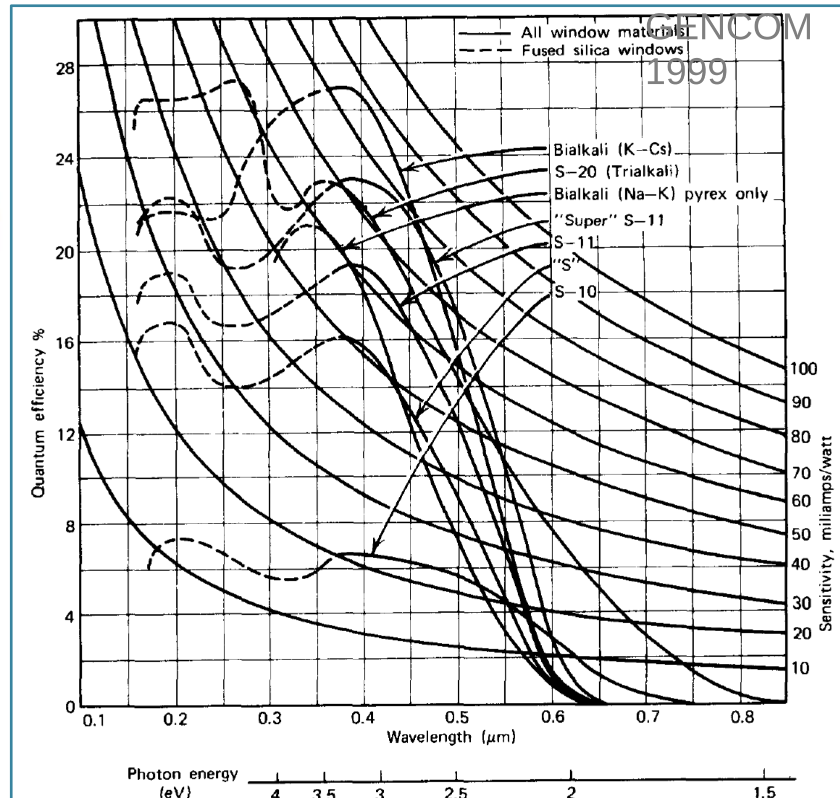

Photomultiplier tubes (PMTs)

- The multiplier portion of a PMT is based on the phenomenon of **secondary electron emission**
  - Electrons from the photocathode are accelerated and caused to

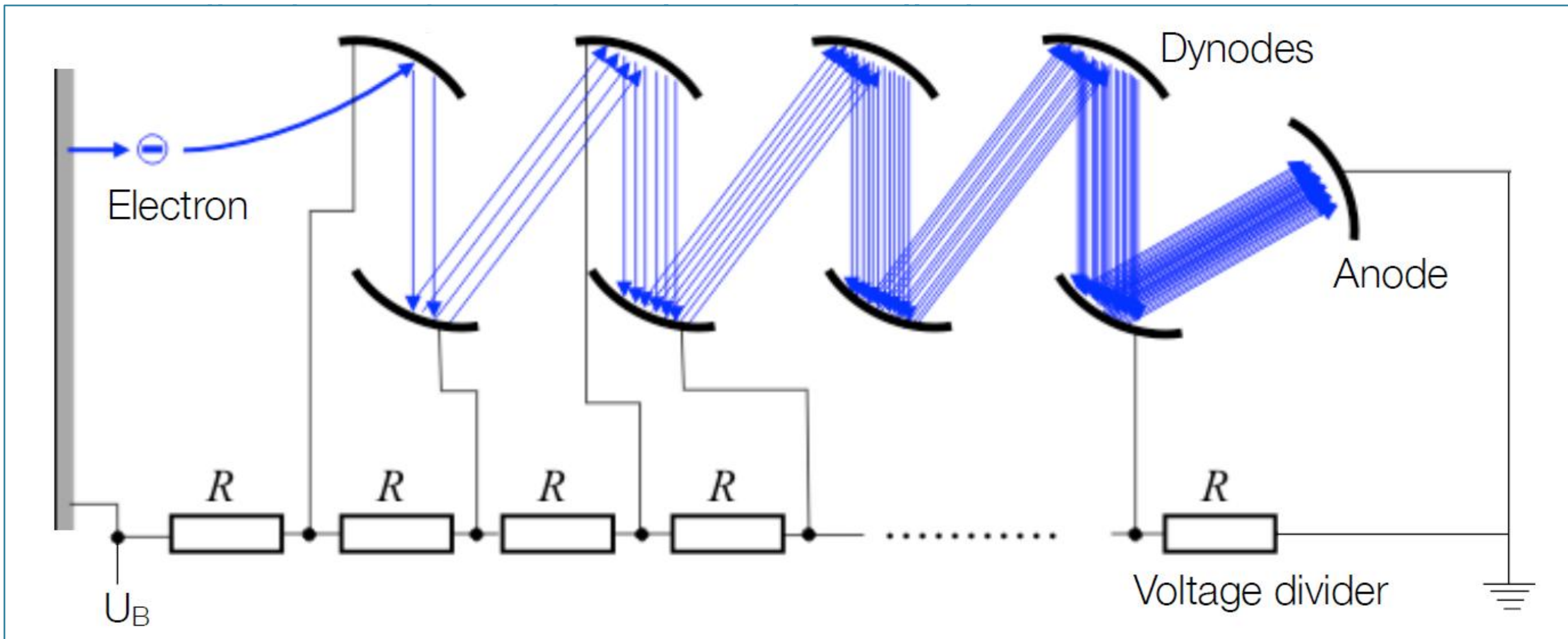

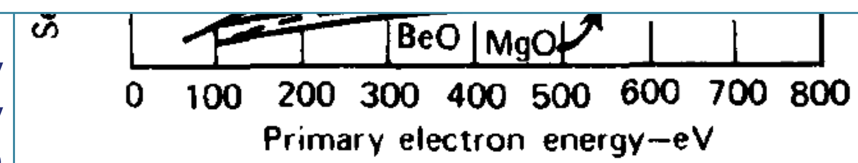

Variation of the secondary emission yield with primary electron energy for dynode materials

Photomultiplier tubes (PMTs)

MULTIPLE STAGES

- Created to achieve **electron gains on the order of $10^6 - 10^8$**
- If N stages are provided in the multiplier section: Overall gain given by

$$G = \alpha\,\delta^N$$

  - α = Fraction of all p.e. collected by the multiplier structure
  - δ = Number of electrons for each incident photoelectron
    - Conventional dynode materials: $\delta = 2 - 10$ and $N = 8 - 15$
    - GaP $\delta = 55$ and $N = 4$

Krall+1970

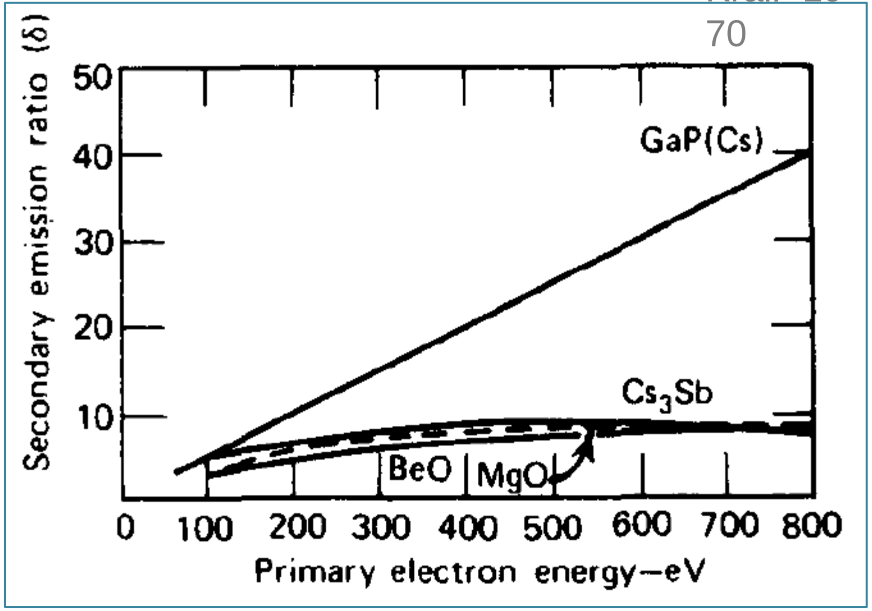

Variation of the secondary emission yield with primary electron energy for dynode materials

Photomultiplier tubes (PMTs)

Statistical broadening of the secondary electron yield from the first dynode

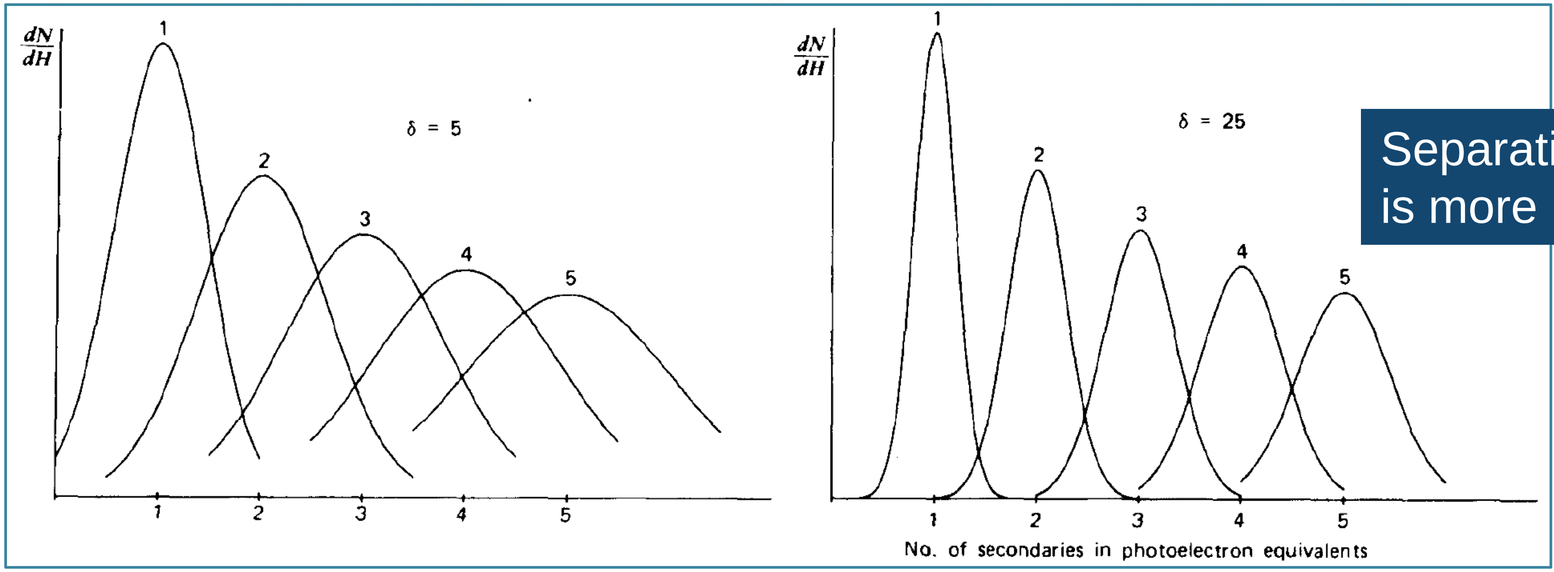

Separation is more

Knoll+1999

- Emission of secondary electrons is a **statistical process**
  - The specific **value of δ** at a given dynode **fluctuates from event to event** about its mean value
    - The shape of the single p.e. pulse height spectrum observed from a real PMT is an **indirect measure of the degree of fluctuation in δ**
      - The production of secondary electrons at a dynode can be assumed to follow a **Poisson distribution** about the average yield

Photomultiplier tubes (PMTs)

- **Time characteristics** determined exclusively by the electron trajectories
  - **Electron transit times**:
    - Time difference between the arrival of a photon at the photocathode and the collection of the subsequent electron burst at the anode
      → **Of the order of 20 – 80 ns**
  - **Spread in transit time:**
    - Can be minimized by **curving the photocatode** and by **using a large voltage difference** between phot

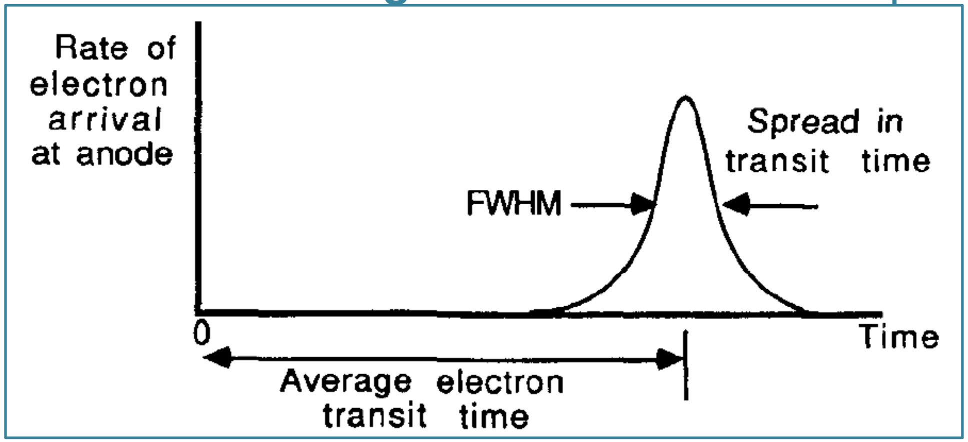

Knoll+1999

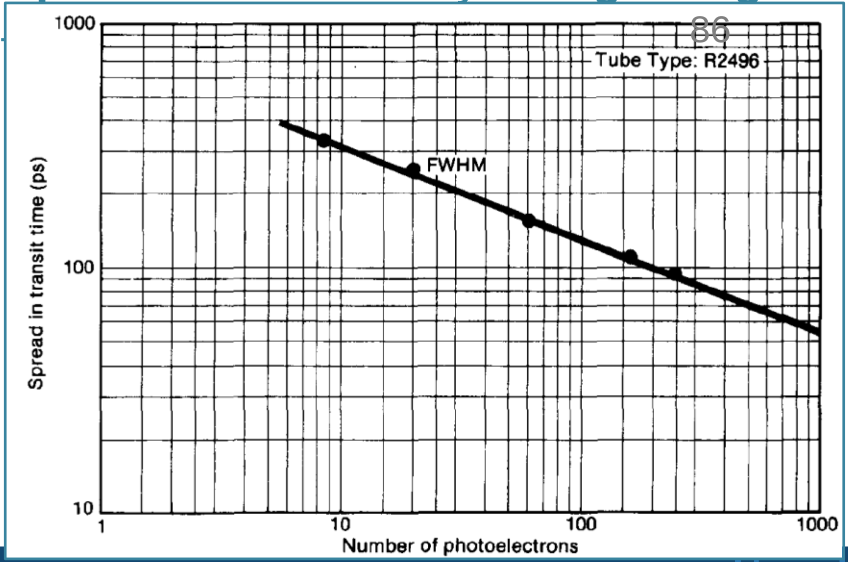

Kume+1986

Photomultiplier tubes (PMTs)

PHOTOMULTIPLIER TUBE SPECIFICAT

1. **OVERALL LUMINOUS SENSITIVITY**

- Ratio of the measured anode **current** at opera
light source of specified temperature incident o

2. **CATHODE LU**

- Same, but with

3. **OVERALL RA**

- Ratio of anode

4. **CATHODE RA**

- Same, but with

5. **DARK CURRE**

- Anode current

6. **ANODE PULS**

- Time taken for t
illuminated by a flash of light of very short dura

7. **ANODE PULSE WIDTH**

- Time width of the output pulse measured at ha
illumination of the photocathode

Dynode chain needs optimization of:

- PMT gain
- Anode isolation
- Linearity
- Transit time
- B-field dependence

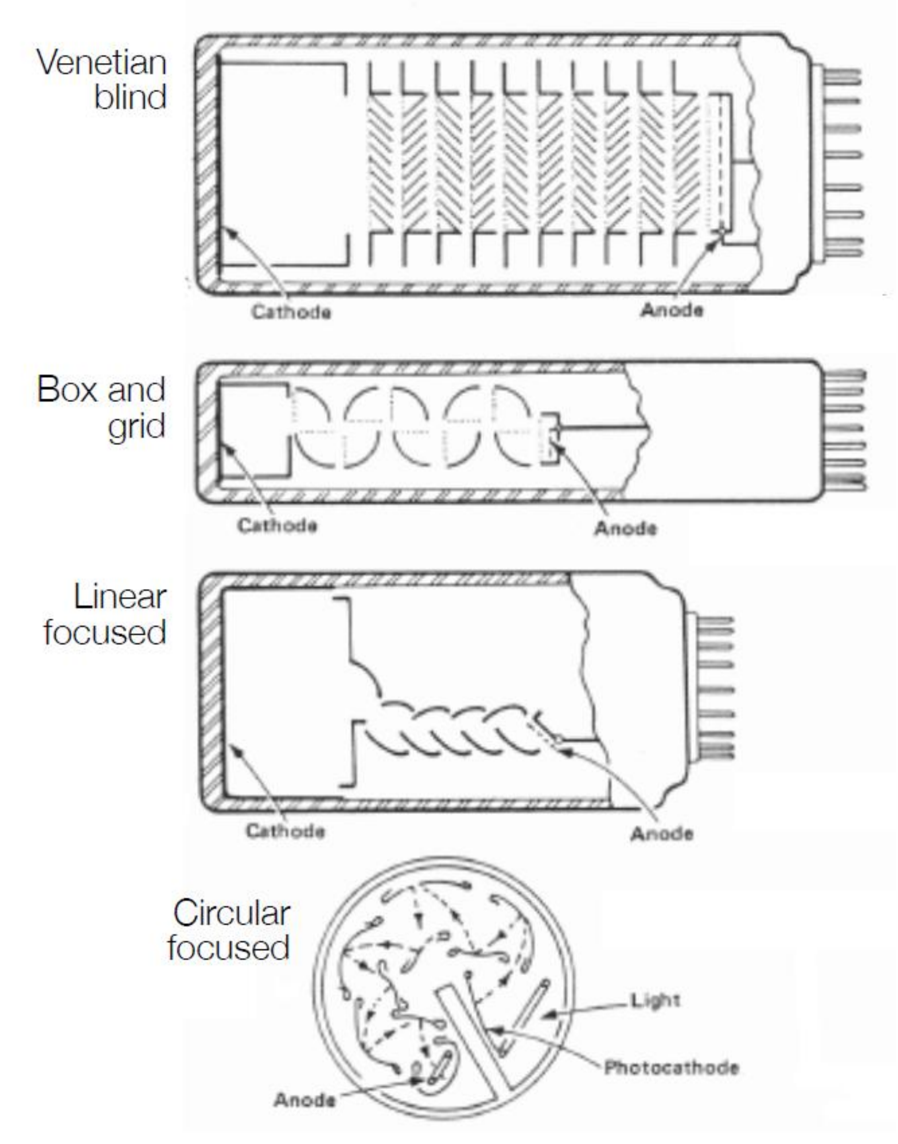

Photomultiplier tubes (PMTs)

A	B	C	D	E	F	G	H	I	J	K	L	M	N
Ham	1635	10	8	L8	BA	1250	1500	1.1	95	76	1	0.8	8.5
Ham	1450	19	15	L10	BA	1500	1800	1.7	115	88	3	1.8	19
Ham	380	38	34	L10	BA	1250	1750	1.1	95	88	3	2.7	37
Ham	1306	51	46	B8	BA	1000	1500	0.27	110	95	2	7.0	60
Ham	3318	51 sq	45	BM10	BA	1000	1500	0.27	110	95	2	4.8	45
Ham	3336	60 h	55	BM10	BA	1000	1500	0.27	110	95	2	6.0	47
Burle	4516	19	13	L10	BA	1500	1800	0.52	66	—	0.2	1.8	20
Burle	S83010E	38	32	C10	RbCsSb	1000	1000	2.4	100	92	1	2.8	32
Burle	S83054F	51	47	B8	BA	800	1200	0.10	10.5[a]	103	3	11	63
Burle	S83020F	60 h	56	L10	BA	1100	1700	0.10	71	100	1	10	69
Burle	S83079F	76 sq	—	B8	BA	800	1200	0.21	11.3[a]	100	3	14	73
Burle	S83006F	130	111	T10	BA	1100	1650	0.07	92	105	1	22	105
ADIT	B29B02H	29											
ADIT	B51B01	51											
ADIT	B76B01	76											
ADIT	B133D01	127											
ETL	9078	19											
ETL	9924	30											
ETL	9266	52											
ETL	9350	200											

C = diameter or dimension of tube outline (sq = square, h = hex) in mm.
D = minimum usable photocathode dimension.
E = dynode structure: L = linear focused, B = box and grid, BM = box and mesh, C = circular.
F = photocathode material: BA = bialkali.
G = recommended operating voltage.
H = maximum tube voltage.
I = gain × 10^6 at voltage in G.
J = cathode luminous sensitivity (μA/lm) measured with 2854 K tungsten source.
K = cathode radiant sensitivity (mA/W) measured at or near the wavelength of photocathode peak sensitivity.
L = dark current (an approximate number due to large variations in the method of measurement between different manufacturers) (nA).
M = anode rise time at voltage in G (ns).
N = transit time at voltage in G (ns).
[a]cathode luminous sensitivity is measured using a blue Corning C.S. No. 5-58 filter.

Photomultiplier tubes (PMTs)

NOISE AND SPURIOUS PULSES

- Most significant source are **thermionic electrons** spontaneously emitted by the photocathode
  - **Pulses correspond to a single p.e.**, so their amplitude is limited to the lowest end of the scale
  - The **rate** at which these pulses are observed is proportional to the area of the photocathode
  - → **Bialkali photocathodes most quiet**
  - Typical **spontaneous emission ra**
    at room T: **10^2 - 10^4 electrons/cm^2/**
    - → Effect reduced by **cooling** the P
- PMT should be stored in the dark
- Natural radioactivity from ^{40}K and Th in the glass envelope
- Afterpulses

«Dark spectrum» due to single electrons emitted spontaneously under dark conditions from the photocatode

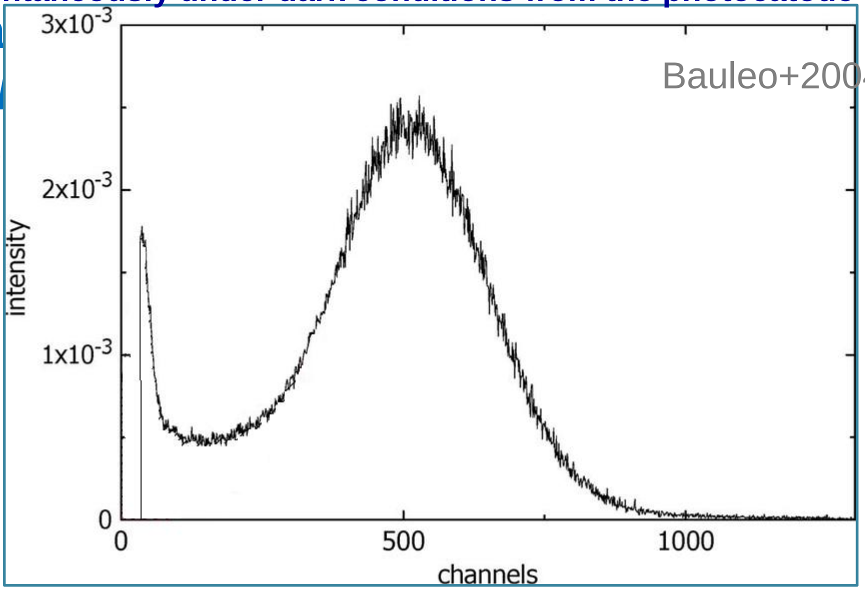

Photomultiplier tubes (PMTs)

HIGH-VOLTAGE SUPPLY AND VOLTAGE DIVIDER

- An **external voltage source** must be connected to the PM tubes in such a way that the photocathode and each succeeding multiplier stage are **correctly biased with respect to one another**
  - First dynode held at a voltage that is **positive** wrt photocathode
    - Each succeeding dynode held at a **positive voltage** wrt preceding one

- **For efficient photoelectron collection**:
  - **Voltage** between **photocathode and first dynode** is often several times as great as the dynode-to-dynode voltage differences
  - **Voltage differences** are provided by a **resistive voltage divider** and a **single source of high voltage**

Photomultiplier tubes (PMTs)

Wiring diagrams for the base of a PM tube

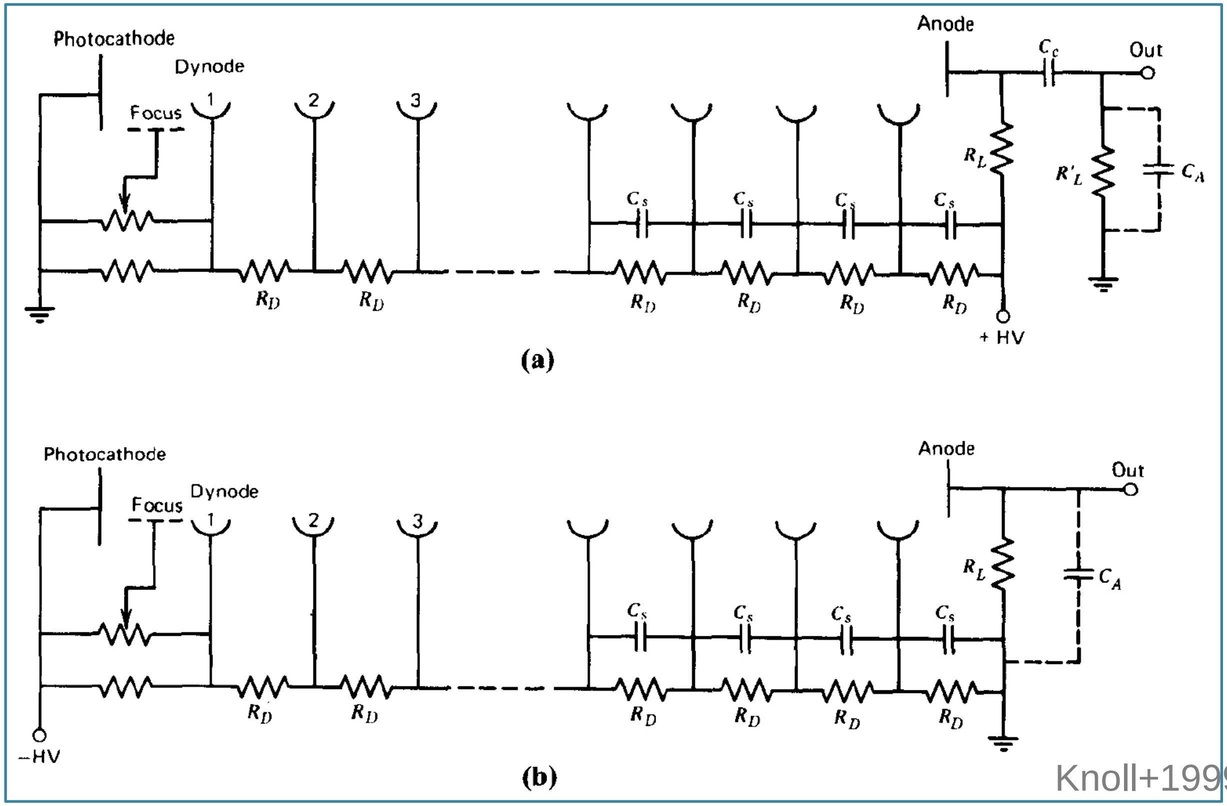

Knoll+1999

Numerical example
Event with 10^3 p.e.
PMT gain: 10^6
→N=10^9 e reach anode
Pulse rate R = 10^5/s
Pulse width w = 5 ns

Average anode current:
I_{avg} = N·e·R = 0.016 mA

Peak anode current
I_{peak}= N·e/w = 32 mA

- **(a) Positive HV and grounded photocatode**
  - The divider string supplies successively increasing positive voltages to each dynode down the multiplying string
- **(b) Negative HV and photocatode isolated** from the ground

Photomultiplier tubes (PMTs)

MAGNETIC SHIELDING

- Electron optics within a PMT are particularly sensitive to magnetic fields because of the **low average energy** (~100 eV) of the electrons traveling from stage to stage.
  Also the **Earth magnetic field** can have an appreciable effect on the electron trajectories!

➔ Magnetic shielding is mandatory to prevent gain shifts

  - Thin cylinder of **mu-metal** (nickel–iron soft ferromagnetic alloy with very high permeability) to fit closely around the glass envelope
  - Shield must be held at **photocatode potential** to avoid noise

Photodiodes

PHOTODIODES AS SUBSTITUTES FOR PMTs

- Advantages:
  - Higher quantum efficiency
  - Better energy resolution
  - Lower power consumption
  - More compact size
  - Insensitive to magnetic fields
  - Comparable time response
- 3 general designs
  - Conventional photodiodes (PIN
  - Avalanche photodiodes
  - Silicon Photomultipliers (SiPM)

® Hamamatsu

Semiconductor diode detectors

- Overcome the limitations by traditional scintillation materials
  - Poor energy resolution: chain of events that take place during conversion of the incident radiation to light and then to an electric signal has many inefficient steps!
    - Energy required to produce 1 p.e.: >100 eV
    - Number of carriers: few thousand
      - Statistical fluctuation greatly affect the energy resolution

➔ Need to increase the number of information carriers

- Electron-hole pairs
- Material: Silicon, Germanium, etc.
  - Semiconductors can have 10 times more carriers than gas chambers and 30 times more carriers than plastic scintillators!

Semiconductor diode detectors

BAND STRUCTURE IN SOLIDS

- Allowed energy bands in the **lattice of crystalline materials** where electrons are confined to:

1. **Valence band**: totally filled by electrons (outer-shell) in the absence of thermal excitation
2. **Conduction band**: hosting electrons when they are free to migrate through the crystal. Electrons in this band contribute to the **electrical conductivity** of the material

➔ **Band separation** by gaps or ranges of forbidden energies

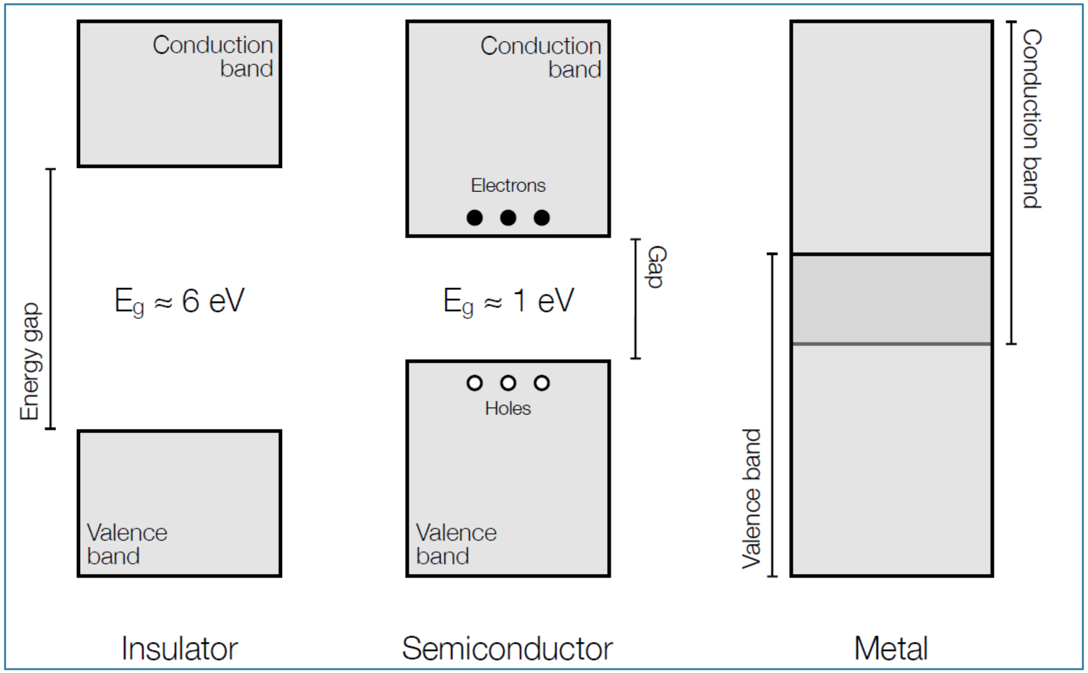

Semiconductor diode detectors

CHARGE CARRIERS

- Electron-hole pair
  1. Valence electron which gained sufficient thermal energy to be elevated across the bandgap into the conduction band
  2. Vacancy called a "hole" in the otherwise full valence band
- By applying an electric field:
  - Electron and hole move in opposite directions

→**Probability per unit time** that an electron-hole pair is **thermally generated**

$$p(T) = C\,T^{3/2} \exp\left(-\frac{E_g}{2kT}\right)$$

- T = absolute temperature
- E_g = bandgap energy
- k = Boltzmann constant
- C = proportionality constant characteristic of the material

Semiconductor diode detectors

MIGRATION OF CHARGE CARRIERS IN AN ELECTRIC FIELD

- Motion of electrons and holes = combination of a random thermal velocity and a net drift velocity parallel to the direction of the applied field
  - **Drift velocities: ~10^7 cm/s**, typical detector dimensions: <0.1 cm → time to collect carriers **<10 ns**
    - Semiconductor detectors among the **fastest-responding** of all radiation detector types
    - Diffusion effects introduce some n

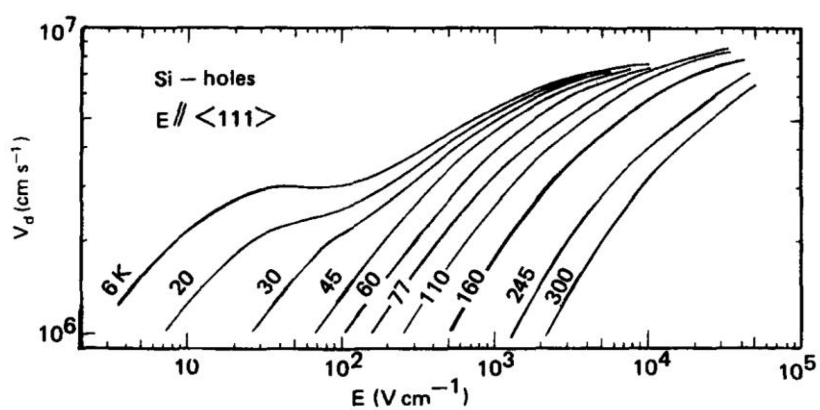

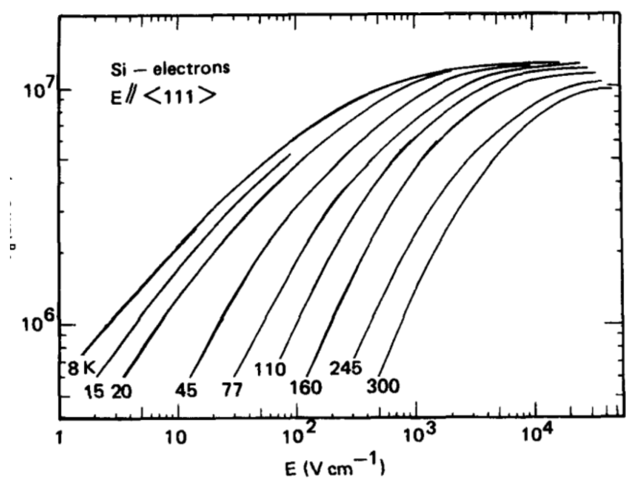

Semiconductor diode detectors

Completely pure or «intrinsic» (i) semiconductor

- Electron density n in the conduction band = Holes density p in the valence band: $n_i = p_i$

n-type semiconductor

- Impurity or dopant with **1 valence e⁻ more** wrt Si.
  Occupies **top** of forbidden gap
- Probability of thermal excitation is high:
  all donor impurities are ionized

$$n \cong N_D \gg n_i$$

- Added concentration of e⁻ in conduction band

➔ e⁻ = majority carriers

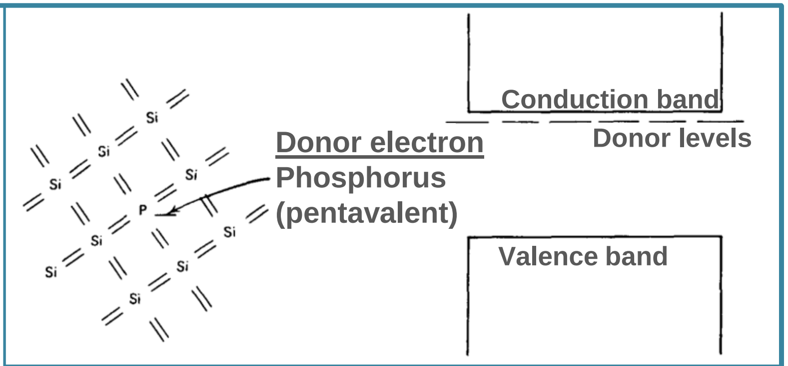

n^+ and p^+ heavily doped materials

p-type semiconductor

- Impurity or acceptor with **1 valence e⁻ less** (vacancy) wrt Si
  Occupies **bottom** of forbidden gap
- Thermally excited e⁻ from valence band fill holes

$$p \cong N_A \gg p_i$$

- Increased availabiliy of holes

➔ Holes = majority carriers

Knoll 1999

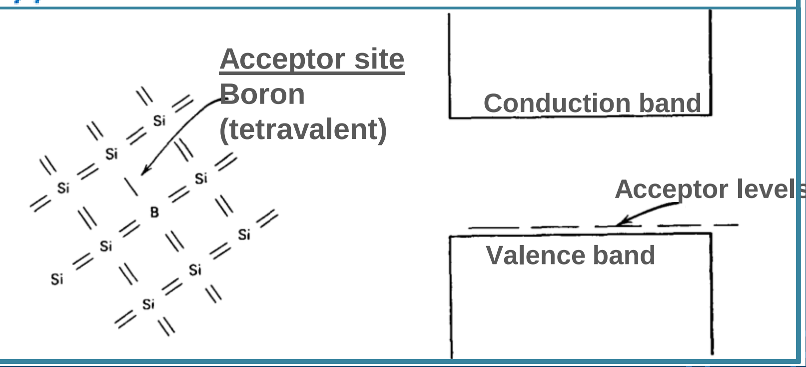

Semiconductor diode detectors

Relationship between electron and hole concentrations in a semiconductor

Lines connecting points on the two logarithmic scales always pass through the center of the diagram (pivot point) for any type or degree of doping

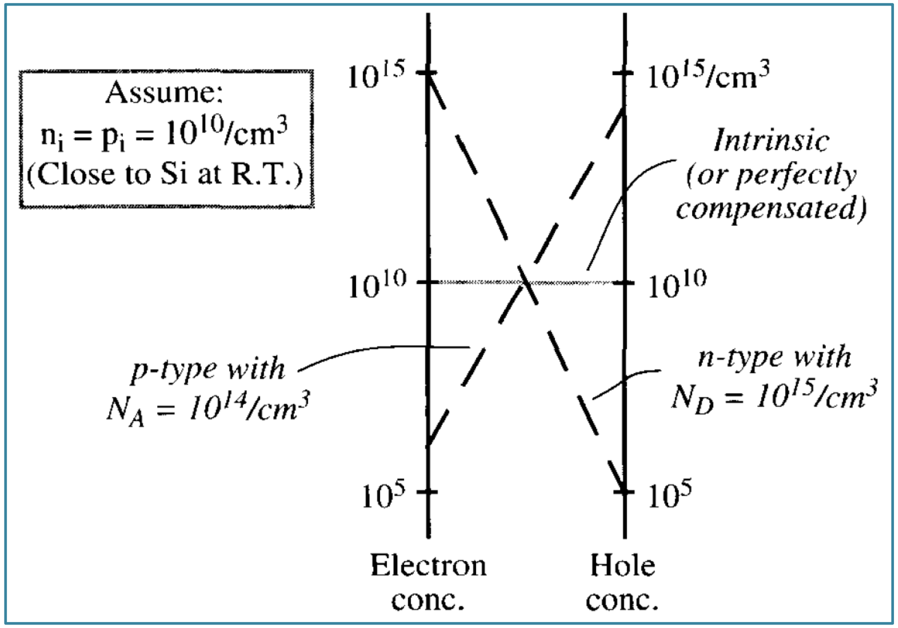

Knoll 1999

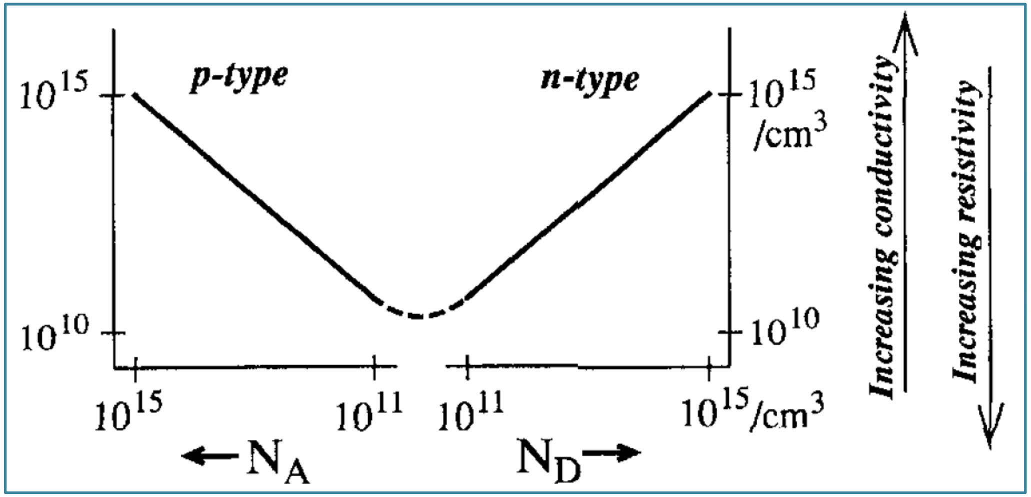

Semiconductor conductivity

as a function of the net concentration of acceptors (N_A) or donors (N_D)

Semiconductor diode detectors

1.ACTION OF IONIZING RADIATION IN SEMICONDUCTORS

- Charged particle passing through the semiconductor: production of many electron-hole pairs along the particle track
- Ionization energy ϵ
  - Average energy expended by the primary charged particle to produce **one electron-hole pair**
  - Independent of the energy of the incident radiation

    ➔ **# of produced pairs** reflects the **incident energy** of the radiation, provided the particle is **fully stopped** within the active volume
  - Value of ϵ in semiconductors is very small: 3 – 4 V
    - # of carriers can be 10 times higher than in scintillators
- Fano factor (adjustment to relate to the Poisson predicted variance)

$$F = \frac{observed\ statistical\ variance}{E\ /\ \epsilon}$$

$F \ll 1$

The semiconductor junction

- Carrier migration between n and p-type semiconductor materials
  - Junction formed within the same crystal by changing the doping conditions from one side to the other

Unbiased junction: very low performance

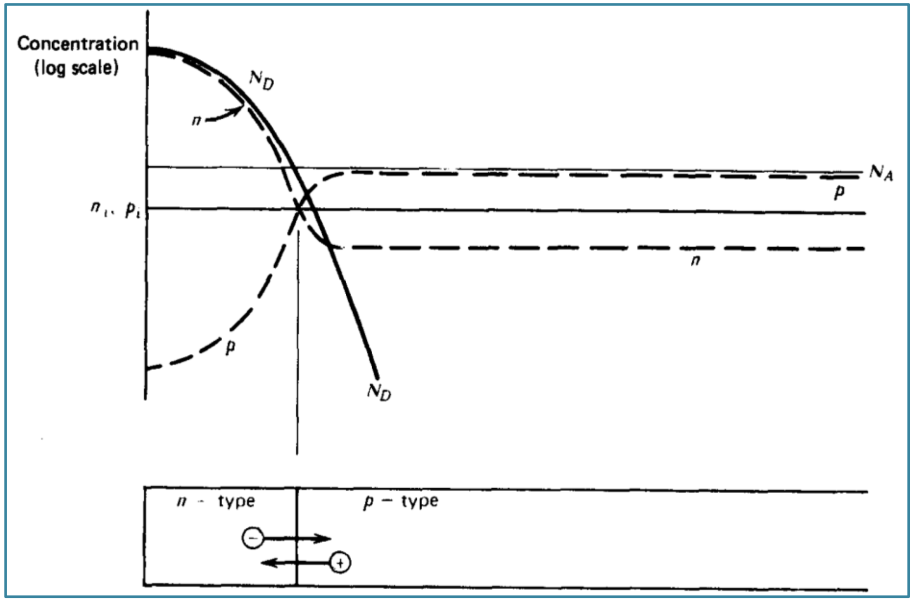

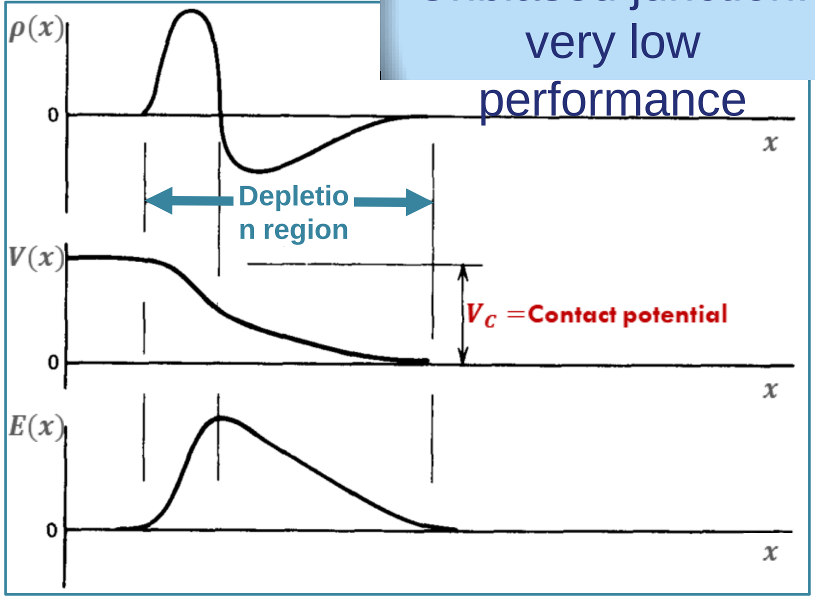

Knoll 1999

- Effect of diffusion:
  - negative space charge ($\rho(x)$) on the p side, positive space charge on the n side
  - → **electric field creation** ($E(x)$), preventing further diffusion
- **Depletion region:** Region in which charge imbalance exists. Extension not symmetric due to differences in initial concentrations

The semiconductor junction

- **Forward bias**
  Attraction of electrons+holes
  (majority carriers)
  → Conductivity grealty enhanced

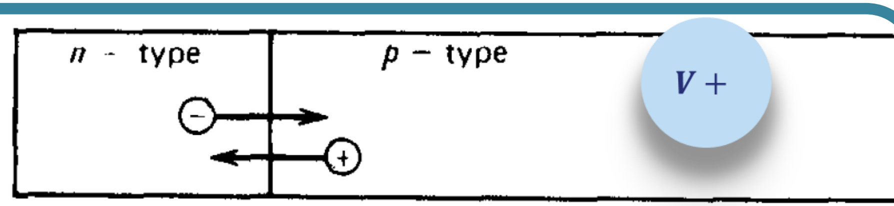

- **Reverse bias**
  Natural ΔV is enhanced, atraction of
  minority carriers → low concentration
  → low «reverse» current, depletion region increased

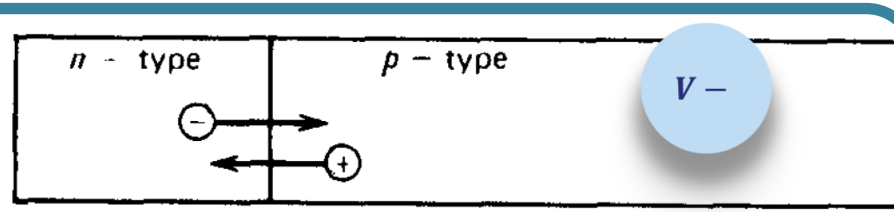

p-n junction

Rectifying element, allowing free current flow in one direction, and large resistance to flow in other direction → Very large bias: sudden breakdown: reverse current increases, destructive effect

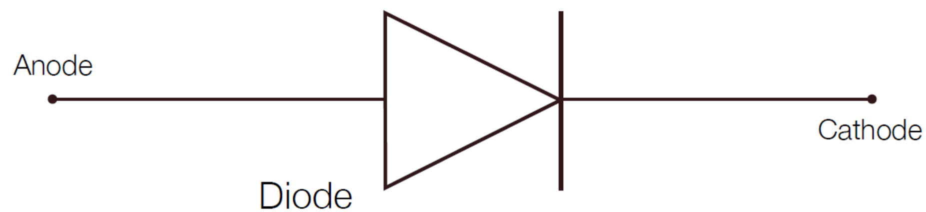

The semiconductor junction

a) The variation of electric potential $V(x)$ across an n-p junction.

b) The resulting variation in electron energy bands across the junction. The curvature is reversed because an increase in electron energy corresponds to a decrease in conventional electric potential $V(x)$ defined for a positive charge.

c) The added displacement of the bands caused by application of a reverse bias V across the junction.

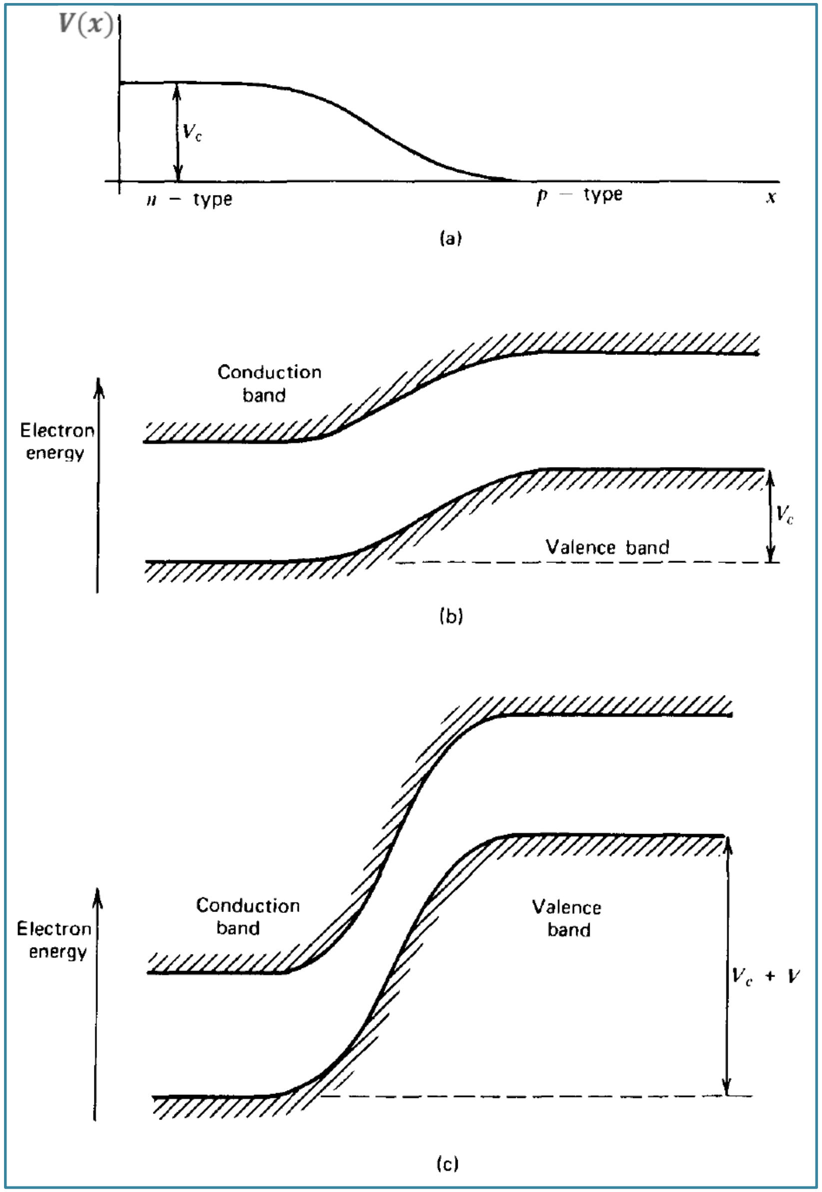

The semiconductor junction

Forward bias

- Majority carriers cross the depletion region. There is a current of e- in the p region and a current of holes in the n region
  - Large current flow

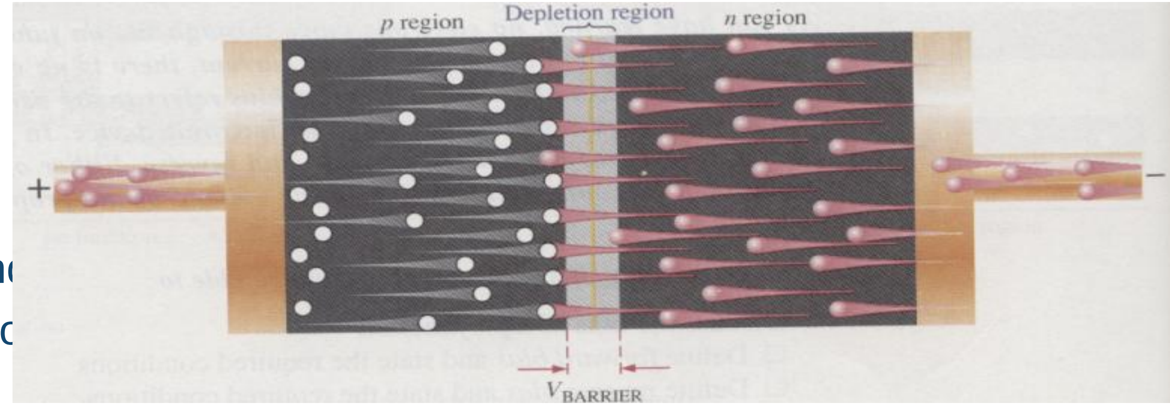

Reverse bias

- Majority carriers are kept away from the barrier
- Minority carriers are attracted across the junction
  - Small current flow!

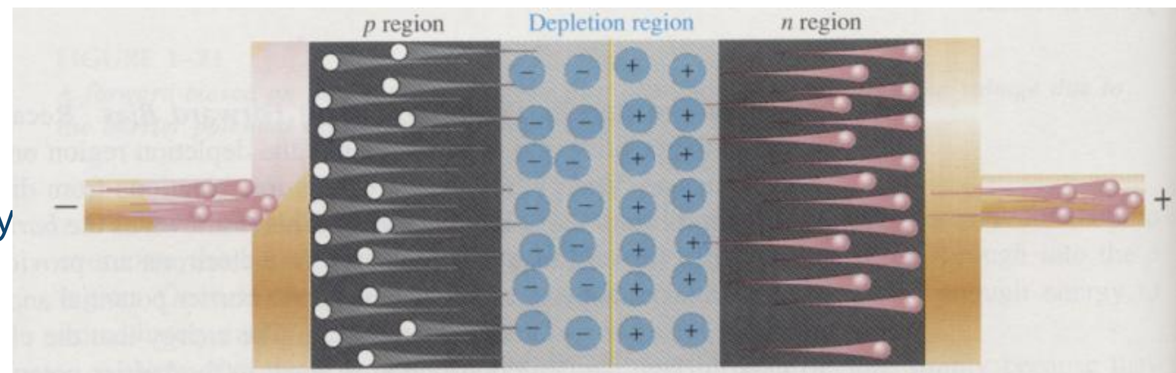

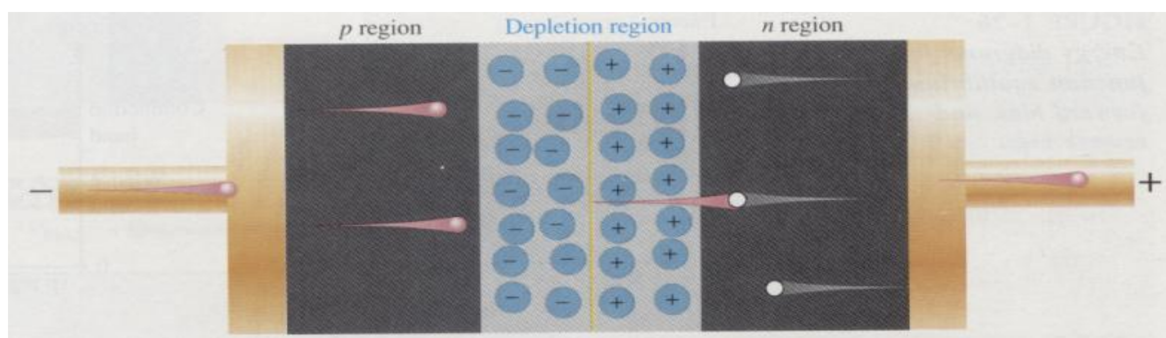

The semiconductor junction

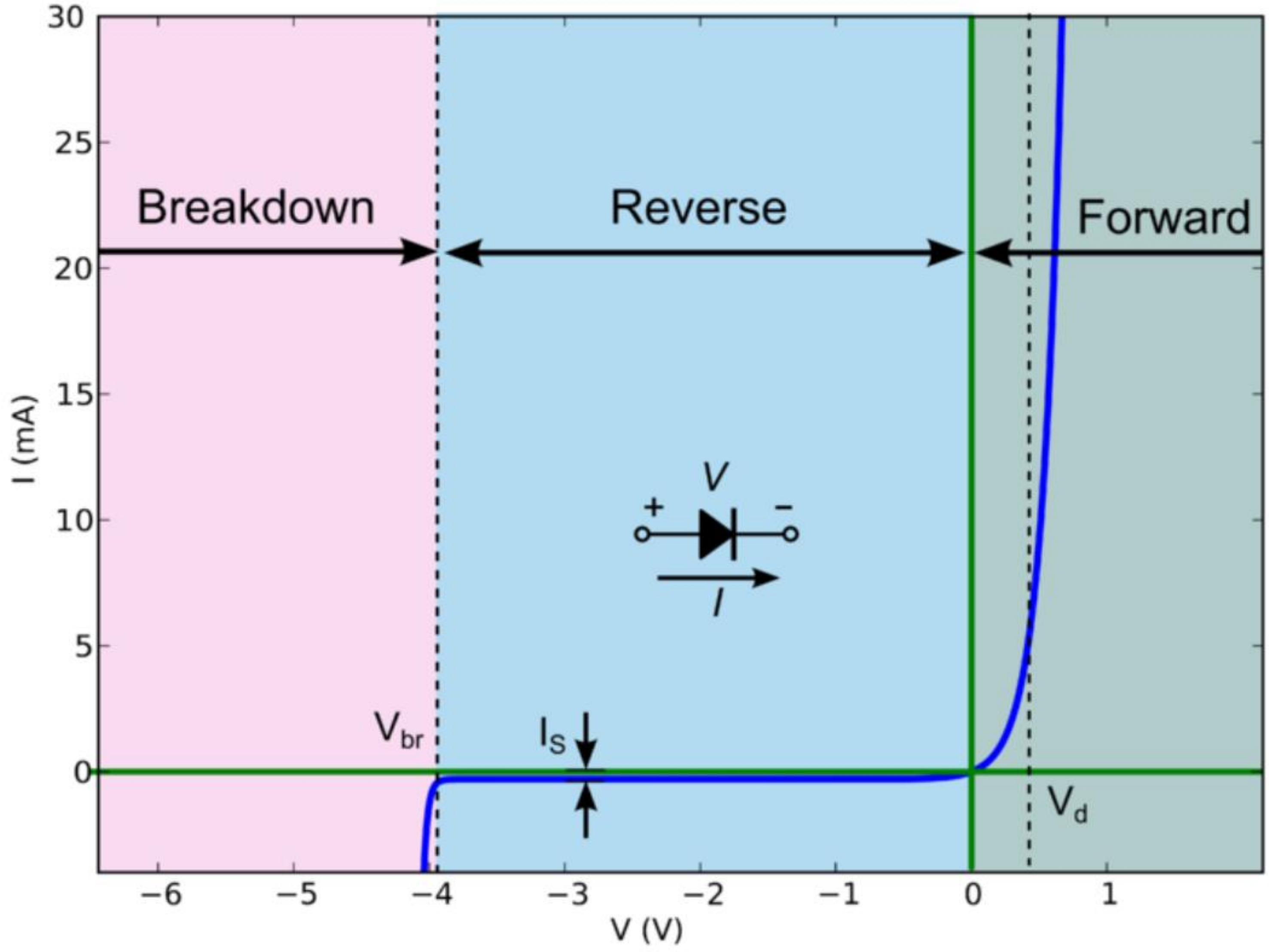

The semiconductor junction

- **Reverse bias condition**

  Thickness of the depletion region: $d \cong \left(\frac{2\epsilon V}{eN}\right)^{0.5} \cong (2\epsilon V \mu \rho_d)^{0.5}$

  - Here $V = V_C + V_B$ where V_0: contact potential; V_B: bias voltage

- In order to have the **largest possible region** d: **resistivity** of doped semiconductor ρ_d should be **high** (μ: mobility of major carriers)
  - If $\rho_d = 2 \cdot 10^4\ W/cm$ and $V_B = 300\ V$ then $d = 1\ mm$.

- Region exhibits properties of a charged capacitor with $C = \frac{\epsilon A}{d} \cong \sqrt{\frac{\epsilon A^2}{2\mu\rho_d V}}$
  - If C is kept small → good energy resolution achieved

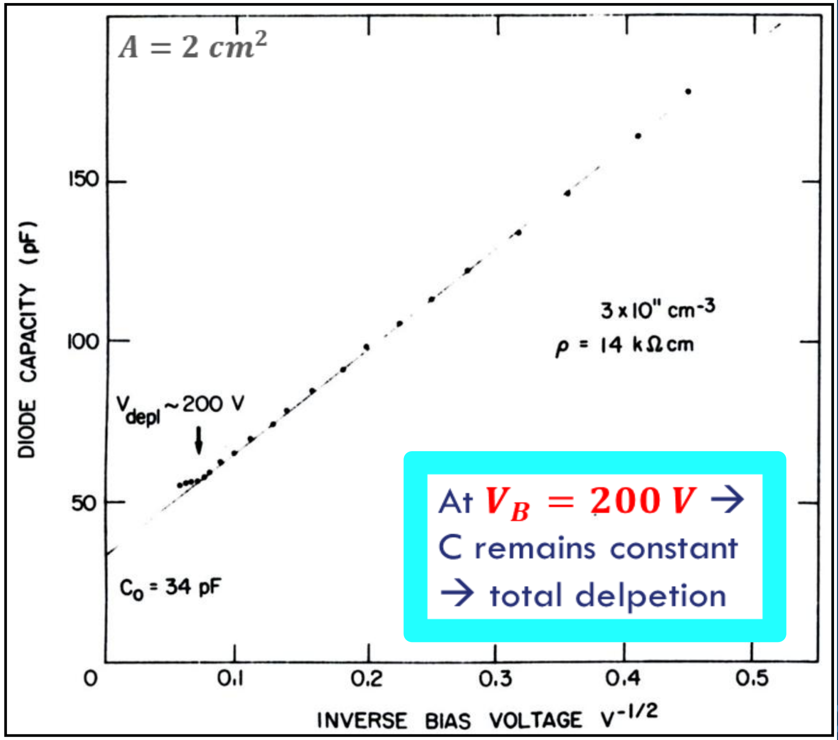

At $V_B = 200\ V$ → C remains constant → total delpetion

Semiconductor detector configurations

1. DIFFUSED JUNCTION DETECTORS

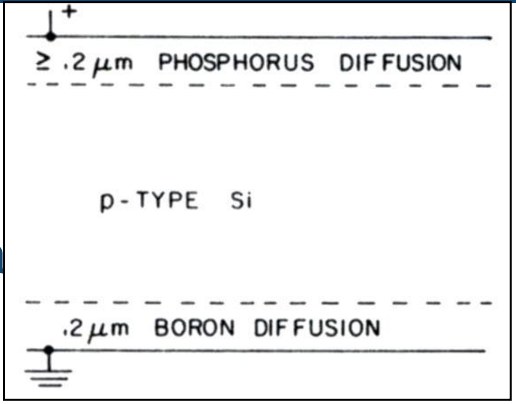

- Earliest fabrication method
- Starts with a homogeneous crystal of p-type material with one surface treated by exposing it to a vapor of n-type impurity (typically phosphorus) at T=1000ºC
  - Junction formed **some distance from the surface** at the point at which the n- and p-type impurities reverse their relative concentration
    - Typical depths of the diffused n-type layer range from 0.1 to 2.0 μm.
    - Depletion region extends primarily into the p side of the junction
  - Much of the surface layer remains outside the depletion region and represents a **dead layer** or **window** through which the incident radiation must pass before reaching the depletion region

    ➔Real **disadvantage**: portion of particle energy lost before the

Semiconductor detector configurations

2. SURFACE BARRIER DETECTORS

- Starts with **n-type crystal** followed by **evaporation of a thin gold layer** for electrical contact, under conditions that promote slight oxidation of the surface; the resulting **oxide layer** between the gold and silicon plays an important role in the resulting properties of the surface barrier.
  - Surface barriers can also be produced by starting with a p-type crystal and evaporating aluminum to form an equivalent n-type contact.
  - Potential **disadvantage**: high sensitivity to light
    - Very high noise level produced by normal room lighting
    - Thin entrance window also make the detector sensitive to damage from exposure to vapors, and the front surface must never be directly handled

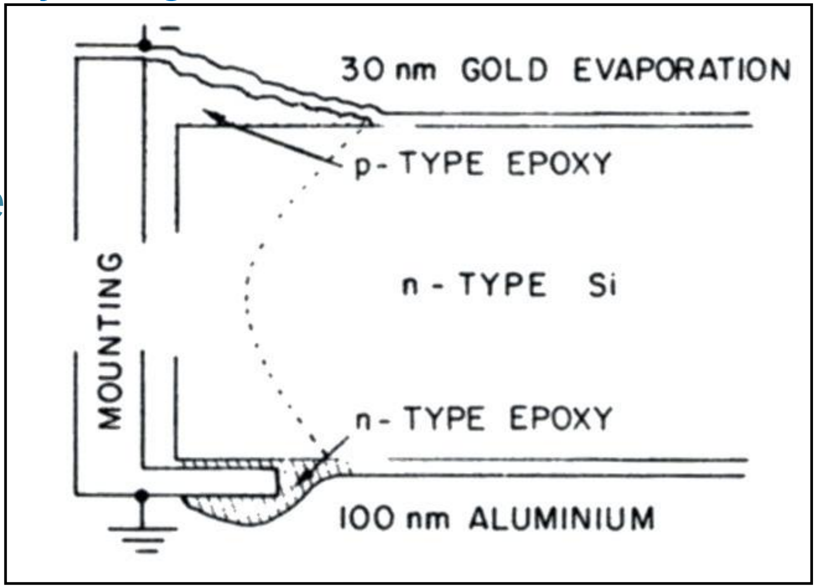

Semiconductor detector configurations

3. ION IMPLANTED LAYERS

- Implantation: Exposure of semiconductor surface to a beam of ions (15 keV) produced by an accelerator at T=600ºC
  - Acceleration of Phosphorus or Boron ions, concentration of added impurity closely controlled
  - Structure of the crystal less disturbed
- Ion-implanted detectors more stable and less subject to ambient conditions

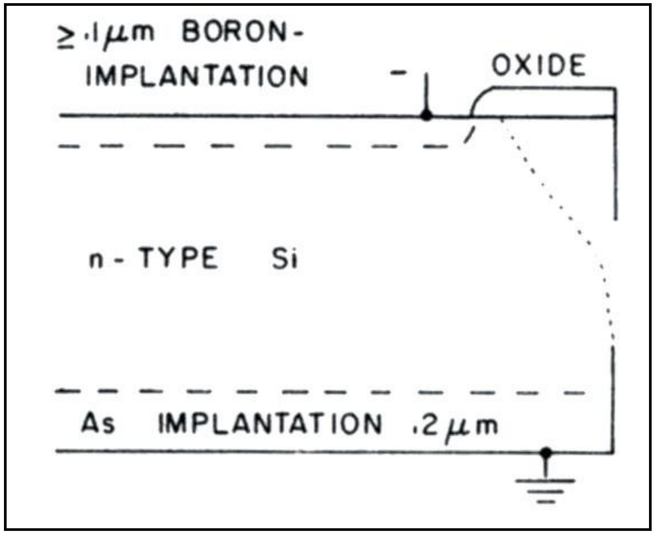

Semiconductor detector configurations

4. FULLY DEPLETED DETECTORS

- Preferred type in most applications
  - Heavily doped **p+ surface layer**
  - High-purity n-type silicon wafer of thickness T
- Raising the reverse bias voltage V
  - *i.* $V < V_d$ and $d < T$: partial depletion
    → Dead layer with $E = 0$, no charge carrier collection
    - Sensitivity only on the front surface
  - *ii.* $V = V_d$ and $d = \tau$: full depletion
    → $E \neq 0$ in the whole wafer
  - *iii.* $V > V_d$: over-depletion
    → E increases and becomes more nearly uniform in the wafer
- Wafer of perfectly compensated material
  Uniform E, "p-i-n configuration"

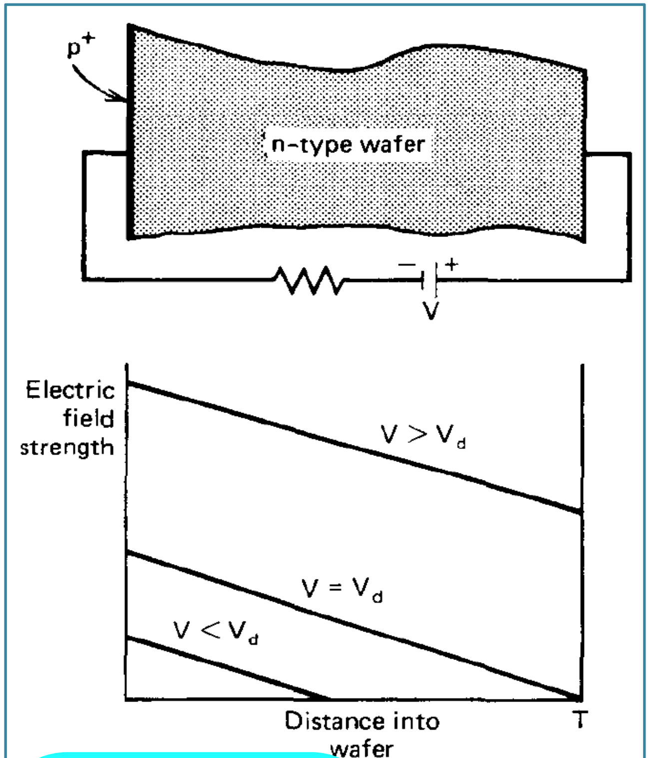

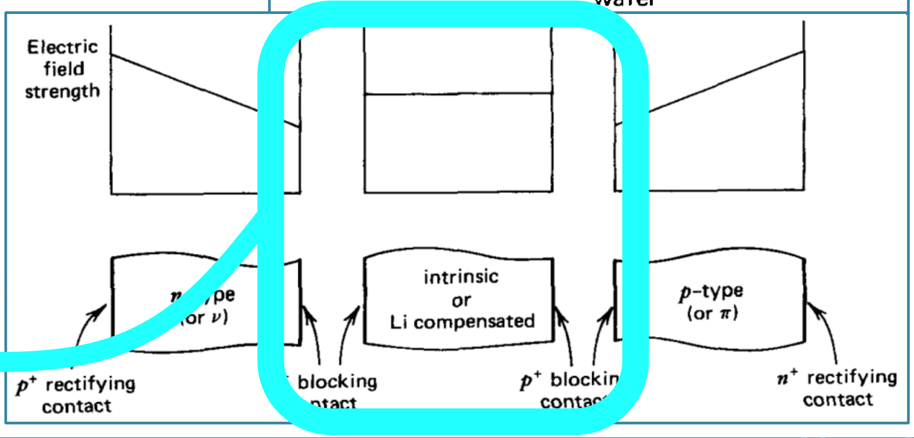

5. PASSIVATED PLANAR DETECTORS

- Combination of techniques to achieve excel operational characteristics

1. High purity Silicon
2. Oxide layer produced at high T
3. Photolitography removes areas where to place the detector entrance windows
4. Thin layers formed by implantation
    1. Entrance windows: p-type
    2. Rear side: n-type
5. Annealing at high T for reducing radiation damage

6./7. Vaporization of Al to provide thin electrica contacts. Separation and encapsulation

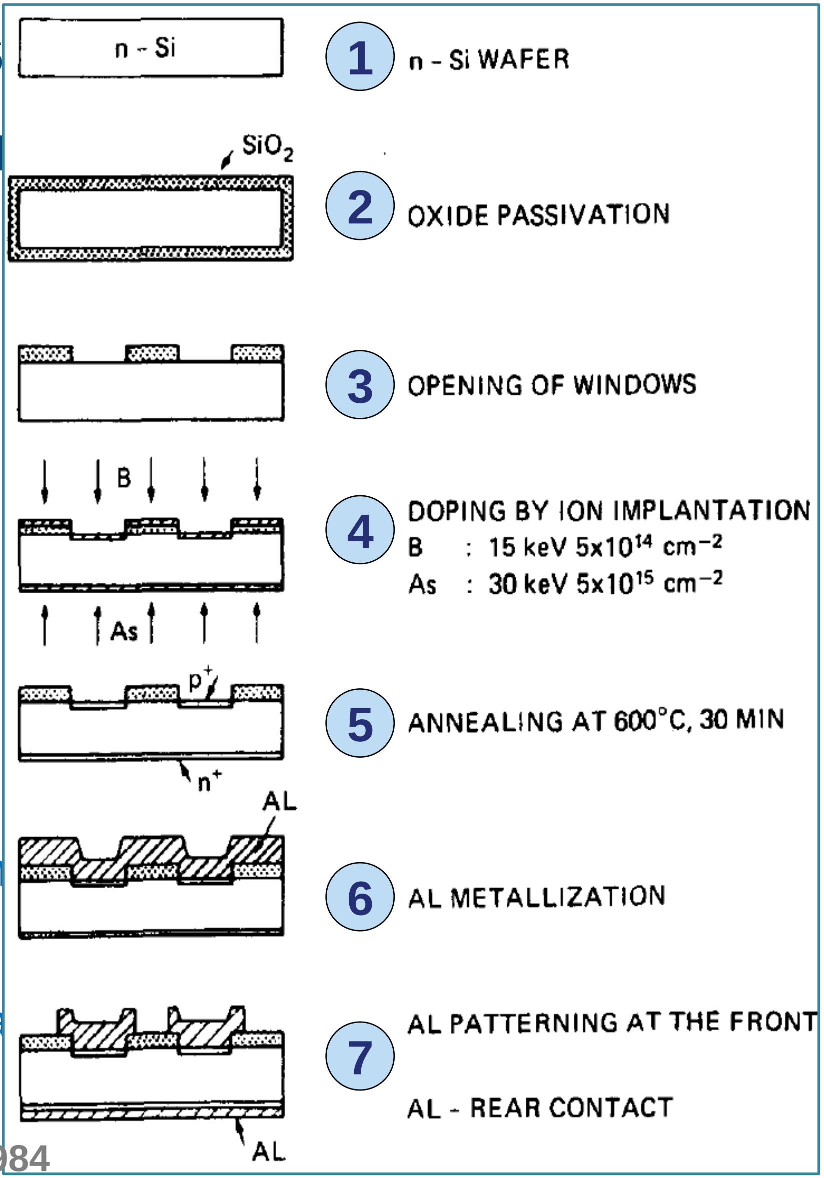

Kemmer+1984

Semiconductor detector configurations

TYPE	STRUCTURE	CHARACTERISTICS	PHOTODIODES
Planar diffusion type	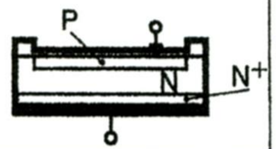	Low dark current	Silicon photodiodes (S2386, S2387 series, S1087, S1133 series etc.) GaAsP, Gap photodiodes
Low Cj planar diffusion type	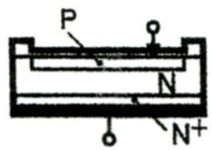	Low dark current Low capacitance High UV sensitivity High IR sensitivity	Silicon photodiodes (S1336 series, S1337 series)
PNN$^+$type	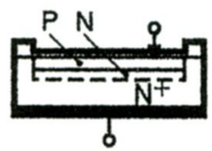	Low dark current High UV sensitivity Suppressed IR sensitivity	Silicon photodiodes (S1226 series, S1227 series)
PIN type	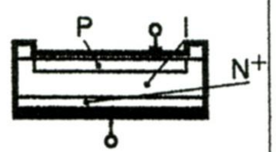	High-speed response	PIN silicon photodiodes
Schottky type	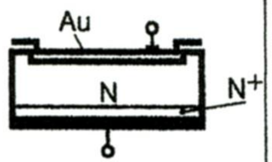	High UV sensitivity	GaAsP, GaP photodiodes
Avalanche type (Reach-through type)	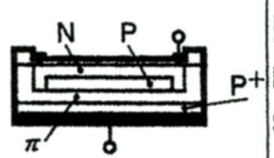	Internal multiplying mechanism, High-speed response	Silicon avalanche photodiodes

Semiconductor detector configurations

MICROSTRIP DETECTOR

- Divided into elements of 20 μm –100 μm with a separated readout. Used for counting particles with high rate and density
- Silicon mictrostrip detectors or pixel detectors are the most performing tracking and imaging detectors in accelerator and space physics

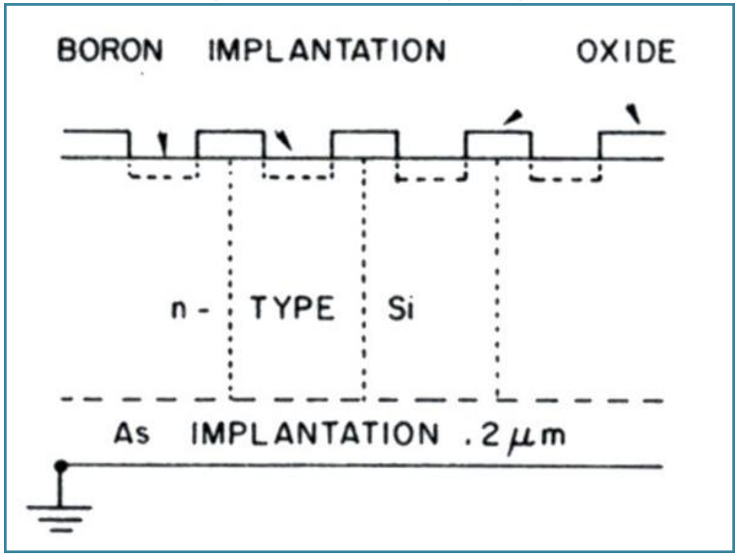

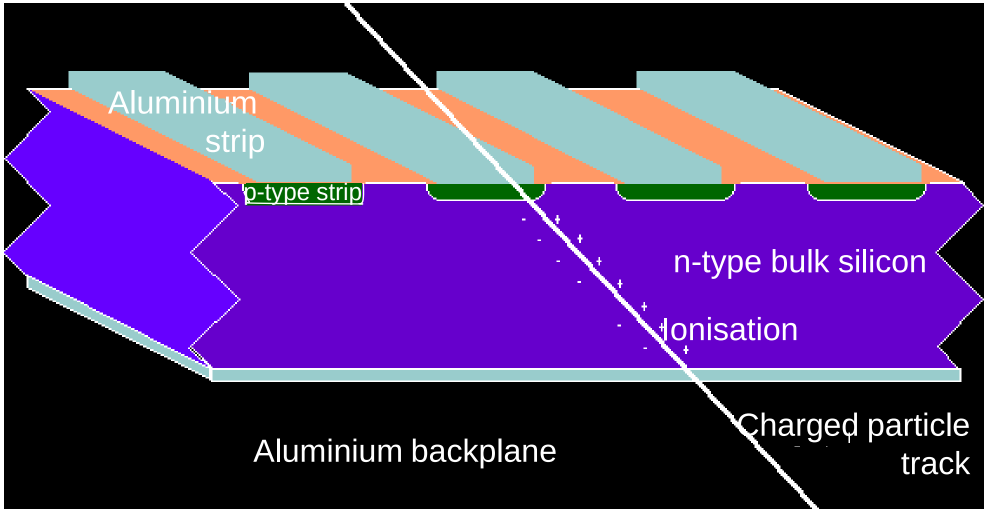

Semiconductor diode operational characteristics

LEAKAGE CURRENT

- **Small current of ~μA** arising internally within the volume of the detector
  - Minority carriers current (negligible)
  - **Thermal generation of electron-hole pairs** within the depletion region
    - Increases with the volume, can be reduce by **cooling**
    - Silicon: room T, Germanium: very low T
  - **Monitoring** of the leakage current in order to mantain a steady value
    - Indicator of possible radiation damage

Semiconductor diode operational characteristics

DETECTOR NOISE AND ENERGY RESOLUTION

- “Parallel” noise
  - Fluctuations in the bulk generated leakage current
  - Fluctuations in the surface leakage current
- “Series” noise
  - Noise associated with series resistance or poor electrical contacts to the detector
- Relative importance of these sources will depend
  - Magnitude of the leakage currents
  - Capacitance of the detector
  - Whether the diode is partially or fully depleted

➔ This noise width combines in quadrature with other sources of peak broadening

- Contributions of charge carrier statistics and fluctuations in particle energy loss in dead layers

Semiconductor diode operational characteristics

PULSE RISE TIME

- Semiconductor diode detectors: among the fastest of all (<10 ns)
  - Contribution of the detector: charge transit time + plasma time

CHARGE TRANSIT TIME

- Migration of electron and holes formed by incident radiation in a certain point across the delpetion region
- Minimized by
  - High E field
  - Small depletion widths (bias voltage increased)

PLASMA TIME

- Observed in case of heavy charged particle radiation
- Electron-hole pairs are too dense: plasma-like cloud shielding from the influence of E
- Gradual cloud "erosion" or disperse until normal charge collection proceeds

α part: 1-3 ns
heavy ions: 2-5 ns

Applications of Silicon diode detectors

1. General **charged particle** spectroscopy
2. **Alpha particle** spectroscopy
3. **Heavy ion** and **fission fragment** spectroscpy
4. Energy loss measurement – **particle identification**
5. **X-ray spectroscopy** with p-i-n diodes
6. **Photovoltaic** mode operation
7. Silicon diodes as **personnel monitors**

Applications of Silicon diode detectors

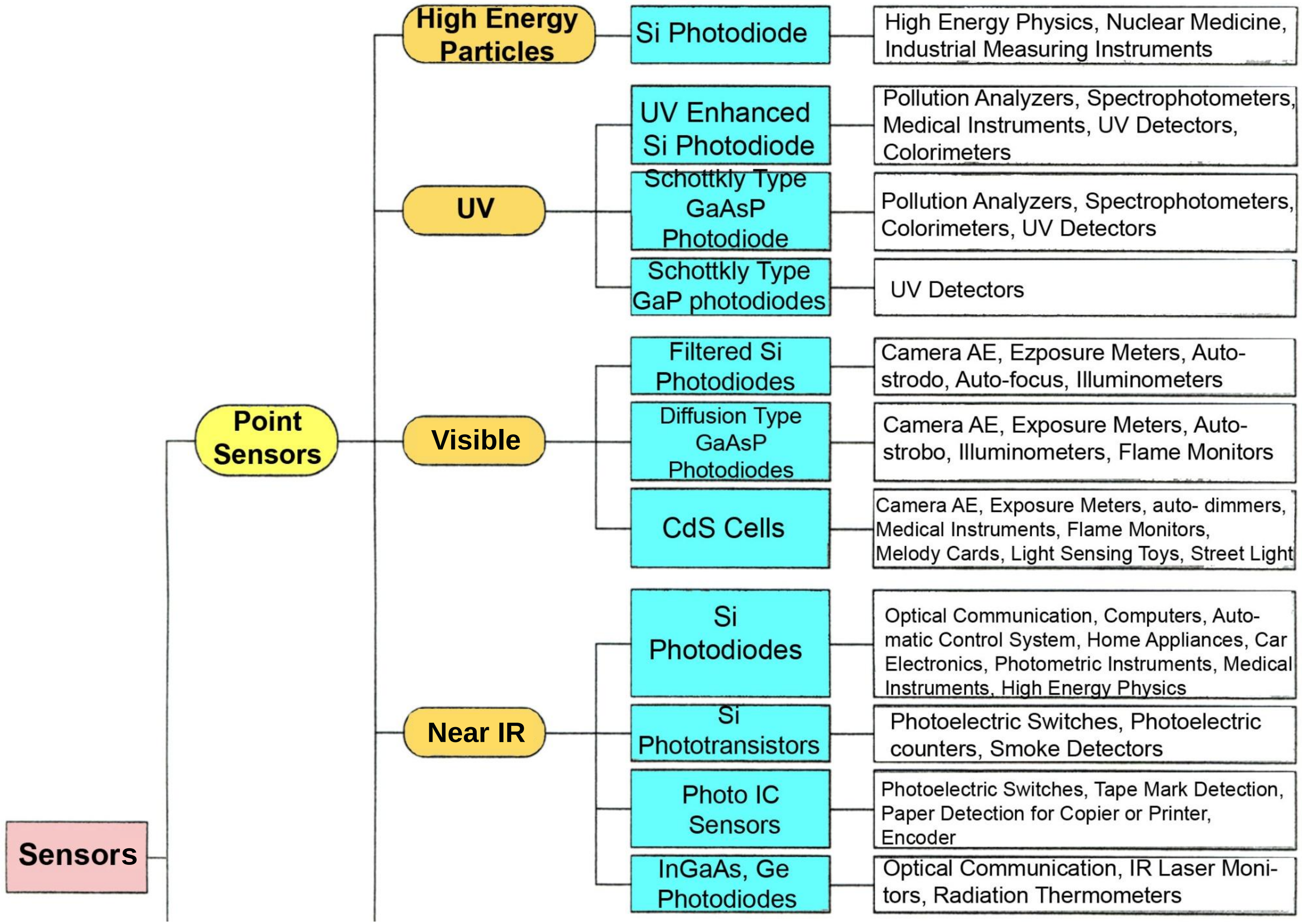

Applications of Silicon diode detectors

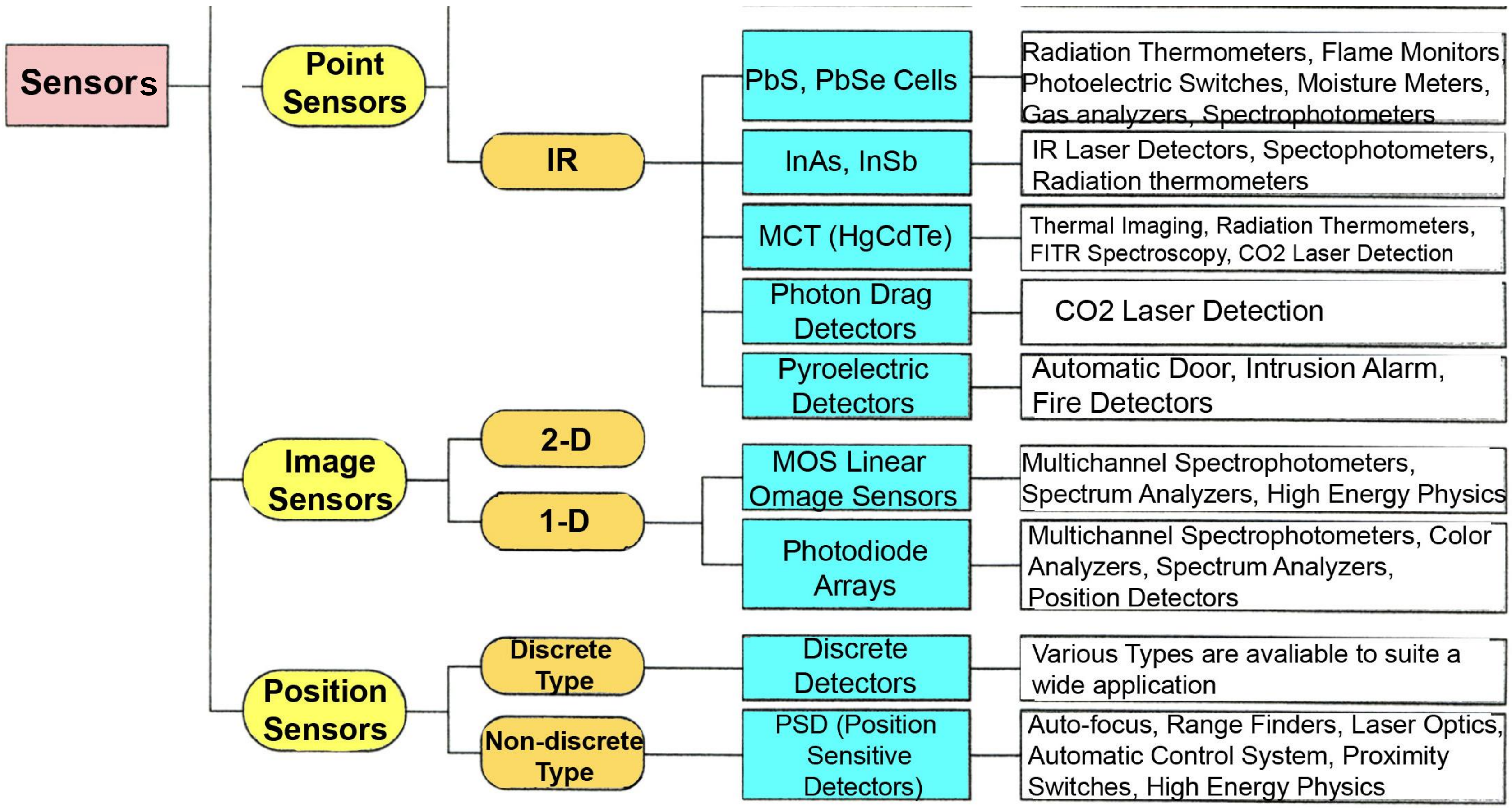

Applications of Silicon diode detectors

Spectral response Range (nm) (200 400 600 800 1000 1200)	Features	Major Applications
Silicon Photodiodes		
190 – 1100	UV to IR range, for precision photometry	Spectrophotometer, analytical instrument, environment monitor, medical equipment, etc.
190 – 1000	UV to visible range with suppressed IR sensitivity	
320 – 1100	Visible to IR range, for precision photometry	Copier, optical power meter, laboratory equipment, cash drawer/deposit, etc.
320 – 730	Visible range, for general photometry	Camera, exposure meter, illuminometer, auto-strobe, light dimmer, copier, etc.
320 – 1100	Visible to IR range, for general photometry	Photoelectric switch, tape reader, card reader, smoke detector, etc.
PIN Silicon Photodiodes		
320 – 1000	High-speed response	Optical communication, optical data link, spatial light transmission, bar code reader, business machine, high-speed photometry, etc.
320 – 1060		
320 – 1100		
800 – 1100	Visible-cut sensitivity	Optical remote control, etc.

Applications of Silicon diode detectors

Spectral response Range (nm) 200 400 600 800 1000 1200	Features	Major Applications
Silicon Avalanche Photodiodes		
400 1000	High-speed response High gain	Optical communications, high-speed photometry, low-light-level detection, etc.
GaAsP Photodiodes (Diffusion Types)		
300 680	Visible range	Camera, exposure meter, illuminometer, auto-strobe, flame monitor, laboratory equipment, colorimeter, etc.
400 760	Extended red sensitivity	
GaAsP Photodiodes (Schottky Types)		
190 680	UV to visible range	Spectrophotometer, analytical instrument, UV detector, etc.
190 760	Extended red sensitivity	
GaP Photodiodes (Schottky Types)		
190 550	UV to green range	UV detector, etc.

Conventional photodiodes

- Generally designed as fully depleted detectors (PIN configuration)
- Photons o typical scintillation light: 3-4 eV of energy, creating electron-hole pairs with a bandgap of approximately 1-2 eV
- Maximum quantum efficiency QE~60-80% (much higher than PMTs)
  - QE also spans a much wider wavelength range: much higher primary charge usually is created by the light from the scintillator
- BUT: No subsequent amplification of this charge as in a PM tube

  → Output signal smaller by orders of magnitude

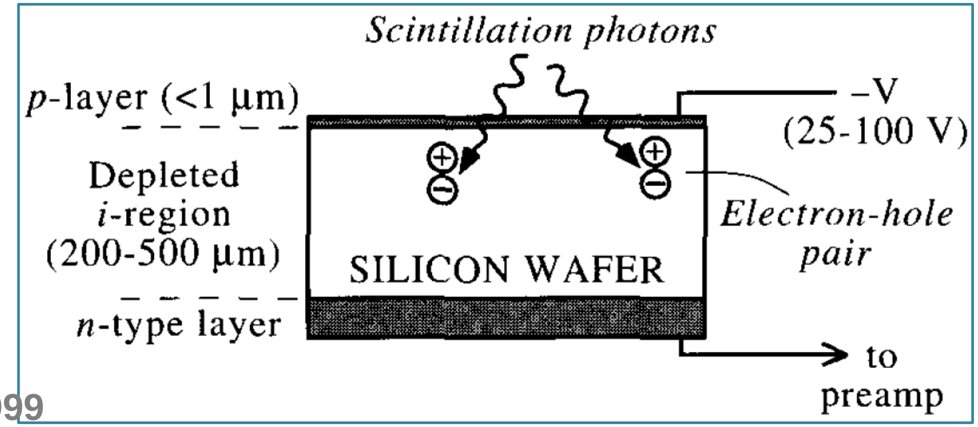

Knoll 1999

Conventional photodiodes

- Because of the small signal amplitude, electronic noise is a major problem in pulse mode operation, especially for large-area detectors and low-energy radiations
- Successful applications
  - High-energy radiation
  - Small-diameter diodes
  - → Small dark current and capacitance
- Photodiodes with A>1 cm^2 **too noisy**
  - C decreases as thickness is increased, but leakage current increases
- Thickness of Si wafers: 300-500 μm
- Quantum efficiency reaches **higher values** ar **extends much farther** into the long waveleng region than PMTs
  - Particularly important for scintillators such as CsI(T1) or BGO

Comparison of quantum efficiencies

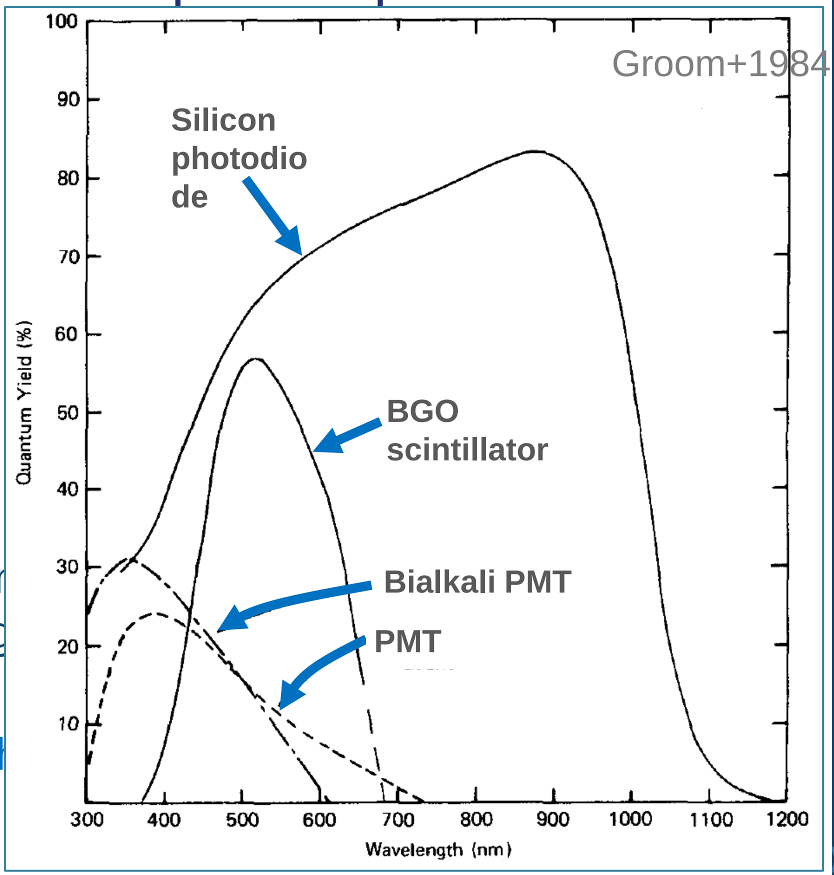

Conventional photodiodes

Major noise contributor: dark (leakage) curren

- **Methods of noise reduction**
  - **Cooling** of the photodiode
    - Rapid rise in dark current above roo temperature generally **prevented th use** of silicon photodiodes in applica requiring operation **at elevated T**
  - **Choosing semiconductor materials** w **wider band gap** than silicon
    - Mercuric iodide crystals
  - Reducing the capacitance
    - ➔ Silicon drift photodiodes

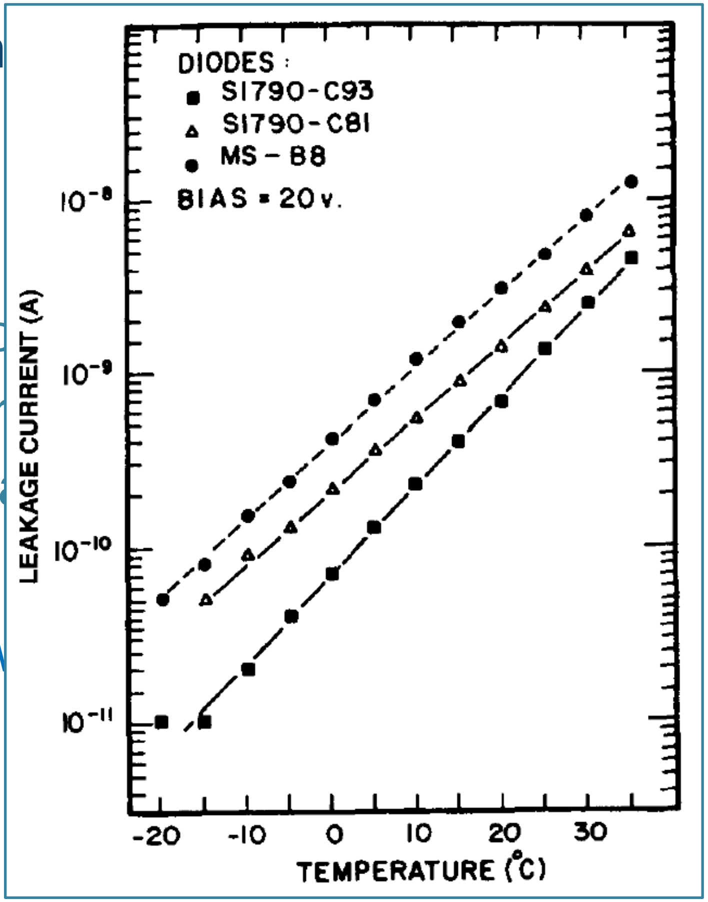

Conventional photodiodes

Silicon drift detectors (SSD)

- Construction process of the passivated planare detectors
- Capacitance not directly depenedent from the area
  - Can be kept low by incorporating an on-chip JFET preamplifier stage
- Resolution as good as <3%
- Can be arranged into monolithic arrays

One-sided

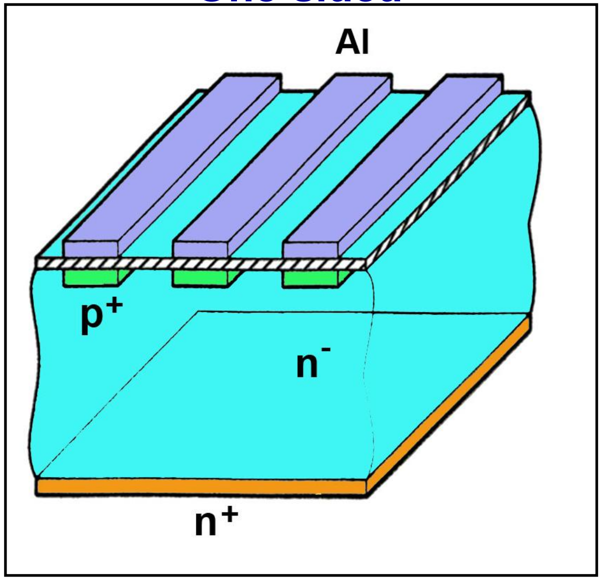

Double-sided

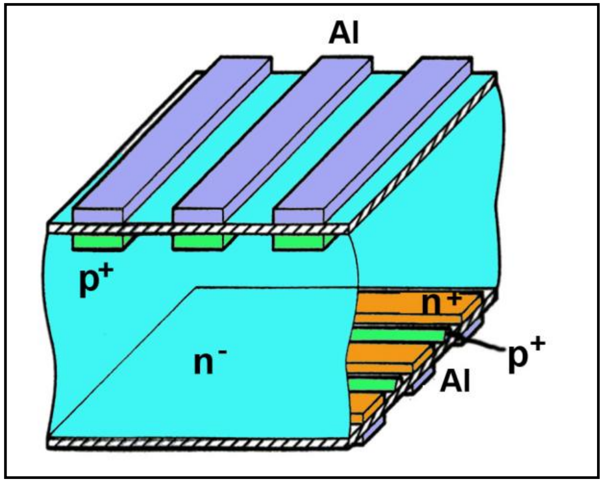

Conventional photodiodes

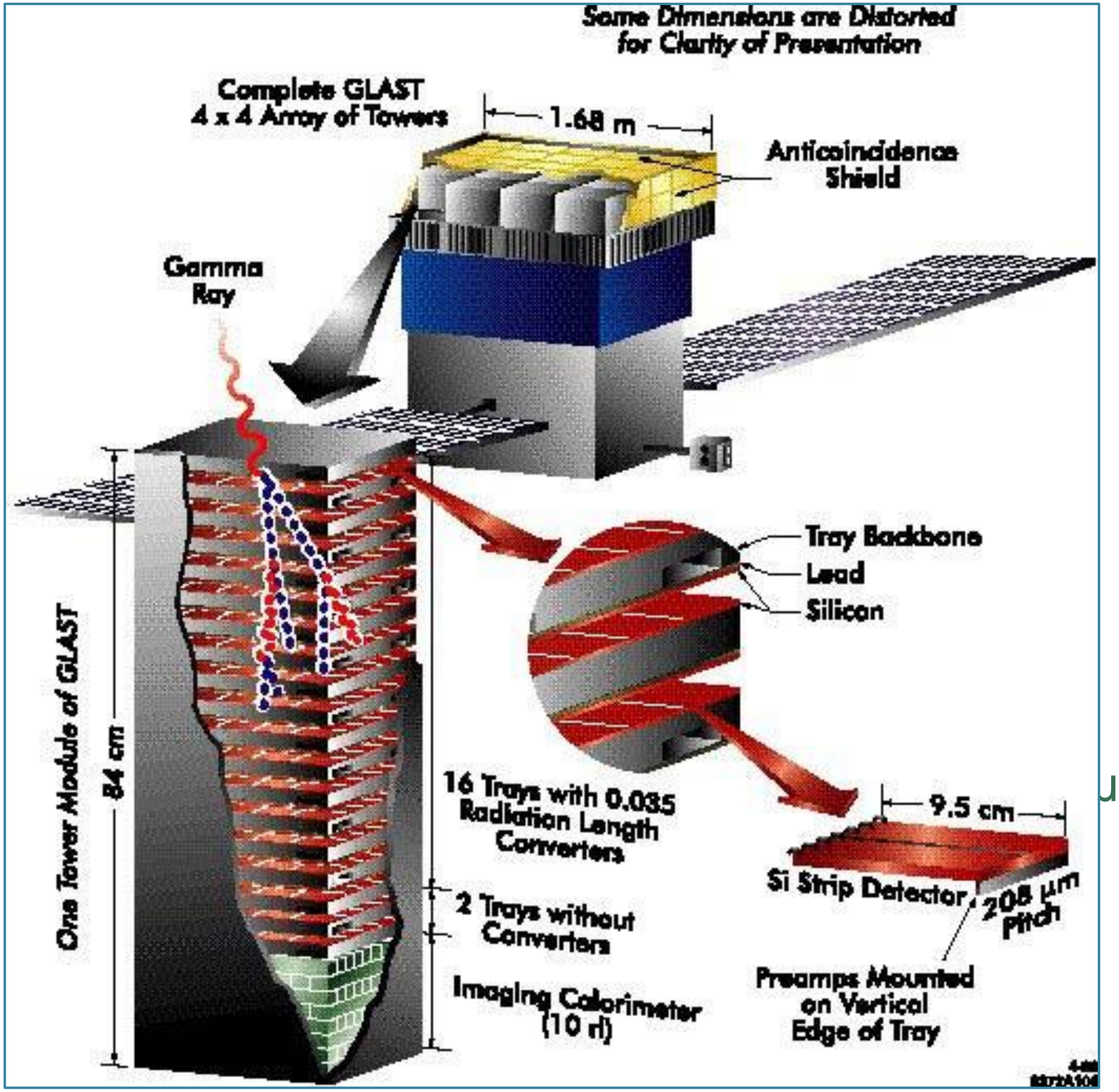

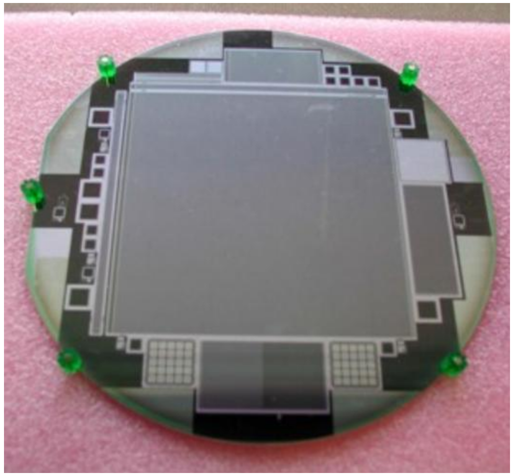

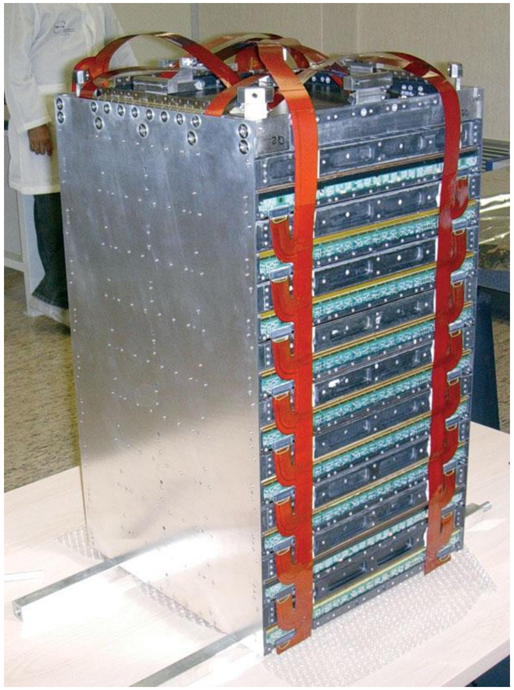

um.

Avalanche photodiodes

- Also called APDs
- The small amount of charge that is produced in a conventional photodiode by a typical scintillation event can be increased through an avalanche process that occurs in a semiconductor at high values of the applied voltage

  → Charge carriers are accelerated sufficiently between collisions to create additional electron-hole pairs along the collection path

    - Better energy resolution in pulse mode at low radiation energy than conventional diodes
- Gain factor is very sensitive to temperature and applied voltage
  - Decrease in gain of ~2% per ^{o}C increase
  - Stabilization of high-voltage supplies required

Avalanche photodiodes

- Fabricated in the "**reach-through configuration**"

1. Light enters through thin p+ layer and interacts somewhere in the p region constituting the diode thickness
2. Formation of electron-hole pairs
3. Electron is drawn to the right into the multiplying region where a high electric field exists
4. More electron-hole pairs created
   - Gain factors: few hundreds
   - Sufficient for low incident light leve

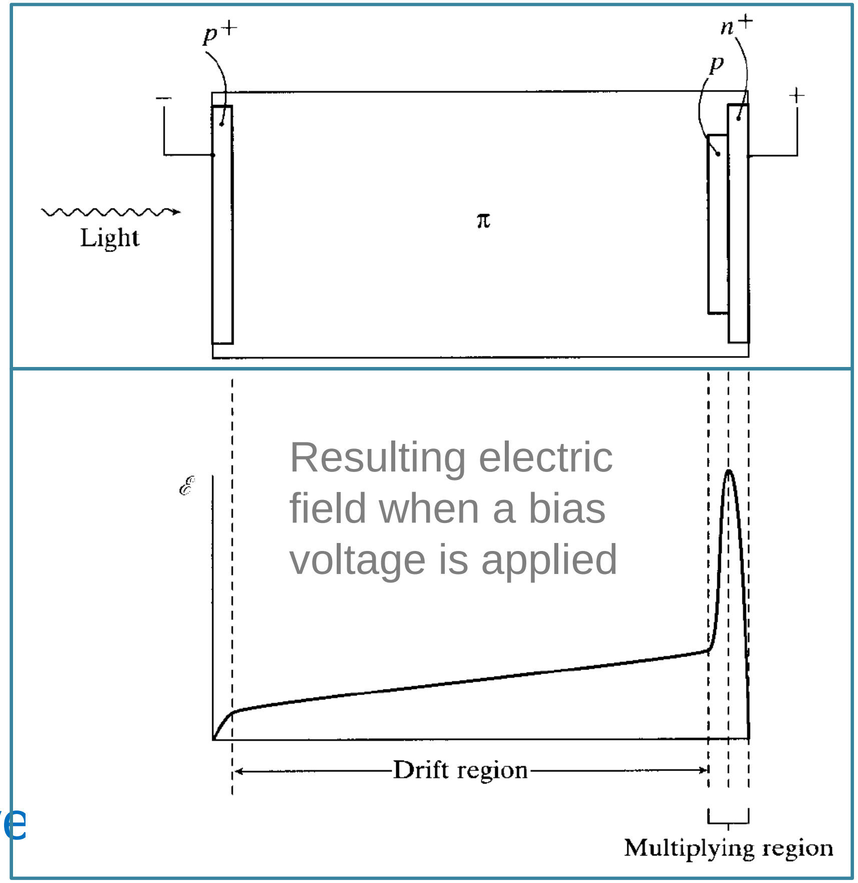

Knoll 1999

→ Quantum efficiencies of 80% are possible

→ Peak wavelength of the response 500-600 nm

Avalanche photodiodes

- The applied voltage is always kept below the breakdown voltage
  - Normal operation in the «linearity regime»: **current signal proportional** to **number of incident photons**
- Timing resolution: <1 ns (best), few ns (typical)
  - Higher rate operation and better timing resolution than conventional diodes

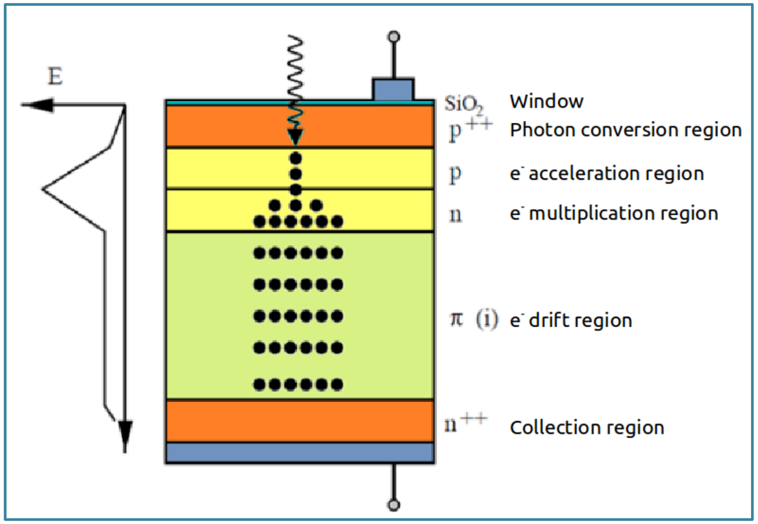

- Relation between n_0 (number of electron-hole pairs created), N number of electrons making up the output signal) and σ_N (relative fluctuations in the output signal):

$$\left(\frac{\sigma_N}{N}\right)^2 = \frac{J}{n_0}$$

  - J Excess noise factor: reflects the degree of variability within all avalanches that make up a pulse ($J \cong 1 - 3$).

Geiger Mode APDs

- Diodes in which the voltage is raised high enough in order for the avalanche process to «run away»
  - As V approches the breakdown voltage, the multiplication regions from various photoelectrons begin to merge together to form a **SINGLE AVALANCHE**
    - Diode enters the so-called **«Geiger mode»**: **Charges** produced in the initial interaction of photons are in principle **multiplied without limit**
    - Creation of a **large output pulse** from as little as a SINGLE INCIDENT PHOTON
    - **SPAD: single photon avalanche photodiode**
- Avalanche self-sustaining, unless it is quenched by some passive or active circuit
  - Large resistor in series with the diode: avalanche current leads to a voltage drop. Electric field gets lowered, multiplication ceases, device

The Silicon Photomultiplier

- For normal scintillation applications, in which a proportional amplification of the original number of electron-hole pairs is wanted, the single-cell Geiger mode is of LITTLE INTEREST
  - All the information on its original number is lost!
- In order to overcome this limitation:
  Developmente of the Silicon Photomultiplier (or SiPM)
  - **Array** of **small avalanche photodiode cells**, each with dimensions of only **tens of μm**, produced using CMOS (complementary metal-oxide semiconductor) processes on a silicon chip.
    - Size of individual photodiode cell is ideally **small enough** so that the probability is low that a cell is hit by a scintillation photon DURING a scintillation pulse: **AT MOST a single**

The **NUMBER OF CELLS** producing an avalanche is **proportional** to the **NUMBER OF INCIDENT PHOTONS**

The Silicon Photomultiplier

- In case of collection of scintillation photons (many thousands at the output window)
  - Number of cells must be a large multiple of the number of collected photons
    - Arrays with >10^4 cells
  - Output of each cell is very close to the same amplitude
    - Uniformity of the cells and the individual quenching resistors
    - Adding the output by connecting them in parallel produces an analog pulse whose amplitude is proportional to the number of detected photons
  - Array dimensions: ~some mm

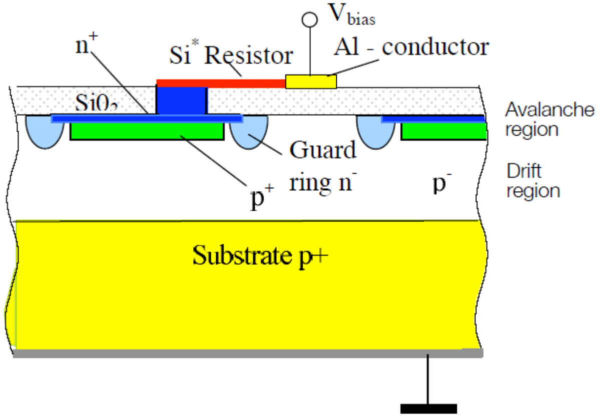

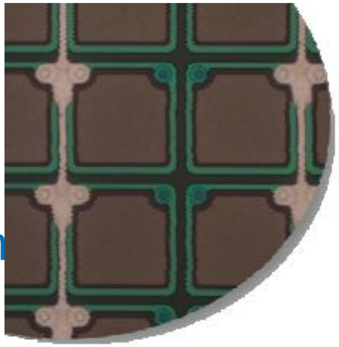

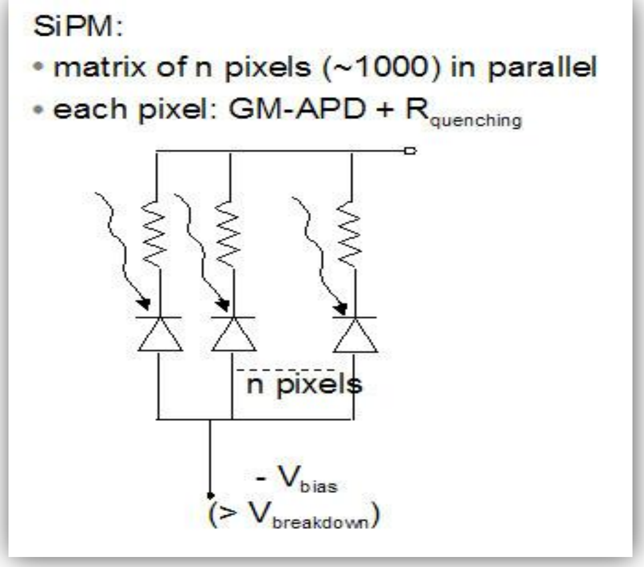

The Silicon Photomultiplier

ELECTRICAL MODEL

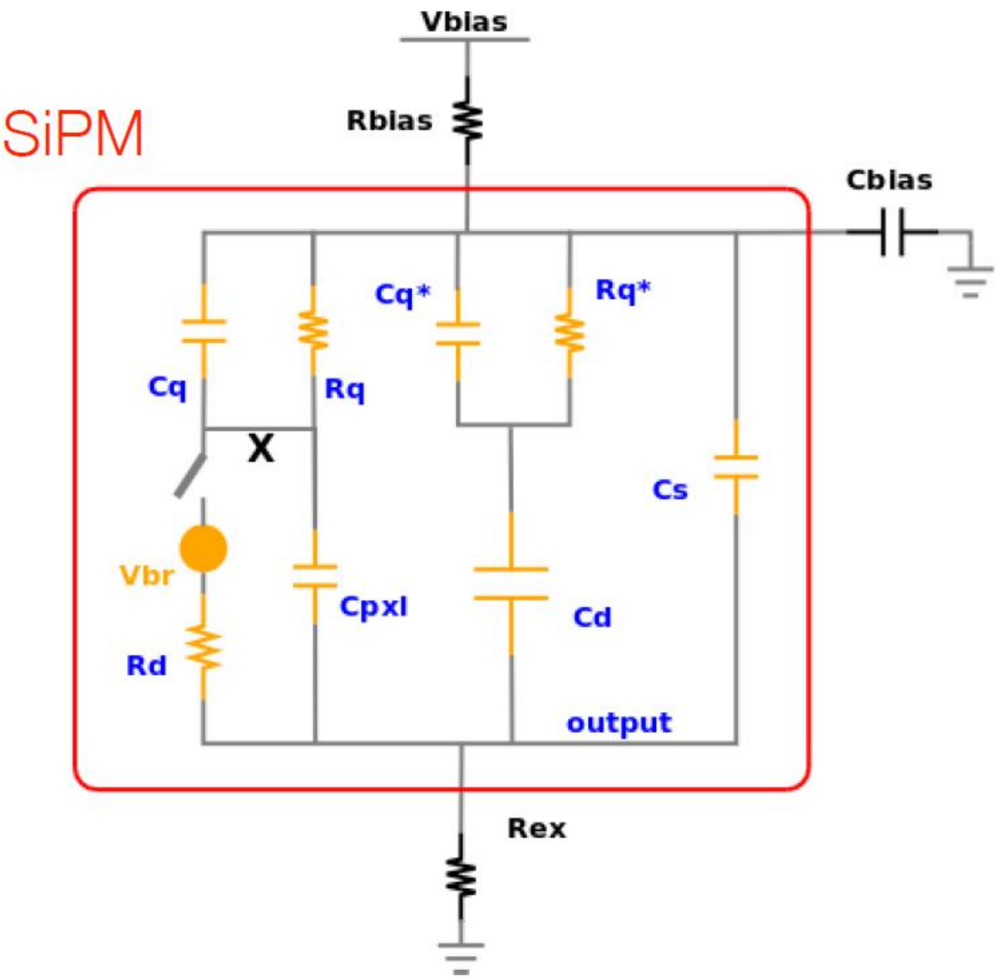

C_{pxl}	Pixel capacitance
C_q	Parasitic capacitance
C_d	Capacitance of inactive pixels
C_s	Stray capacitance
R_q	Quench resistor
R_d	Space charge resistance

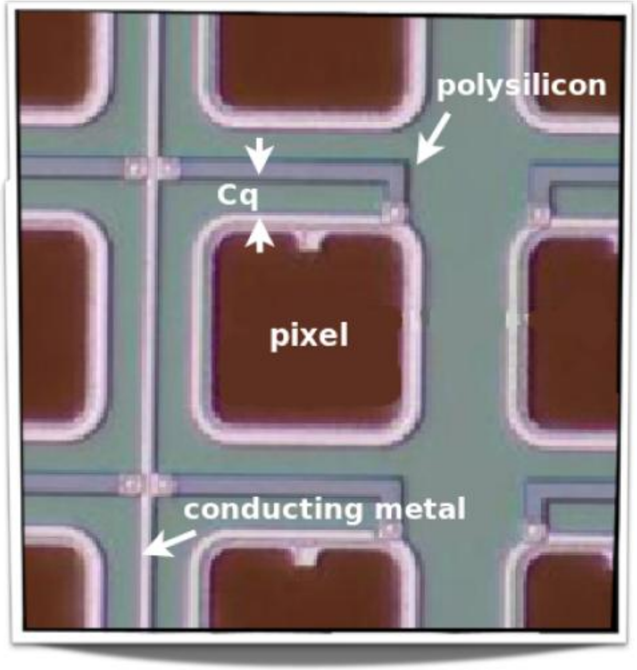

The Silicon Photomultiplier

DEVELOPERS AND PRODUCTS

- MEPhI/Pulsar (Moscow) - Dolgoshein
- CPTA (Moscow) - Golovin
- Zecotek (Singapore) - Sadygov
- Amplification Technologies (Orlando, USA)
- **Hamamatsu Photonics (Hamamatsu, Japan)**
- **SensL (Cork, Ireland)**
- **AdvanSiD (former FBK-irst Trento, Italy)**
- STMicroelectronics (Italy)
- KETEK (Munich)
- RMD (Boston, USA)
- ExcelitasTechnologies (former PerkinElmer)
- MPI Semiconductor Laboratory (Munich)
- Novel Device Laboratory (Beijing, China)
- Philips (Netherlands)

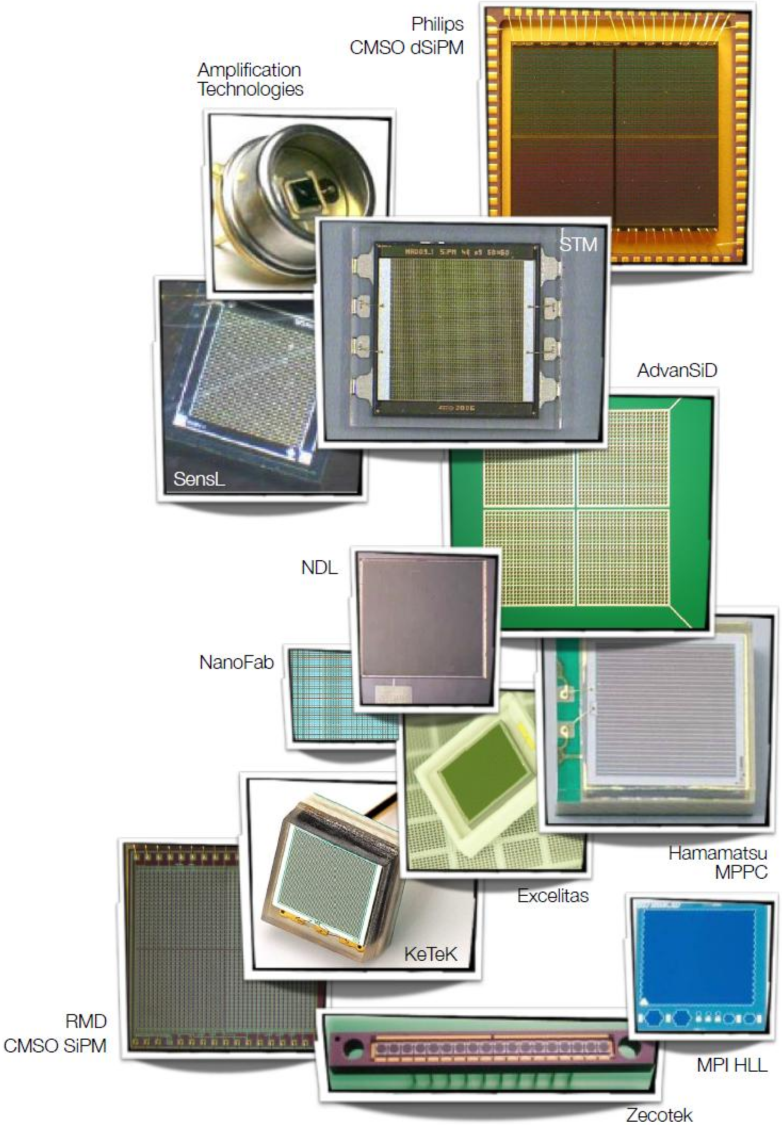

- Note: Every producer uses its own name
  MRS APD, MAPD, SiPM, SSPM, MPPC, SPM, DAPD, PPD, SiMPl , dSiPM

The Silicon Photomultiplier

Hamamatsu MPPC 400 pixels

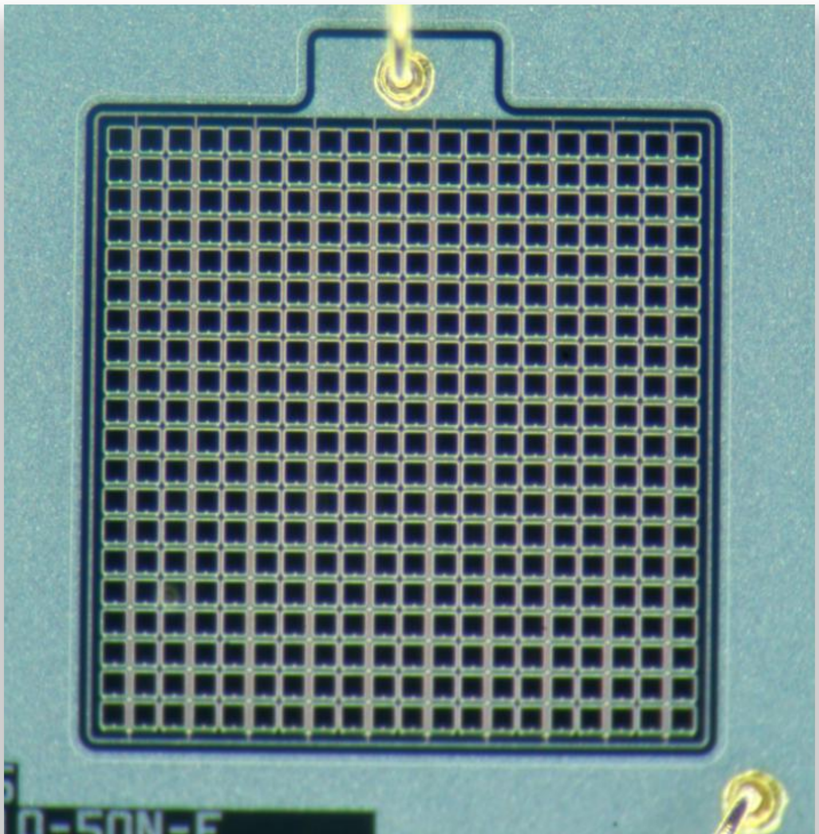

One of the first SiPM (FBK – Trento, Italy)

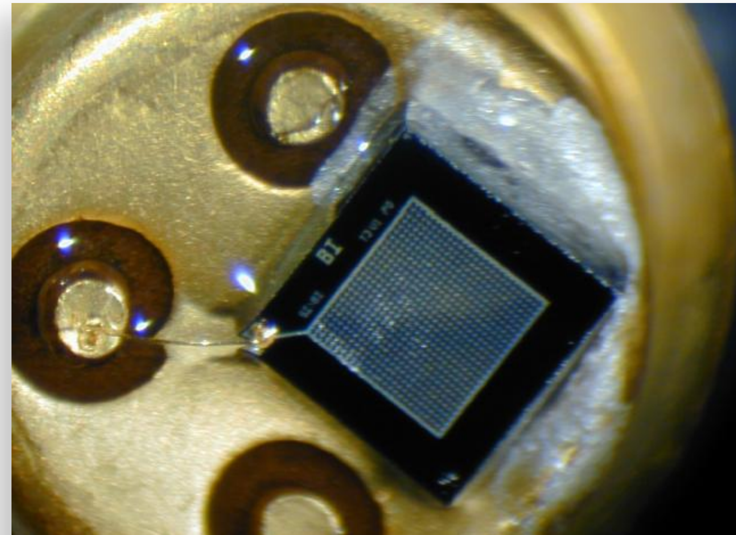

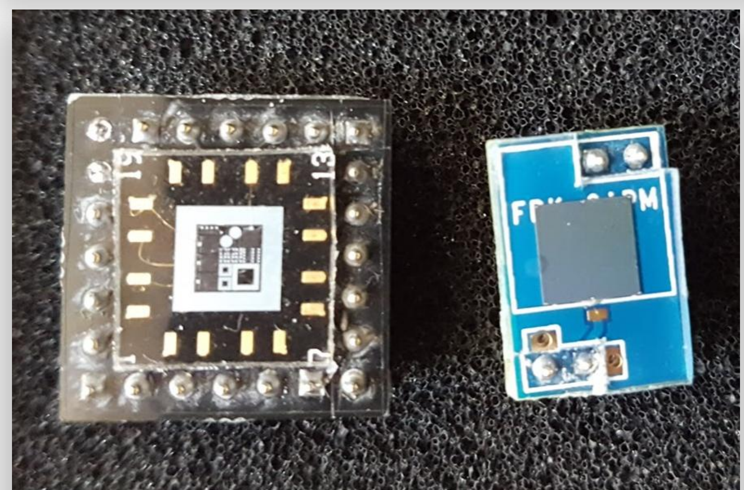

Latest SiPM for the CTA experiment (FBK – Trento, Italy)

TRIGGERING PROBABILITY

- Avalanche generated next to n-edge
- Av
- “R
  - Deep p-edge → n/p device
- “Blue” photon (small wavelength
  - Surface p-edge → p/n devic

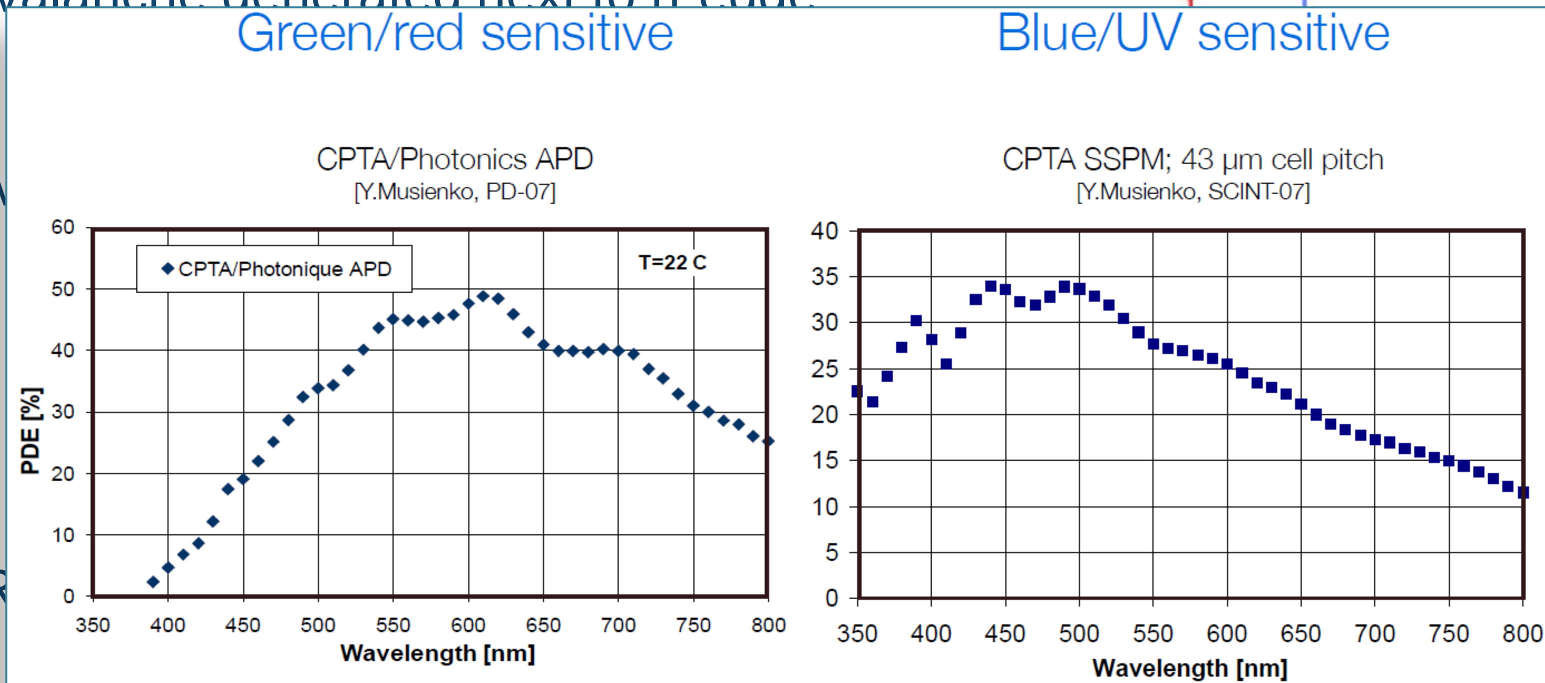

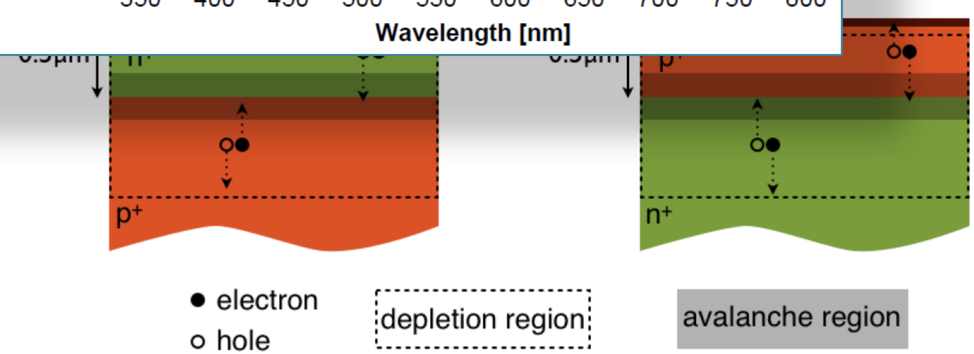

The Silicon Photomultiplier

Comparison with other devices regarding the IV chatacteristics

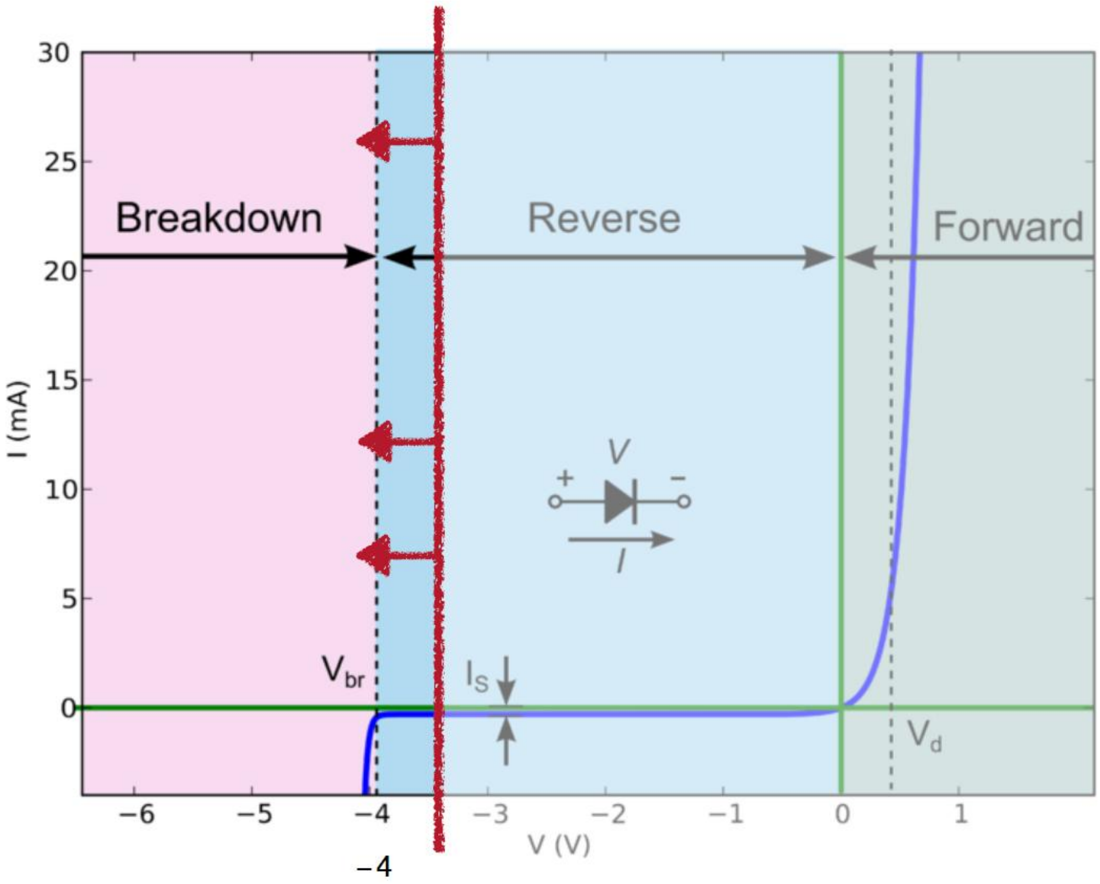

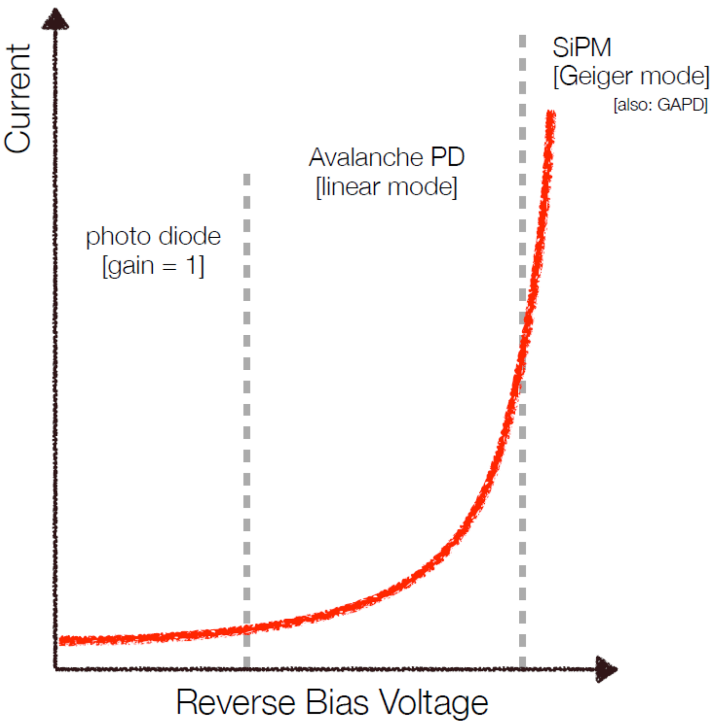

The Silicon Photomultiplier

Single photon spectrum

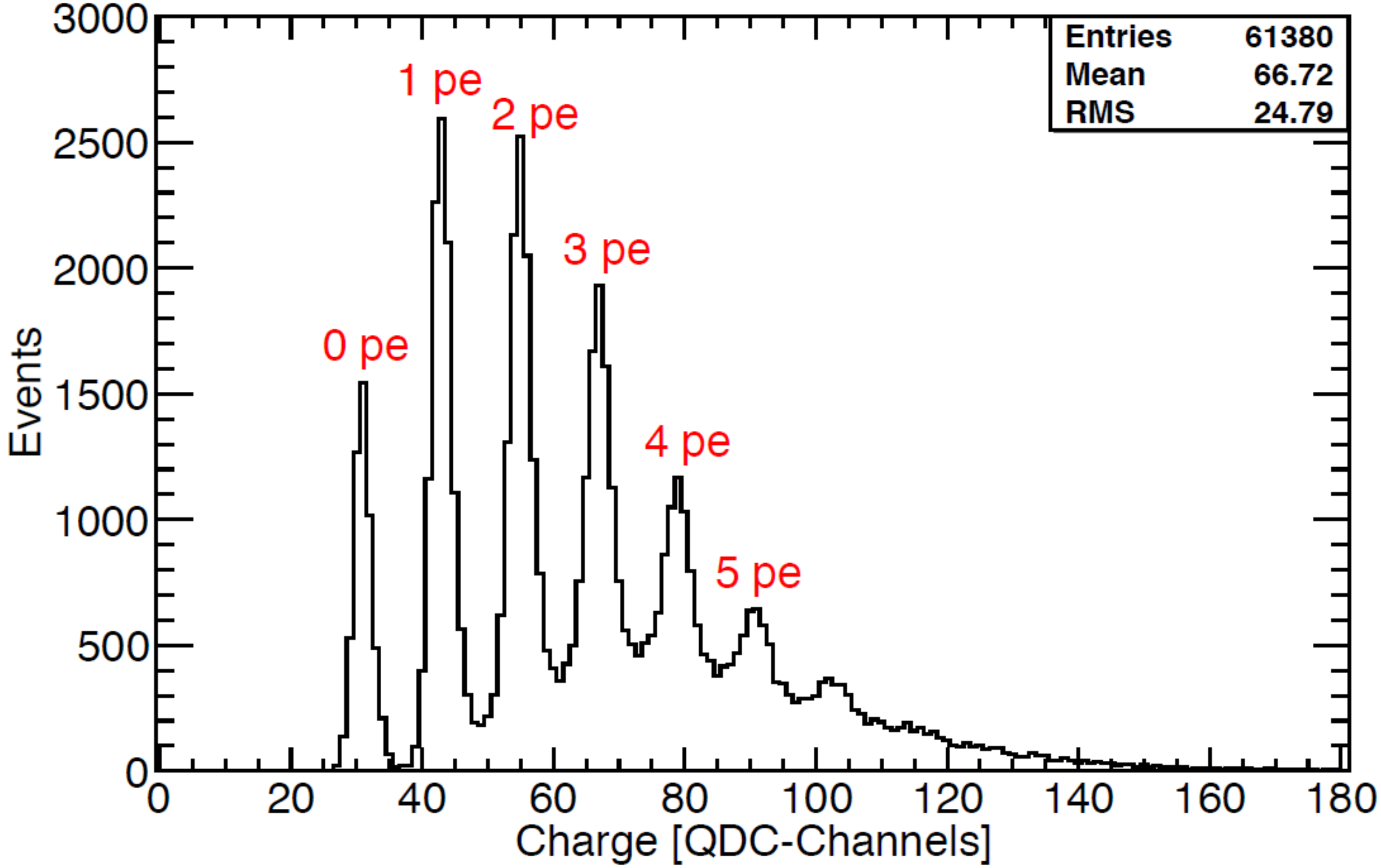

The Silicon Photomultiplier

- Array of SPADs connected in parallel
  - One quenching resistor per SPAD (from 100kΩ to several MΩ)
  - Common bias applied to SPADs (10 – 20% over breakdown voltage)
  - SPADs fire independently

OUTPUT
Sum of signals by individual cells → for small light pulses, SiPMs work as analog photon counters

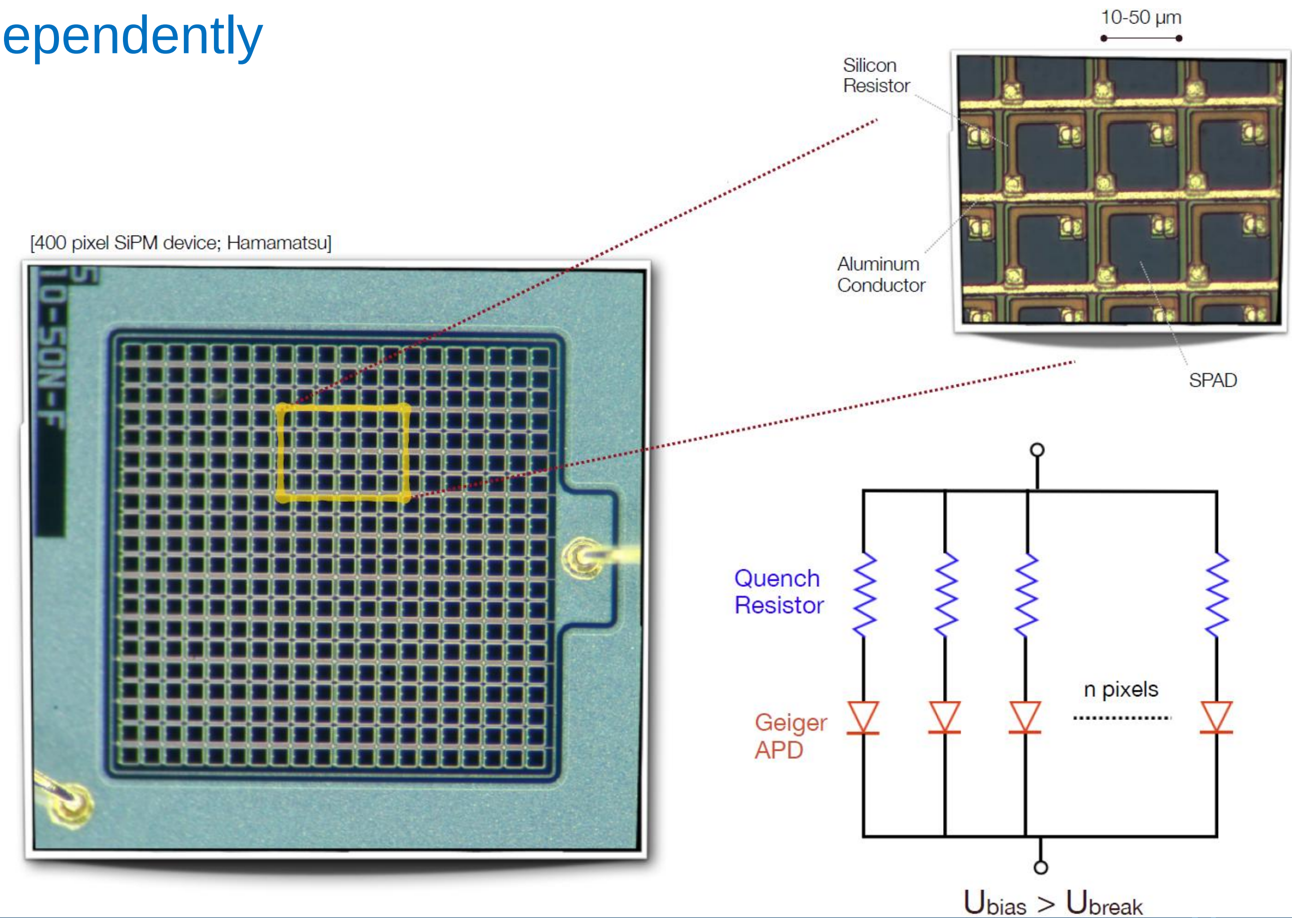

The Silicon Photomultiplier

A. SiPM biased at $V > V_{br}$
   - As long as no charge carrier is present in the high electric field region, no current flowing

B. Avalanche breakdown, initiated by photon, thermal noise, etc.
   - Internal diode capacitance starts to discharge, the rising current flowing through the device induces voltage drop

C. Avalanche quenched
   - Recharge of internal device capacitance
   - Return to initial state

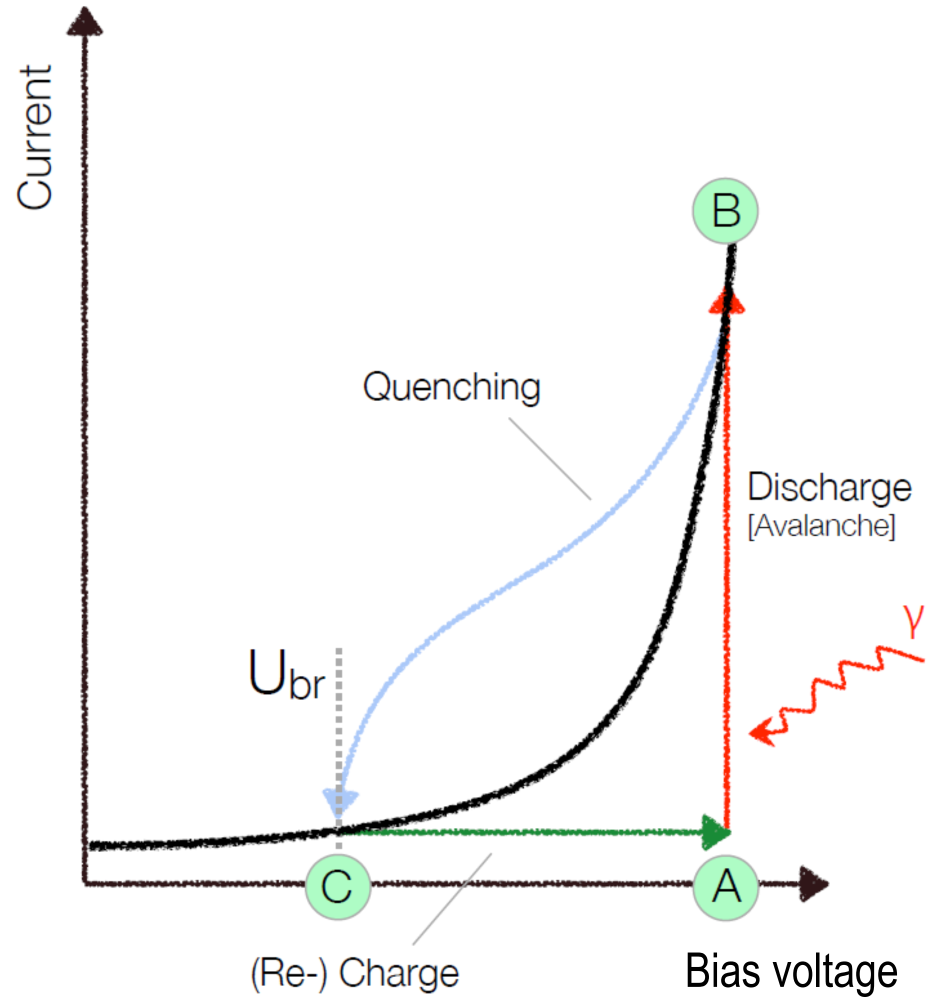

The Silicon Photomultiplier

Typical signal shape

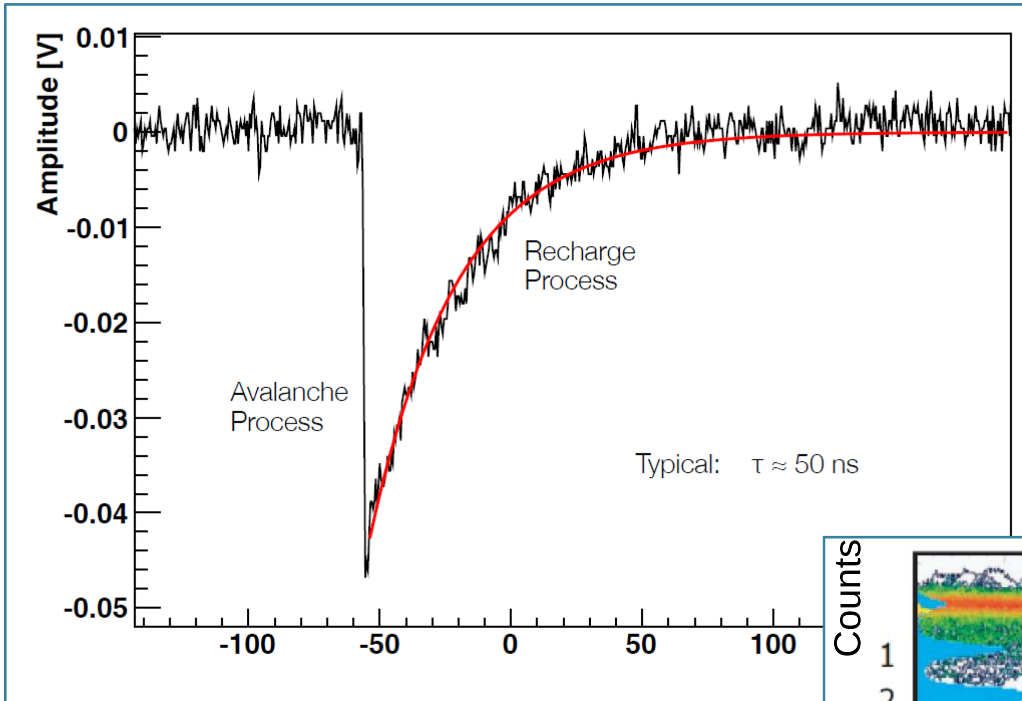

Photon

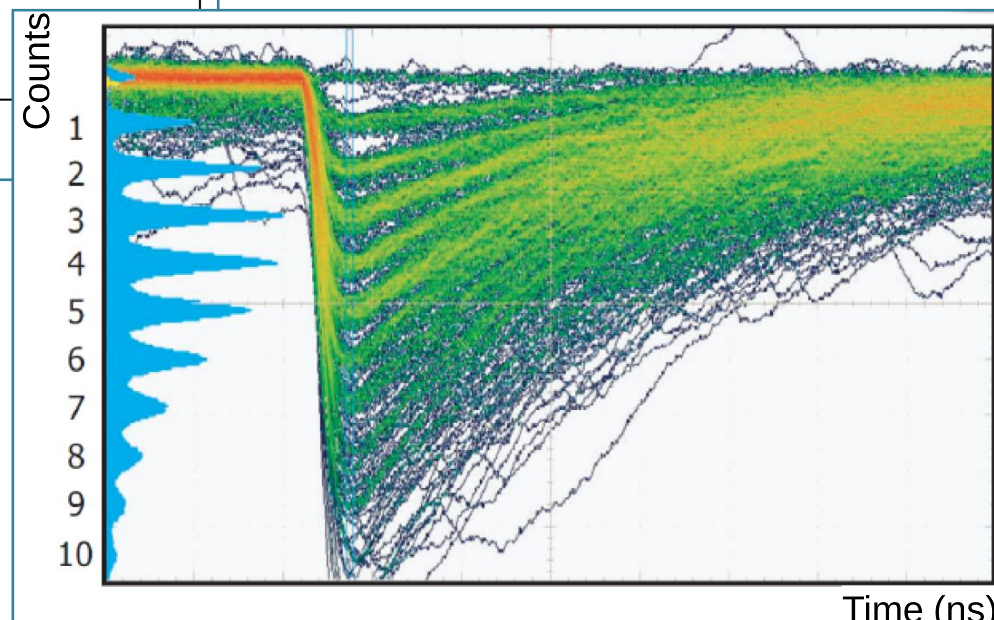

The Silicon Photomultiplier

SUMMARY OF PROPERTIES

- Pros
  - High gain — 10^5 to 10^5
  - Compactness — 1 to 3 mm^2
  - Insensitive to magnetic fields — up to few T
  - Low operation voltage — 30 – 70 V
- Cons:
  - Limited dynamical range — $N_{pxl} = O(1000)$
  - Cross-talk, after-pulsing — 1–10 %
  - High dark-rate — 0.1 to few MHz
  - Temperature sensitivity — 20 – 50 mV/K

The Silicon Photomultiplier

GAIN AND SINGLE PIXEL CHARGE

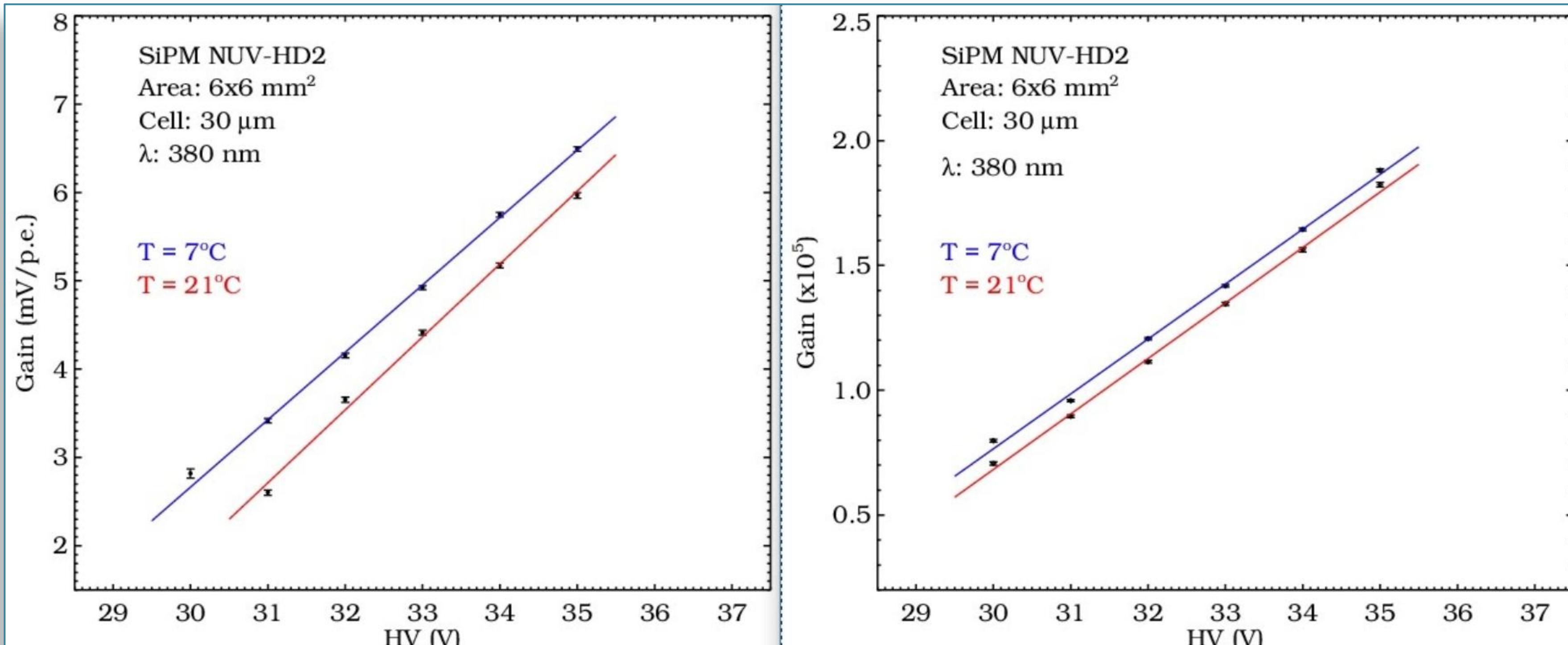

- SiPM Gain (for low noise):

$$G = \frac{Q_{pxl}}{Q_e} \propto V_{OV}$$

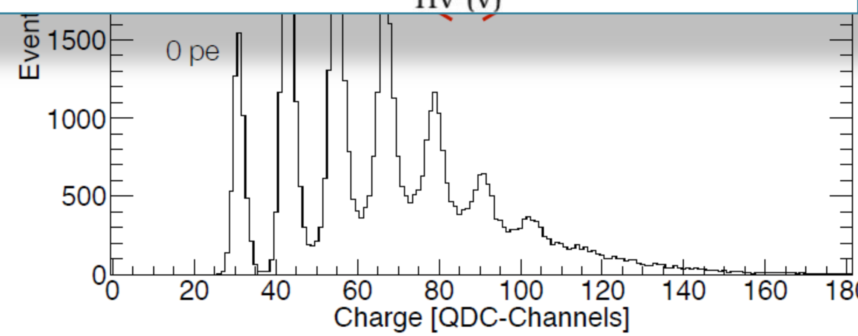

The Silicon Photomultiplier

PHOTO DETECTION EFFICIENCY (PDE)

$$PDE = FF \cdot QE(\lambda, T) \cdot p_t(\lambda, V, T)$$

- FF: geometrical fill factor
- $QE(\lambda, T)$: quantum efficiency
- $p_t(\lambda, V, T)$: triggering probability

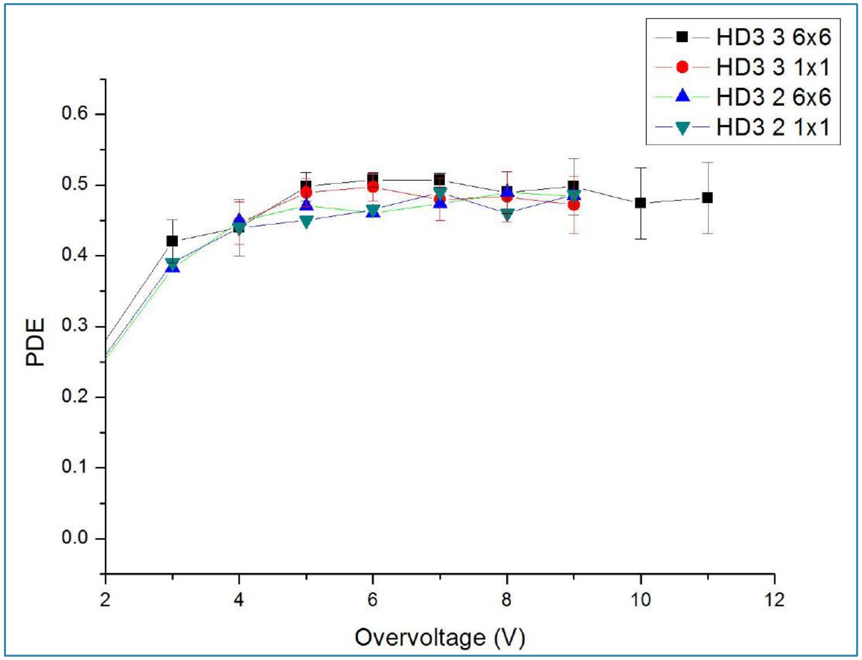

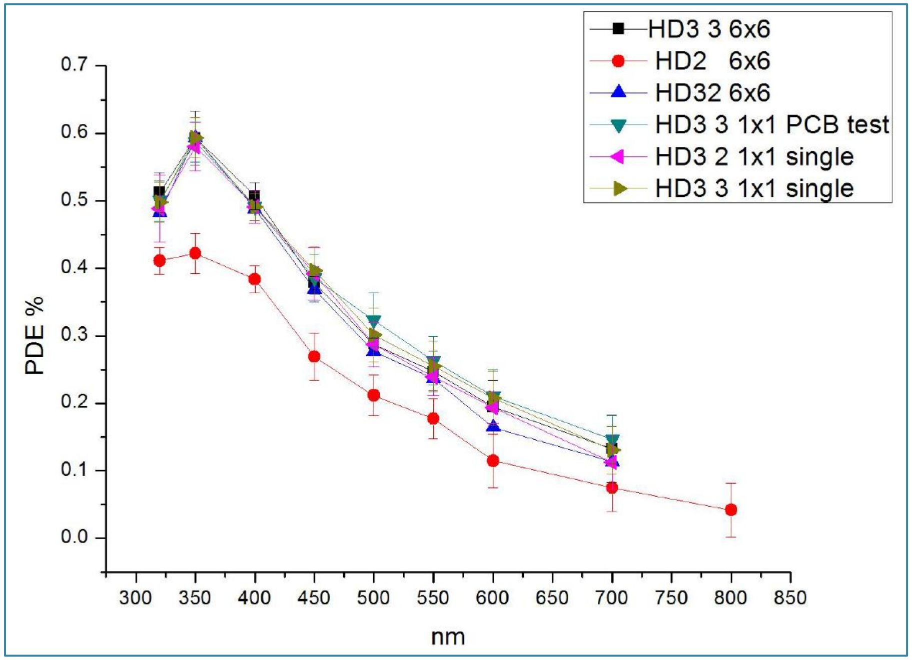

THE GEOMETRICAL OR FILL FACTOR FF

- Non-sensitive zones between cells which reduce the PDE
  - Silicon resistors and aluminum conductors are not photon-sensitive and hence reduce the active area
- Smaller pixel size yields small FF
  - Tradeoff between dynamic range and PDE
  - Typical $FF = 60 - 80\%$
- Improved FF using metal quench resistors (MCR technique)

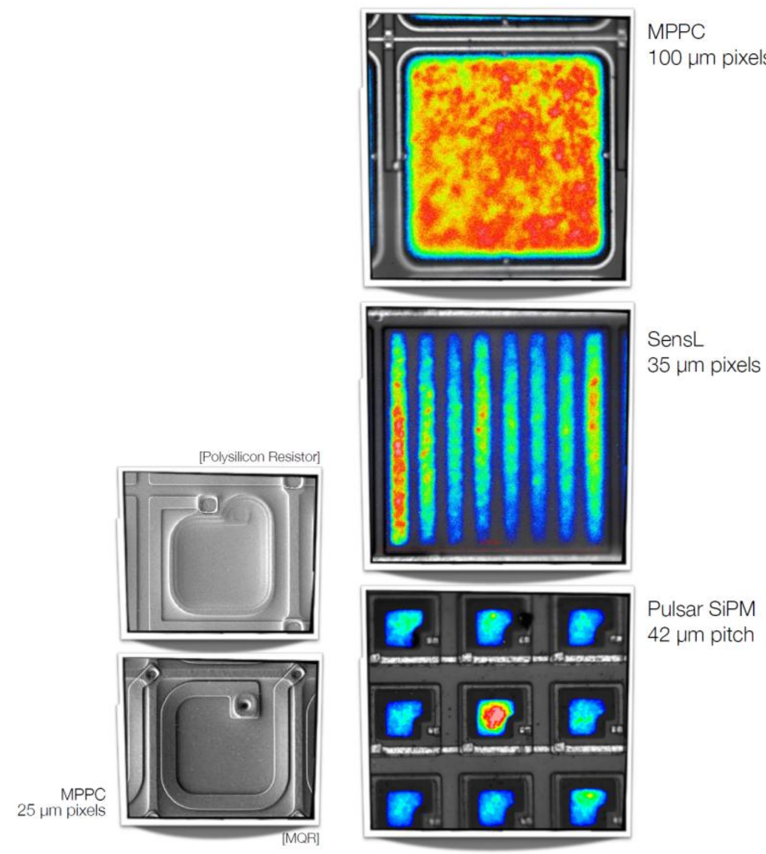

DARK PULSES AND NOISE

- **Unwanted noise** due to creation of electrc hole-pairs without involvement of photon Prcoesses:
  - Thermal exitation
  - Field assisted excitation

  → Electron (hole) drifts to high-field area creating an avalanche

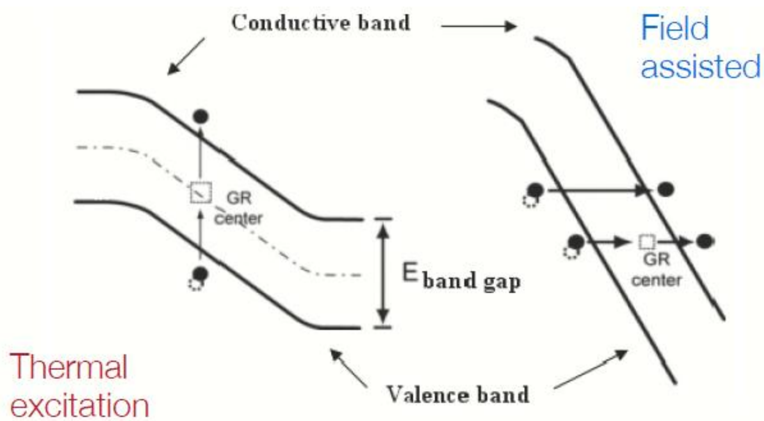

→Resulting signal **indistinguishable** from genuine photon induced SiPM signal

- Dark rate can be as high as 10^6 pulses/s/m at room temperature. Can by reduced by:
  - Setting a **discrimination level** (numbe simultaneously fired cells)
  - **Cooling** the device

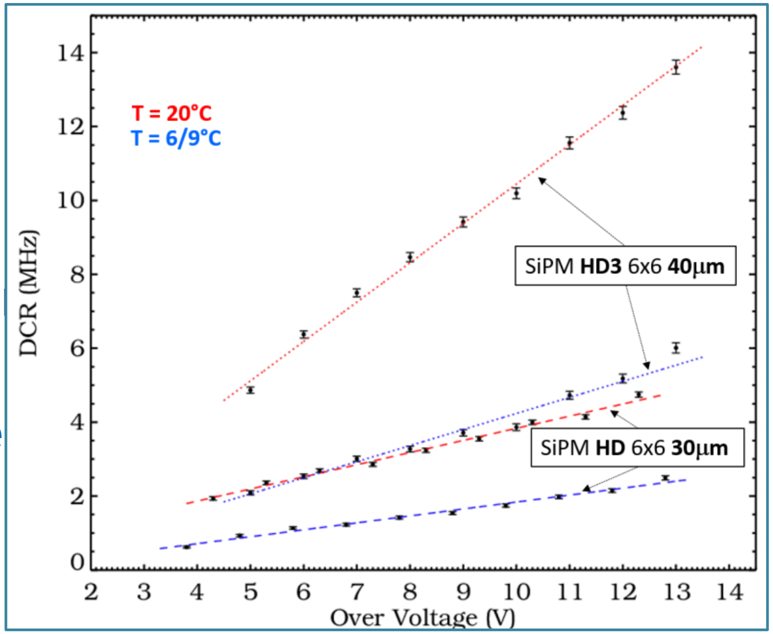

The Silicon Photomultiplier

CORRELATED NOISE

1. **Afterpulse (AP)**
   - Carriers trapped in medium's defects. Released after some recovery time, during the recharge phase
     → Delayed discharge **pulse observed on the tail of the previous one (usually smaller)**

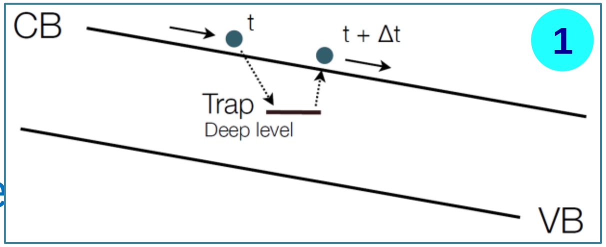

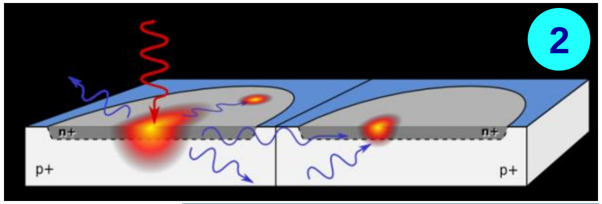

- **Optical cross talk (CT)**
  - Carriers generated by absorption of photons emitted during the avalanche process in neighbouring cells.

2. **DIRECT CT**: photon absorbed in the active region of the device, triggering an additional avalanche in the same instant of the original avalanche. → D**ouble pulse.**
3. **DELAYED CT**: photon absorbed in the inactive region of the device. Generated pair must diffuse to the active region in order to trigger a discharge.
   Result is a pulse occuring a few ns after the original one

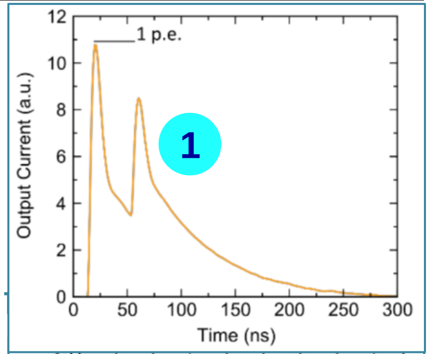

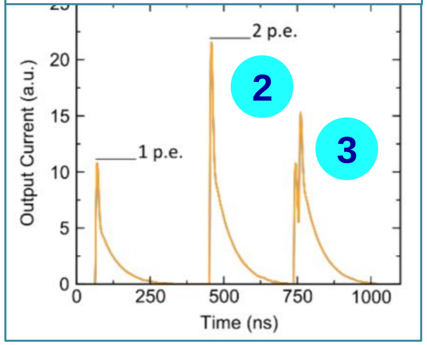

The Silicon Photomultiplier

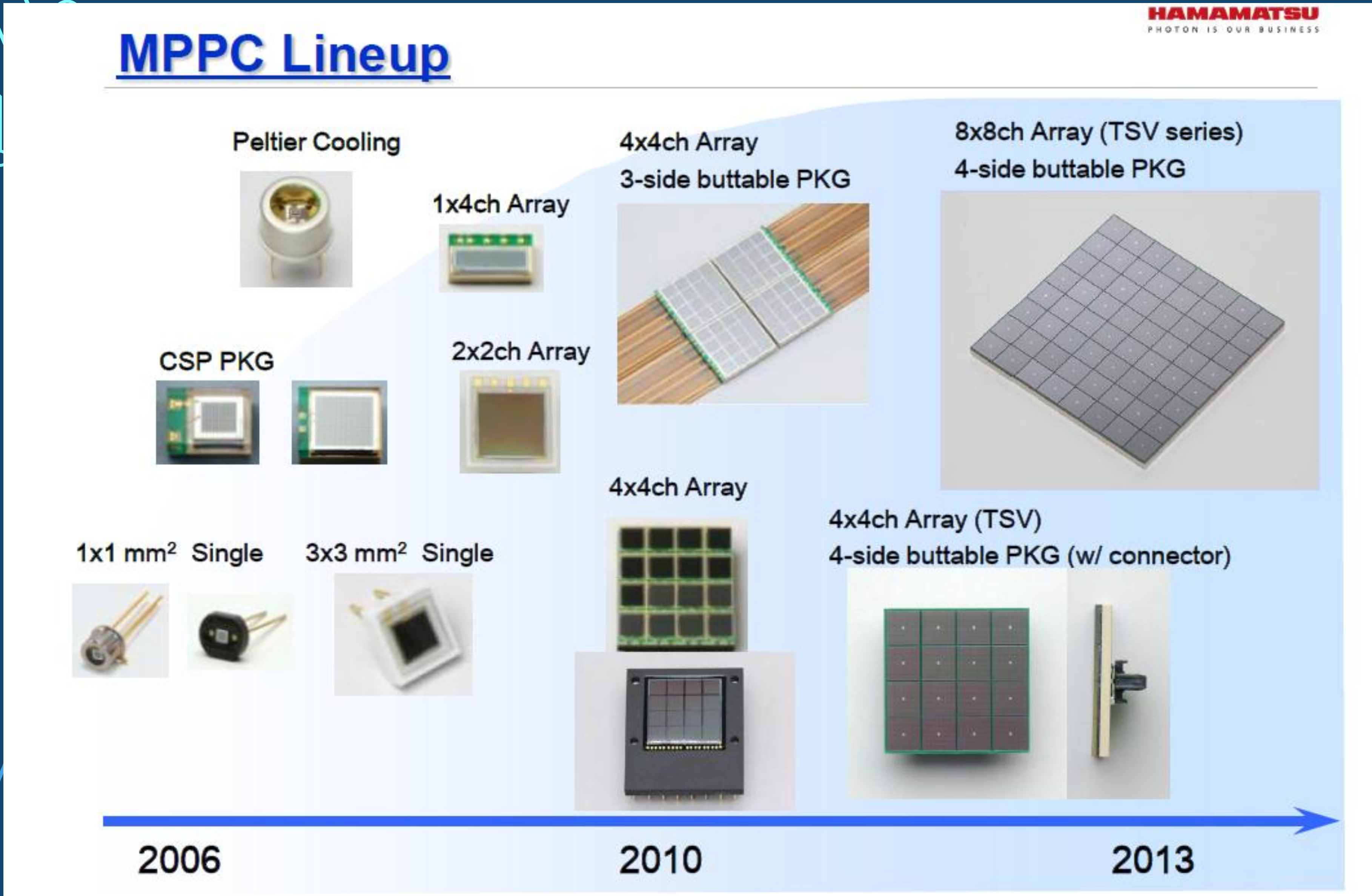

The Silicon Photomultiplier

- R&D of FBK NUV SiPM sensors

NUV sensors: Specifically designed for near ultra-violet light detection

Technologies aimed to the **optimization of different parameters** in order to **improve performances** and **match device's features** with the **specific applications' requirements** they are designed for

2013

- 1 x 1 mm^2 – NUV SiPM 50 um cell
  - 12 pcs, **initial test**
- 3.6 x 3.6 mm^2 – NUV SiPM 50 um cell
  - 50 pcs, **initial test**
- 3.1 x 3.1 mm^2 – NUV SiPM 50 um cell
  - 214 pcs, used for **test, measurement, Matrix assembly of 16**
- 3.1 x 3.1 mm^2, 6 x 6 mm^2 – NUV SiPM 40 um cell
  - used for **test, measurement, Matrix assembly of 16**

2015

- 6 x 6 mm^2 – CTA-HD SiPM 30 um cell
  - [production CTA_HD 2015]: 164 SiPM good, **for pSCT**
- 6 x 6 mm^2 – CTA-HD2 SiPM 30 um cell
  - 289 SiPM good, not ideal for pSCT

2018

- 6 x 6 mm^2 – CTA-HD3 SiPM 40 um cell
  - Final design
  - CTA HD3 2017: 600 SiPM mass production for pSCT

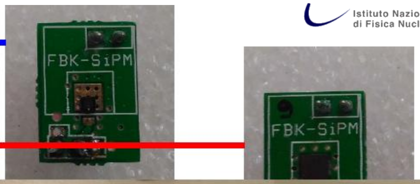

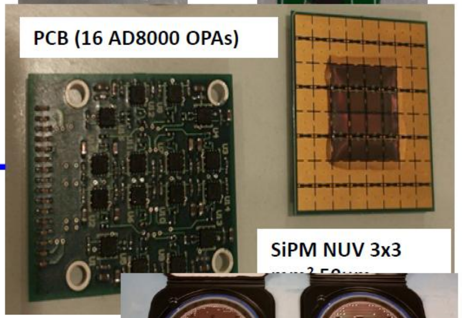

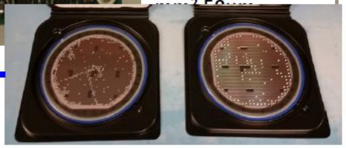

SiPM NUV da 3x3 e 6x6 mm^2 su fette da 6”

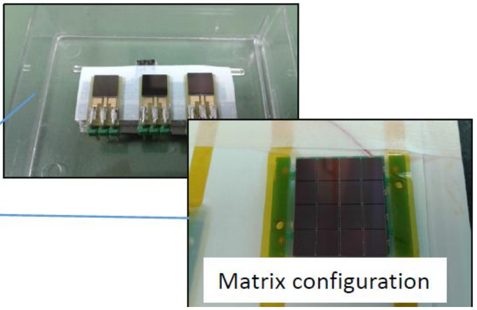

The Silicon Photomultiplier

FBK NUV HIGH-DENSITY (HD) SIPM SENSORS

- Produced at Fondazione Bruno Kessler (FBK, Trento, Italy)*

SiPMs mounted on single sensor test PCB

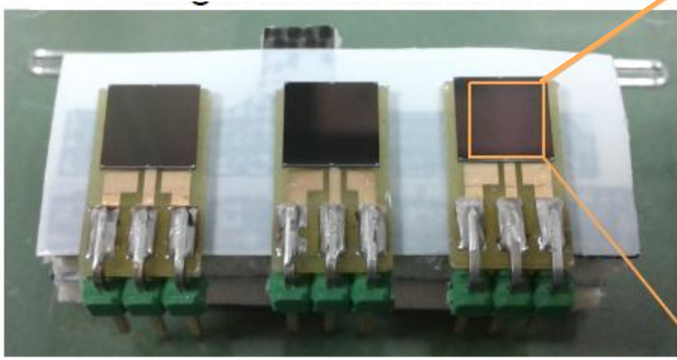

6 x 6 mm^2

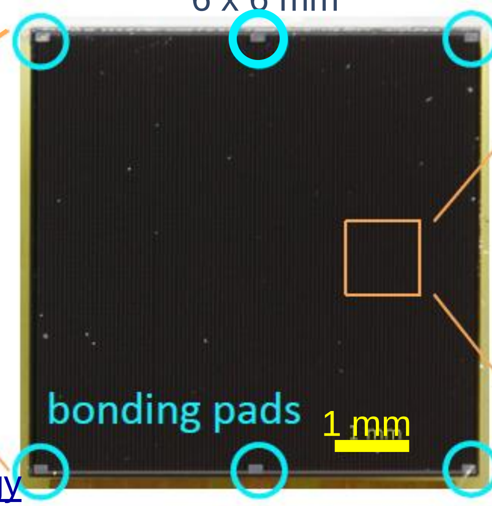

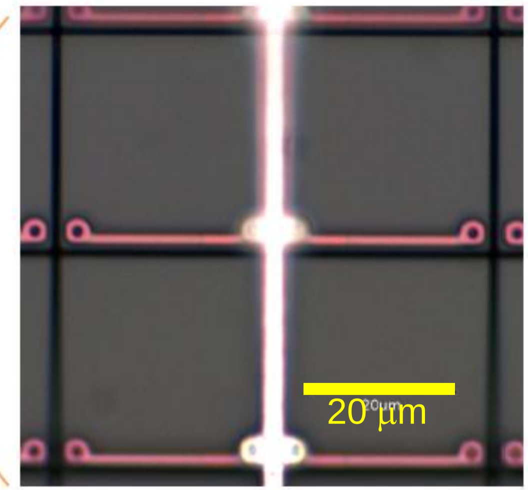

* http://srs.fbk.eu/optimization-sipm-technology

- This technology presents HIGH FILL FACTOR wit increased PDE, LOW CORRELATED NOISE and WIDE DYNAMIC RANGE, due to the high cell-density of the device

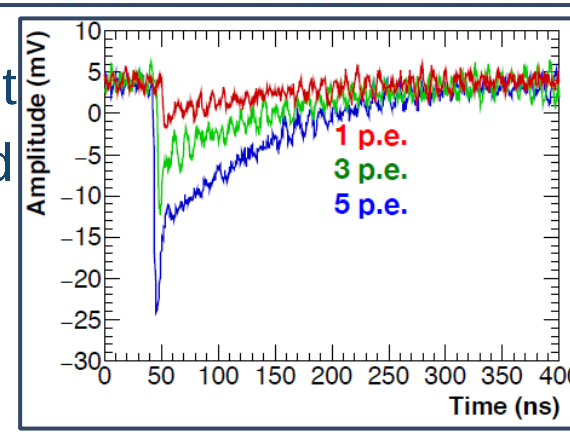

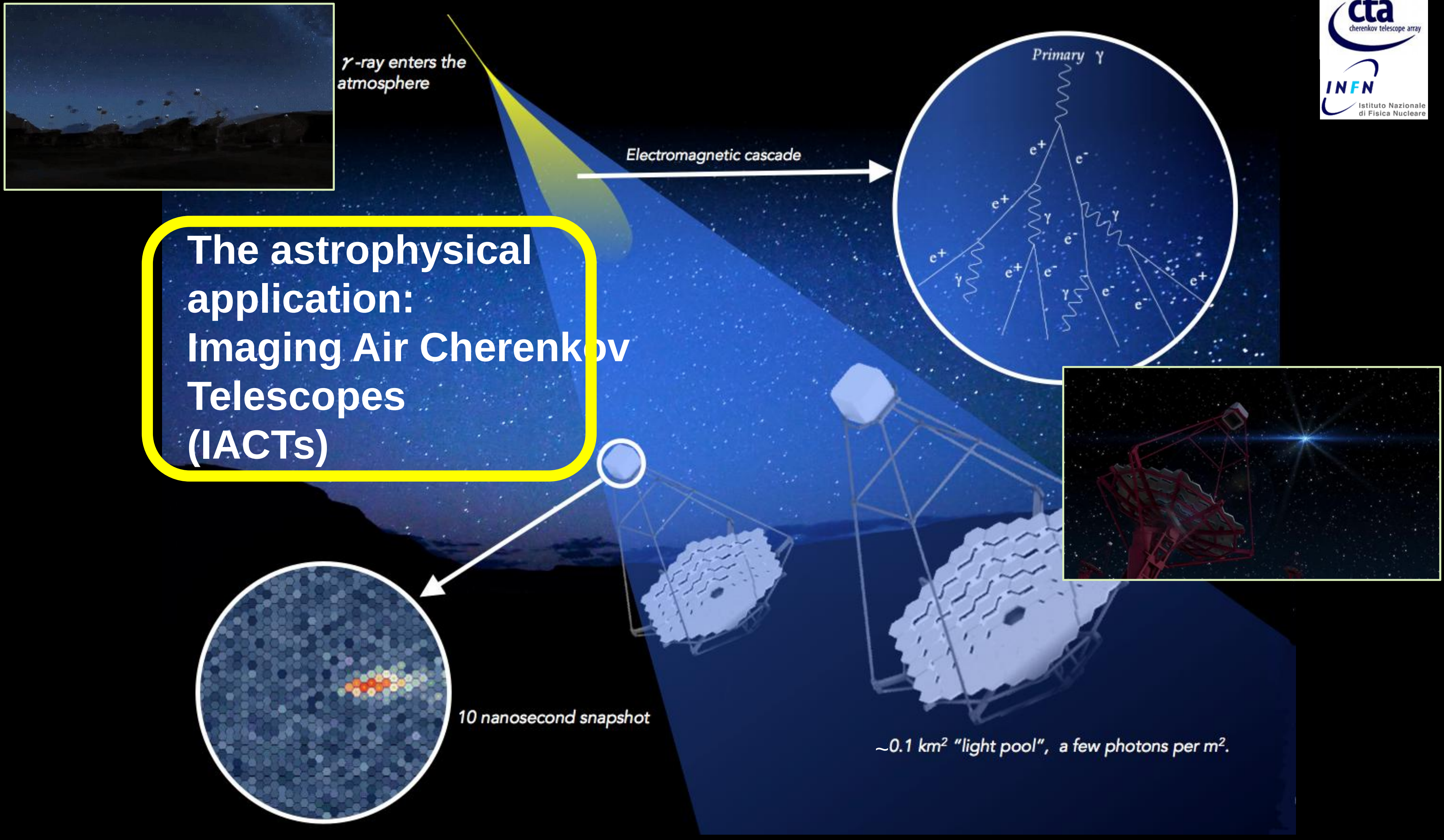

The astrophysical application:
Imaging Air Cherenkov Telescopes (IACTs)

https://www.cta-observatory.org

The Silicon Photomultiplier

- Characterization of FBK NUV SiPMs for the CTA experiment

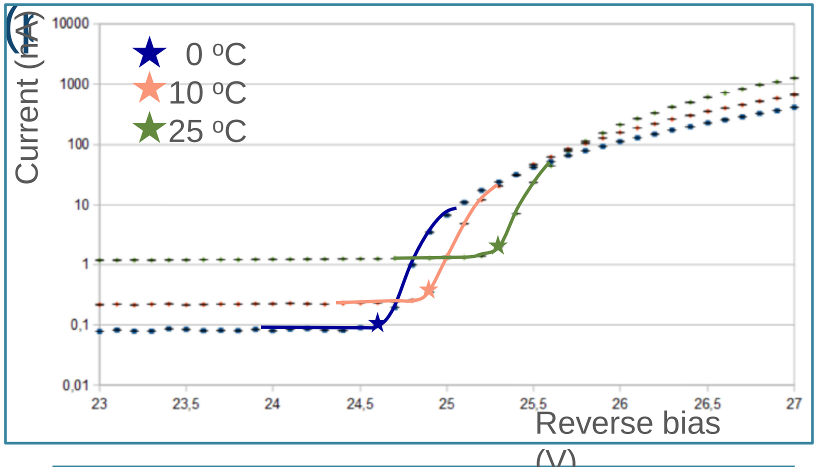

- Low breakdown voltage @ 26V
- Little temperature dependance ~25 mV/°C
- High bias resistance >800 kΩ

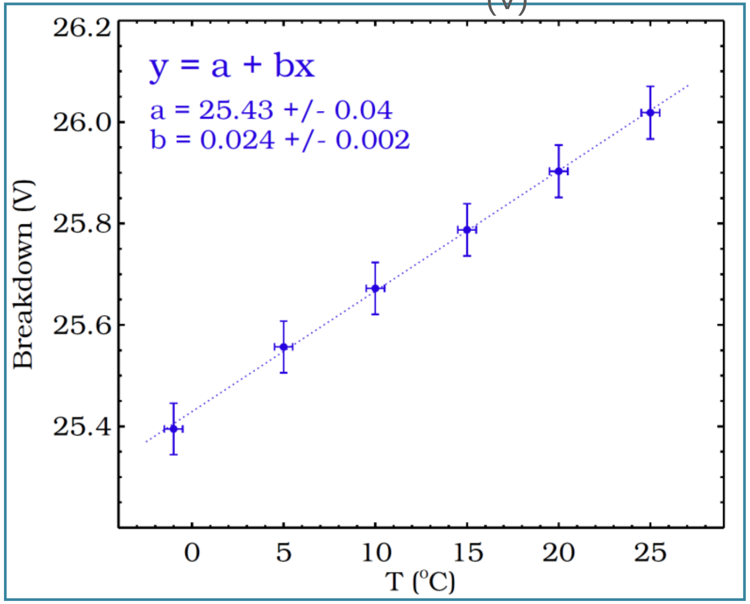

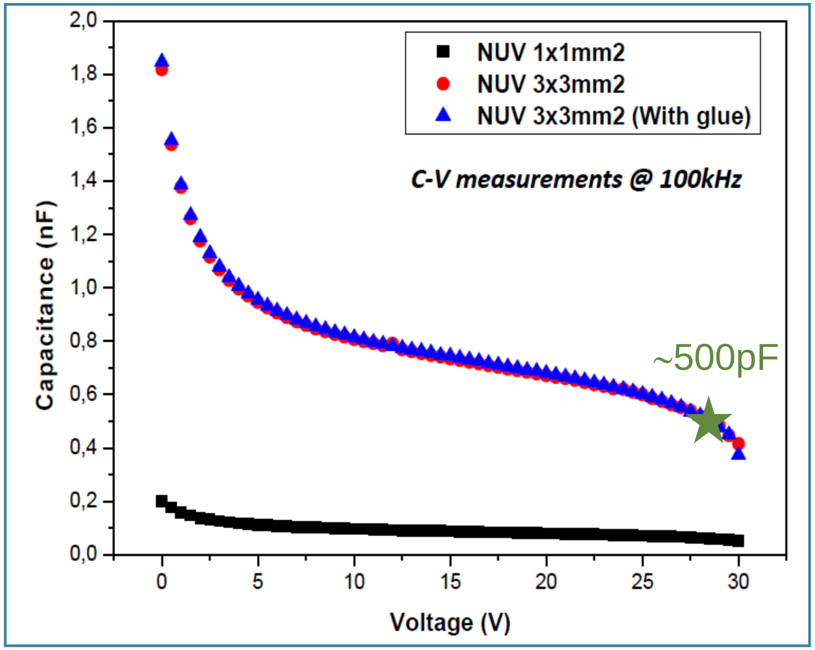

The Silicon Photomultiplier

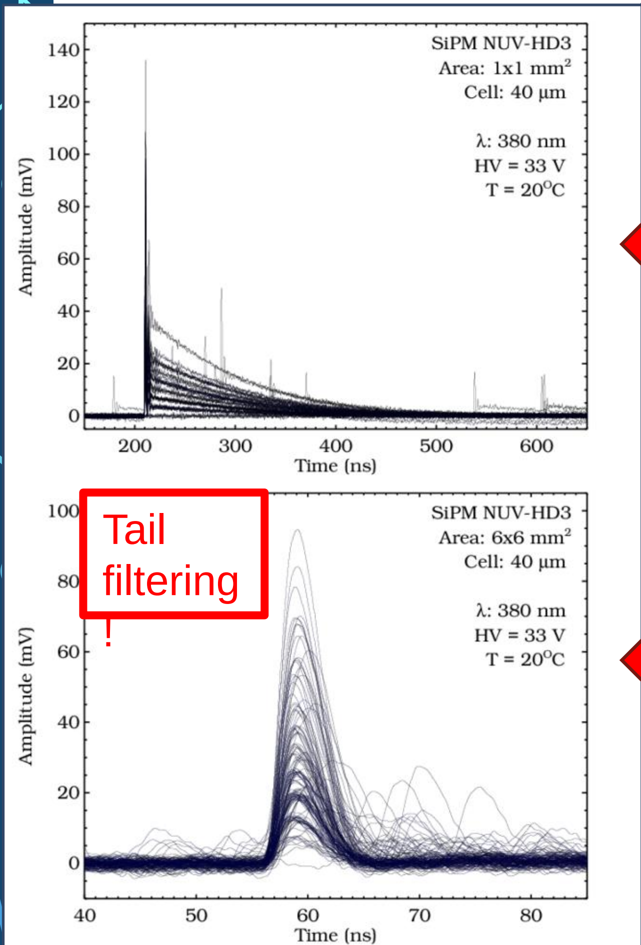

Tail filtering !

- For a full characterization: we tested devices with **different active areas** read out with different front-end electronics circuits

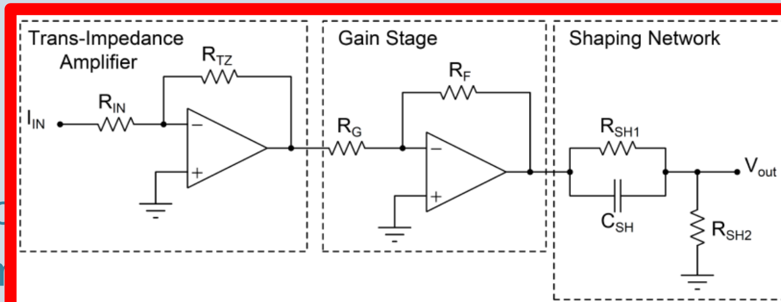

- **1 x 1 mm²**
  - Study o
    SiPM n

nm
Room temperature
HV = 28 – 40 V

- **6 x 6 mm²**
  - Study of **correlated noise** and of **signal-to-noise ratio (SNR)**

The Silicon Photomultiplier

Compound Poisson distribution*

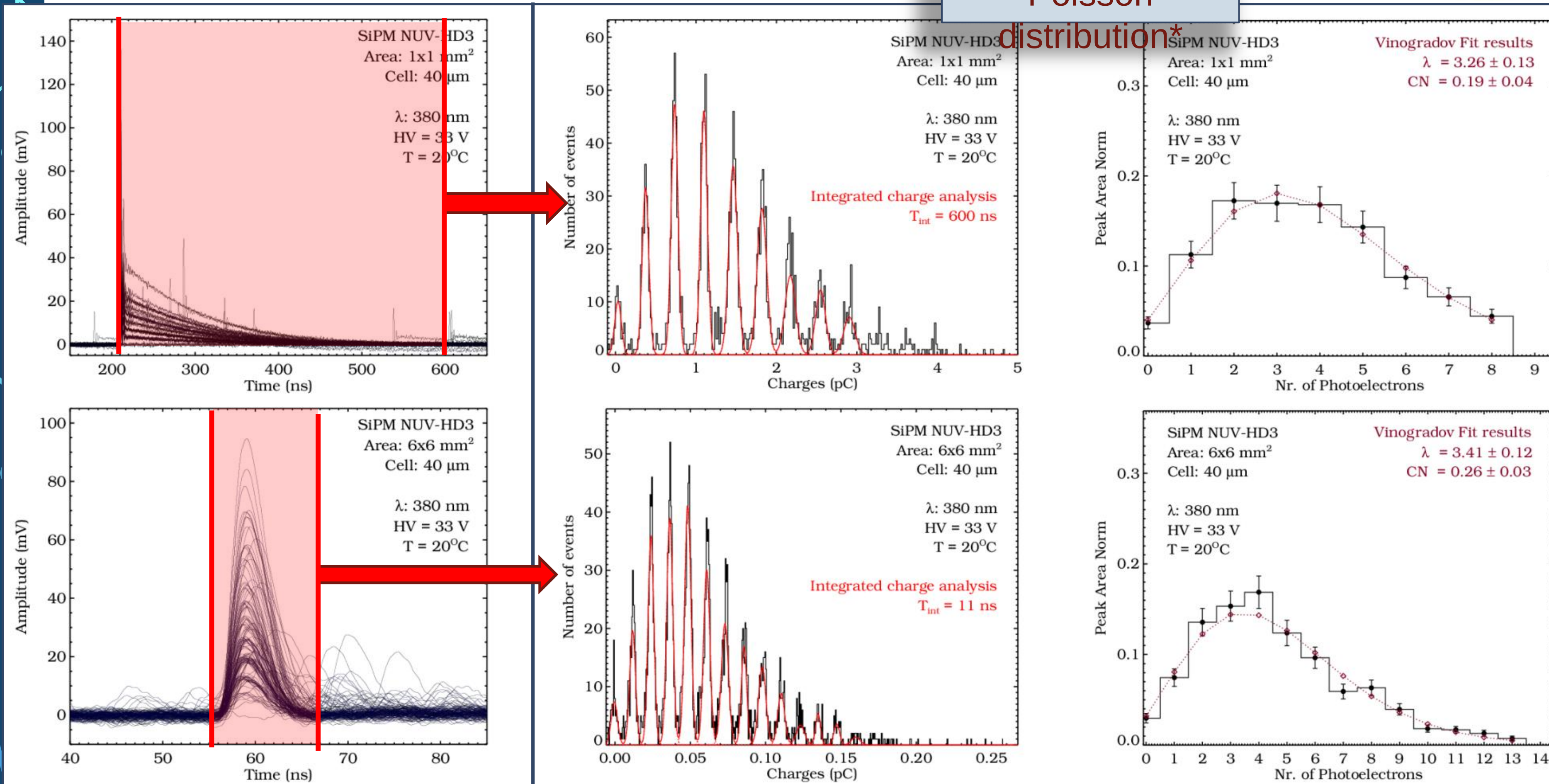

The Silicon Photomultiplier

NUV-HD performances are **compliant** with **minimum requirements** specified to equip the focal planes of **CTA telescopes**

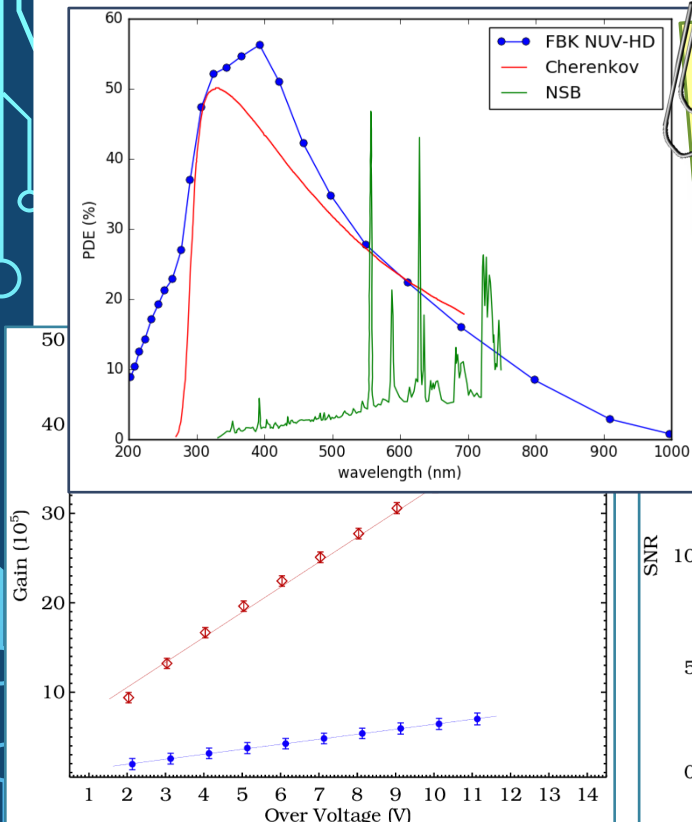

SNR

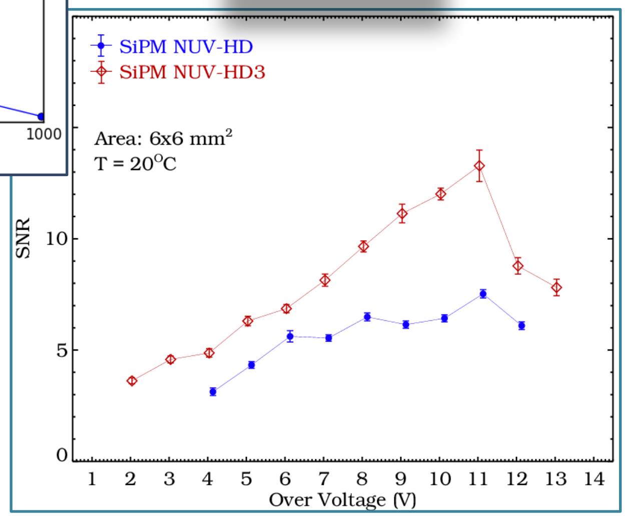

DCR

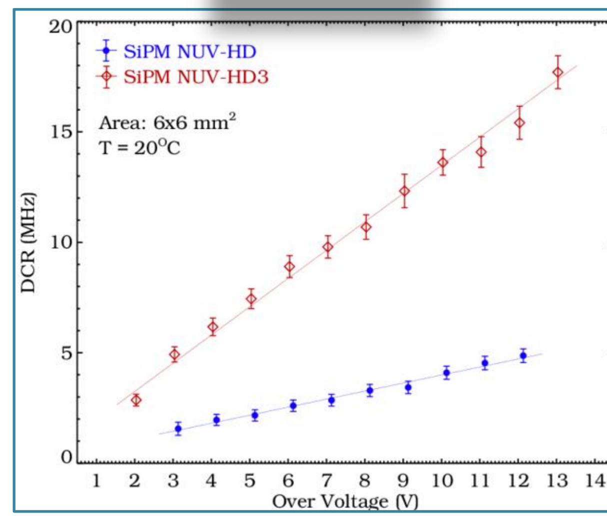

- Despite larger DCR, **HD3 devices** prove to be the best sensors, given the much **higher gain** and **better SNR**.

  ➔ The ideal **working point** lies around **5 ÷ 6 V of OV** (HV = 32 ÷ 33 V).

SiPM applications

THE SCHWARZSCHILD-COUDER TELESCOPE FOR CTA

Dual mirror optics

YESTERDAY!

Prototype demonstrator (pSCT) currently **under construction** at the **Fred Lawrence Whipple Observatory** (→ Veritas site) in Arizona.

LIVE http://cta-psct.physics

SiPM applications

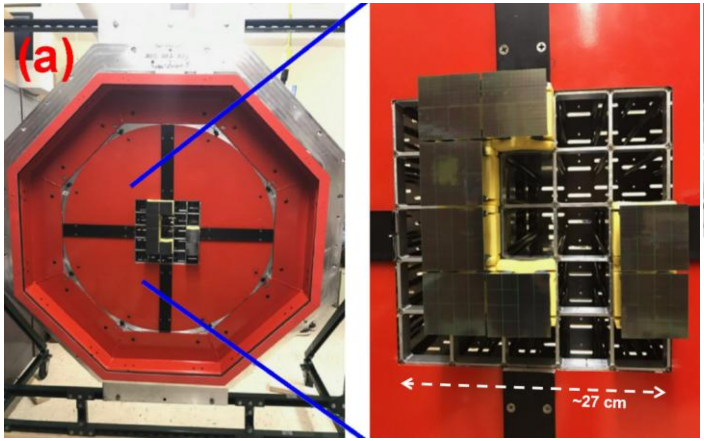

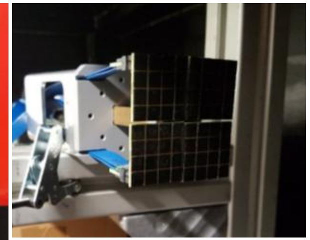

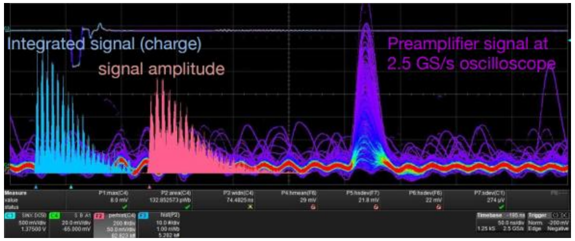

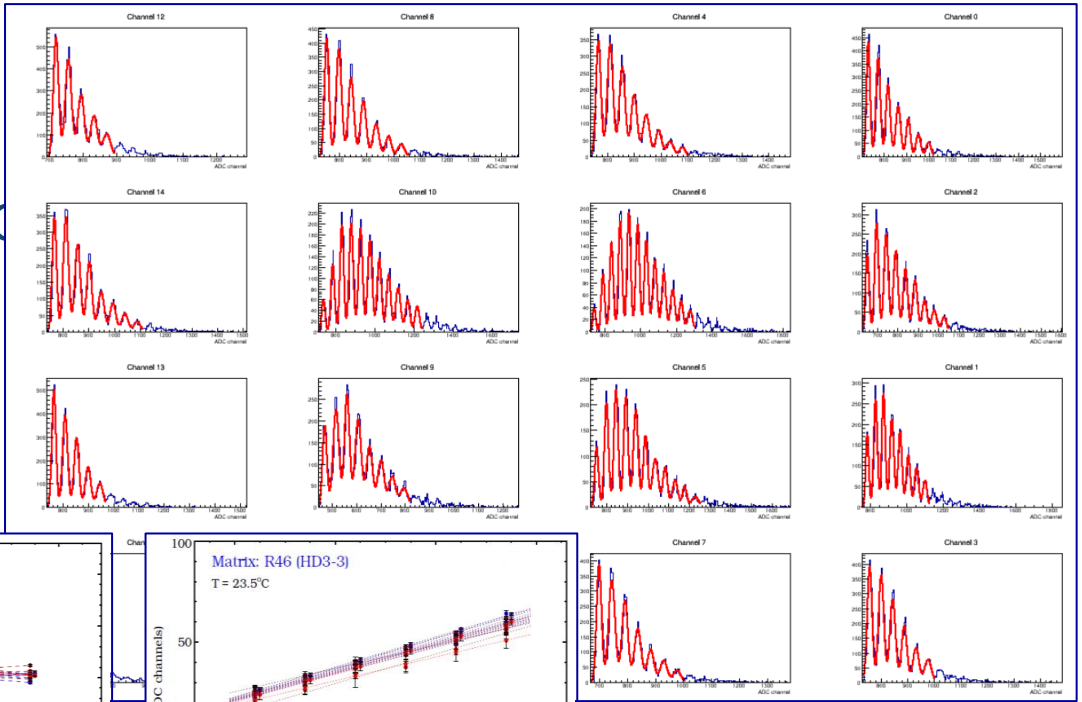

SiPM mass production for pSC

- 672 SiPMs on **42 matrices**

  Matrix = 4x4 units of 6x6 mm^2

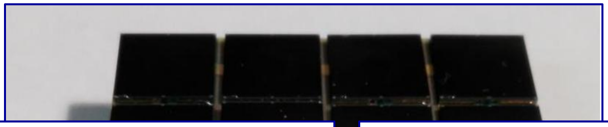

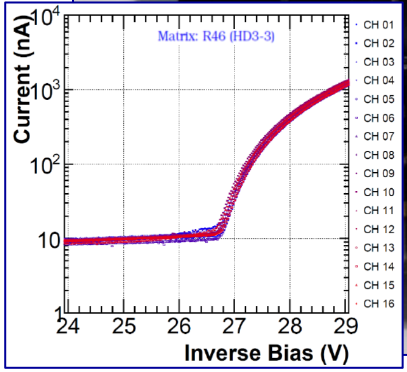

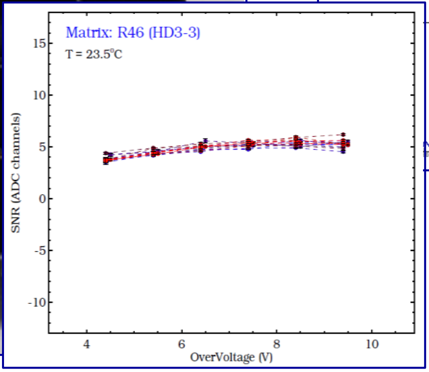

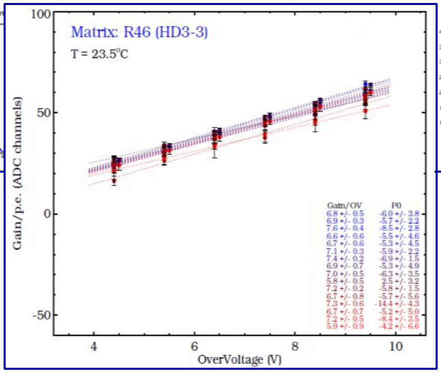

Study of SiPM matrix uniformity